Potential Impacts of Climate Change on Hydrological Extremes in the Incomati River Basin

Master's dissertation

by

Tlakale Mogebisa (MGBTLA002)

presented towards the degree of Master of Science

in Environmental and Geographical Science

University of Cape Town

February 2021

Supervisor: Associate Professor Babatunde J. Abiodun

PLAGIARISM DECLARATION

1. I know that plagiarism is wrong. Plagiarism is to use another's work and pretend that it is one's own.
2. I have used the Harvard convention for citation and referencing. Each contribution and quotation in this dissertation from the works of other people has been attributed and has been cited and referenced.
3. This dissertation is my own work.
4. I have not allowed, and will not allow, anyone to copy this work with the intention of passing it off as his or her own.

Signature: Signed by candidate

February 2021

ABSTRACT

Climate change has been shown to influence extreme rainfall and flooding events over many river basins, yet there is a dearth of information on how to mitigate future risks and vulnerabilities in the Incomati River Basin (IRB), a basin known for extreme devastating flood events. This thesis investigates the potential impacts of climate change on extreme hydrological events that induce flood in the Incomati River Basin (IRB). A series of climate and hydrological simulation datasets were analysed for the study. The climate simulation datasets were acquired from the Global Meteorological Forcing Dataset (GMFD) and the CO-ordinated Regional Downscaling Experiment (CORDEX), but the hydrological simulation datasets were generated with the latest version of the Soil and Water Assessment Tool (called SWAT+), using GMFD and CORDEX as the climate forcing data. The CORDEX dataset was biased-corrected with GMFD, using the Quantile Delta Mapping (QDM) method. The SWAT+ was calibrated and evaluated over the basin to investigate the role of objective functions in SWAT+ calibration, four sensitivity experiments were performed using four objective functions (hereafter, 1-NSE or RMSE, 1-R^2 and PBIAS). To study the influence of the bias correction of CORDEX on hydrological simulations, the SWAT+ simulations were performed using the original and biased-corrected CORDEX datasets as the climate forcing. The impacts of climate change on the mean hydroclimate variables and on characteristics of extreme hydrological events (*i.e.* the intensity and frequency of extreme precipitation and streamflow events) were examined at four global warming levels (*i.e.* GWL1.5, GWL2.0, GWL2.5, GWL3.0) under the RCP8.5 future climate scenario.

The results of the study show that SWAT+ gives realistic simulations of hydrological processes in the basin, although with notable biases in the simulated streamflow. The SWAT+ calibration over the basin is sensitive to the choice of objective function for the calibration. The calibration converges faster with 1-NSE or RMSE than with R^2 or PBIAS. The performance of SWAT+ in simulating the streamflow over the basin depends on the statistical metrics used in the evaluation, while the NSE of the model SWAT+ simulation is poor (*i.e.* NSE ≈ -0.08) over all the stations, the PBIAS is very good (*i.e.* PBIAS ≈ 13.7%) at some stations. The bias correction of CORDEX datasets substantially reduces errors in the climate datasets and improves the quality

of SWAT+ simulations over the basin. Moreover, it also reduces the level of uncertainty in the simulations. With global warming, a future increase in temperature is projected over the basin, but a decrease in annual precipitation is indicated over most part of the basin except at the south-west tip of the basin (*i.e.* around Nooitgedacht Dam), where precipitation is projected to increase. The changes in hydrological extreme events generally follows the precipitation pattern, in that, while less intense and less frequent extreme precipitation and streamflow events are projected over most parts of the basin, more intense and more frequent precipitation and streamflow are indicated in the vicinity of the dam. However, the projection also suggests that an increase in extreme precipitation and streamflow activities surrounding this water body could induce extreme streamflow events downstream of the basin. The results of this thesis have applications in mitigating the impacts of climate change on extreme hydrological events in the basin.

TABLE OF CONTENTS

LIST OF FIGURES

LIST OF TABLES

LIST OF ABBREVIATIONS

CORDEX	Co-Ordinated Regional Downscaling Experiment
CRIDF	Climate Resilience Infrastructure Development Facility
DEA	Department of Environmental Affairs
DEM	Digital Elevation Map
DWAF	Department of Water Affairs
ENSO	El Niño Southern Oscillation
GDP	Gross Domestic Product
GMFD	Global Meteorological Forcing Dataset
ICMA	Inkomati Catchment Management Agency
IRB	Incomati River Basin
IPCC	Intergovernmental Panel on Climate Change
JIBS	Joint Incomati Basin Study
NDELI	Natural Disasters Economic Loss Index
QDM	Quantile Delta Mapping
QGIS	Quantum Geographic Information System
QSWAT+	Quantum Soil & Water Assessment Tool Plus
RCP	Representative Concentration Pathways
SRES	Special Report on Emissions Scenarios
SSP	Shared Socioeconomic Pathways
SWAT+	Soil & Water Assessment Tool Plus
SST	Sea Surface Temperature
SRTM	Shuttle Radar Topography Mission
TPTC	Tripartite Permanent Technical Committee
UNEP	United Nations Environment Programme
UNFCCC	United Nations Framework Convention on Climate Change

ACKNOWLEDGMENTS

I would first and most importantly like to give thanks to the Almighty God for His overwhelming presence throughout this journey. I would then like to extend my deepest gratitude to my supervisor, Associate Professor Babatunde J. Abiodun, for his commitment, guidance and support throughout this process. I am sincerely grateful for the financial support I received from the National Research Fund, the Water Research Commission, the Schroeder Scholarship, and UCT bursary, without which the completion of this degree would not have been possible. I would like to acknowledge Mr Elias Nhlapo from the Department of Water Affairs in providing me with streamflow datasets.

I want to give gratitude to my fellow colleagues, Nokwethaba Makhanya and Myra Naik for the shared knowledge, intellectual input, support, and the long working and editing hours. A special thanks to my friends Lillian Maboya (for also editing my work), Precocious Lekgothoane, Ntando Nyalungu, Nelia Manamela, Sandra Lekota, Mahlape Moloisane, Dimakatso Sethebane and Letlotlo Maluka for their continued support, advice, and motivation. And to my family, my grandmother, Francisca Mogebisa, my mother Kgaugelo Mogebisa, my uncle Pontsho Mogebisa and my sister Palesa Mogebisa, I can never thank you enough for the love, support, and prayers that you've given me throughout my academic journey. This dissertation is dedicated to you!

CHAPTER 1: Introduction

1.1 Background

The Incomati River Basin (IRB), a transboundary basin that is shared amongst three southern African countries (*i.e.* South Africa, Mozambique, and Swaziland), plays a fundamental role in the economies of the riparian countries (Inkomati Catchment Management Agency; (ICMA), 2010; Riddell et al., 2014). In South Africa, the basin covers a small water management area, but contributes a significant 1.3% of the gross domestic product (GDP) (Department of Water Affairs; DWAF, 2003). In 1997 the basin made large economic contributions to various sectors including manufacturing (24.6%), agriculture (18.6%), trade (13.4%) and the government (6.4%) (Riddell et al., 2014). Although the basin contributes to various economic activities (including transportation between Gauteng and the Indian Ocean, as well as mining activities such as coal, gold, nickel and copper mining), its largest economic contributions are to the agriculture and forestry departments. The basin is dominated by rain-fed commercial forestation covering 340 000 ha as well as the cultivation of irrigated sugarcane that covers 42 800 ha. The IRB comprises a total population of 2.3 million, which is estimated to increase to 3 million in a couple of years (Van der Zaag and Carmo Vaz, 2003; Monteiro and Marchand, 2009). Nevertheless, the IRB experiences large precipitation variation, which often leads to hydrological extremes such as flooding and drought. As a consequence, land and water resources are put under unprecedented pressure as these extremes bring about severe and devastating socio-economic risks associated with poverty and economic globalization. Hence, understanding the future characteristics of hydrological extremes is a crucial step toward improving the socio-economic activities of the riparian countries.

1.2 Physical description of the Incomati River Basin

The Incomati River basin (IRB) is located in the east of southern Africa, between latitudes 24^{o}S and 26^{o} 30´S and longitudes 29^{o} 70´E and 33^{o} 35´E (Fig 1.1). The catchment, which is accommodated by South Africa (61.3%), Mozambique (33.2%) and Swaziland (5.5%), covers an area of approximately 46,800 km^{2} (United Nations Environment Programme [UNEP], 2010;

ICMA, 2010; Riddell et al., 2014). The river flows from the south-western part of the basin, across western mountains and plateau of Mpumalanga province (approximately 2000 m above sea level) and continues its flow across Swaziland and the Great Escarpment, before it rapidly descends north through the middleveld, lowveld, and into Mozambique (UNEP, 2010; Riddell et al., 2014). The IRB comprises of seven main sub-catchments namely: Komati (24%), Crocodile (22%) Sabié (15%), Massintonto (7%), Uanetze (8%), Mazimchope (8%) and Incomati (14%) (Vaz and Pereira, 2000; Okello, 2019).

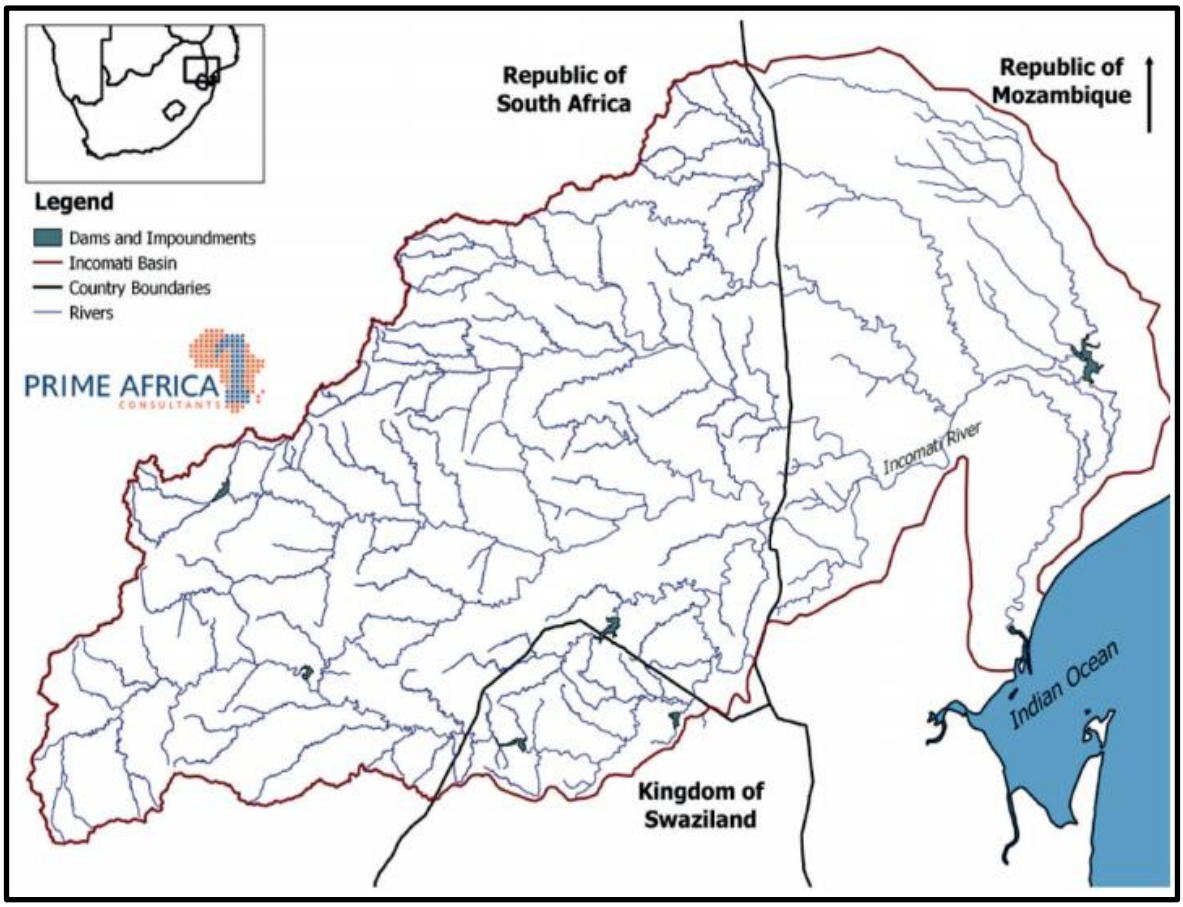

Figure 1.1: The Incomati River Basin watershed (source: Wilkinson et al., 2015).

1.3 Climate of Incomati River basin

The IRB experiences summer rainfall between October and March. The mean annual temperature over this basin is 17°C, with its hottest mean temperatures of 21°C occurring in

January and the coldest temperatures averaging 11.5°C during the month of June (Riddell et al., 2014). Rainfall reaches annual means of approximately 740 mm between October and March, increasing westward. In addition, approximately 1900 mm potential evaporation occurs on average annually. Evaporation in this region decreases westwards (Leestemaker, 2000; Joint Incomati Basin Study [JIBS], 2001). Due to the deficit between rainfall and potential evaporation, the importance of irrigation on crop production becomes pronounced in the east. Incidentally, the IRB generally has light winds with the occasional occurrence of gale winds and thunderstorms. Tropical cyclones during the summer season (January and March) are a predominant influencer of the weather conditions over the flat plateau of Mozambique, mostly resulting in extreme flood events associated with extreme rainfall. The flood experiences are further exacerbated by the opening of dam walls in the riparian countries to reduce the accumulation of water during the summer rainfall season. Nonetheless, the World Bank has estimated increases of 41% in coastal area vulnerabilities and a steep 52% in coastal GDP weakness, stemming from storm surges and flooding events that are attributed to climate change (Holbrook, 2010). Hence, for better mitigation strategy developments, it is important to understand extreme flooding characteristics over the IRB.

1.4 Hydrological Extremes in Incomati River basin

Hydrological extremes are extremes in variability of hydro-climatic variables that lead to natural hazards such as flood and drought in river basins. While floods are associated with precipitation extremes driven by numerous dynamics (such as thunderstorms, tropical storms, tropical cyclones, orographic rainfall, *etc.*), drought is mainly associated with limited or no precipitation as well as extremely high temperatures. Under these extreme dry or wet conditions, enormous economic losses as well as damage to infrastructure that induce unprecedented threats to human lives occur. Over the years, such hydrological extremes have become more frequent, intense, and severe in the IRB. In the past 50 years for instance, the basin has experienced an increase in the severity of hydrological drought events, with the 2015 to 2016 events being more severe than the 2003-2005, 1998-1999, 1991-1995 and 1982-1983 events (Sifudza et al., 2018). In terms of frequency, extreme flood events were less likely to occur more than once in five years

in this basin (Kay and Washington, 2008; Climate Resilience Infrastructure Development Facility [CRIDF], 2018). For example, the basin experienced flood disasters in the years 1976, 1984, 1985, 1996, and 2000 (Gallego-Ayala and Juízo., 2014). In recent times however, the frequency of floods increased sharply. For instance, over a period of twenty-four months, the Crocodile River experienced four major flood events in 2011, 2012, 2013 and 2014 (Sauka, 2016). Hence, more attention should be given towards monitoring these extremes. However, the occurrence of extreme increases in river basin flow, which often lead to flooding, have become even more problematic as they are often localized and take place over a short period of time, yet limited studies have been done in this regard. The year 2000 flood event was the biggest ever recorded, destroying the Moamba bridge, flooding irrigation areas, inundating agricultural lands and taking lives (Van Ogtrop et al., 2005). However, as a result of IRB flooding, the Natural Disasters Economic Loss Index (NDELI) ranked Mozambique as the second highest vulnerable country in the world to experience economic losses between 1980 and 2010 (Holbrook, 2010).

1.5 Causes of flooding in the Incomati River Basin

The occurrence of extreme rainfall and flooding events are largely associated with multiple oceanic and atmospheric drivers. For example, extreme weather conditions are generally driven by induced global mean temperatures and changes in relative humidity (Parry et al., 2007; Solomon et al., 2007; Bernstein, 2008; Zhu & Ringler, 2012). These conditions ultimately influence the occurrence and severity of storms, hurricanes, and precipitation extremes. Consequently, inland flooding and coastal inundation rise, exposing lives, assets, and river basin characteristics to alarming rates of water related disasters and risks. In addition, ocean dynamics such as tropical cyclone landfalls significantly influence weather events (*i.e.* precipitation) that lead to flooding. For example, the year 2000 extreme flooding events over Mozambique, were driven by two consecutive tropical cyclones, namely, Cyclone Eline and Cyclone Hudah which occurred in February and April (Vaz, 2000). Similarly, the 1984 flood event over this basin was a product of Cyclone Domoina, destroying agricultural lands, water supply and roads (Vaz, 2000). Furthermore, the occurrence of El Niño Southern Oscillation (ENSO) modulates these dynamics (*i.e.* tropical cyclones), consequently increasing the occurrence and severity of precipitation

events, storm surges and coastal inundation (Knebl et al., 2005; Tadross and Johnson, 2012; Jury, 2016), thus exacerbating extreme flood events.

Anthropogenic activities have also increased the likelihood of flooding. Due to the high demand of land and freshwater resources for the consequent supply of basic needs, human population as well as socio-economic development have expanded towards the Incomati riverbanks and its floodplains (Kiersch, 2001; Sauka, 2016). Consequently, a steep increase in flood risks and damages has occurred along the flood-prone areas over the years (Jongman et al., 2012; Okello, et al., 2015; Winsemius et al., 2016). Flooded regions are often more affected downstream where the runoff water from overflowing lakes and dams accumulates (Benito et al., 2003; Pomeroy et al.,2016). This is evident over the IRB, where flooding is predominant over Mozambique, which lies on a flat plateau downstream of the basin (Van Ogtrop et al., 2005). The overall impact of all the different drivers of extreme precipitation and flooding thus create great socio-economic losses. With future extreme events being projected to increase because of climate change, the flooding in the IRB raises great concern. Hence, the importance of understanding the future impacts of climate change on hydrological extremes in the IRB that influence flooding events for enhanced mitigation strategy developments.

1.6 Climate change and flooding

Climate change is anticipated to increase temperatures and consequently intensify hydrological processes attributed to it in future (Kruger and Shongwe, 2004; Schulze, 2011). In southern Africa, climate change may not only increase the frequency of extremes, but it may also change the intensity, timing, and circulation of storms that result in flood events (Akoon et al., 2011). With flooding being the main natural hazard in Mozambique and across the basin, future impacts of climate change over the IRB raises even more concern. However, no studies have projected future climate change impact on hydrological extremes associated with flooding over the IRB. Numerous projections have simulated climate separately in the riparian countries, especially over South Africa. For example, precipitation is expected increase in frequency and intensity over the South African part of the basin (Mason et al., 1999; Davis, 2010; Sauka, 2016). Consequently, hydrological extremes such as increases in runoff and streamflow may lead to flooding and have

been projected to also occur in future (Knoesen et al., 2009; Department of Environmental Affairs [DEA], 2010). In Swaziland, future runoff under climate change conditions have also been projected to increase. Although many studies have been done over Mozambique as it is the most vulnerable country to flood disasters and risks in southern Africa, no projections have been made over the IRB region. Nevertheless, the World Bank has estimated increases of 41% in coastal area vulnerabilities and a steep 52% in coastal GDP weakness, stemming from storm surges and flooding events that are attributed to climate change (Holbrook, 2010). Hence, the focus of this dissertation is on the future impacts of climate change on hydrological extremes (*i.e.* flooding) in the IRB.

1.7 Research question

The main research question is:

What are the potential impacts of climate change on extreme climate and hydrological events over the Incomati River Basin?

1.8 Aims and objectives

The aim of this dissertation is to investigate the future impacts of global warming on extreme precipitation and hydrological events over the Incomati River Basin, using a series of climate and hydrological simulations. The overall goal is to provide relevant information for future climate change adaptation and mitigation strategies over the basin. The information may assist governments, the private sector, as well as local communities in sustainably managing water resources and in reducing disaster risk associated with extreme hydrological events (*i.e.* flooding) in future. To achieve the aim, the following are the dissertation objectives:

1. To examine how SWAT+ simulates the hydrology of the IRB and study the influence of different objective functions in obtaining the best SWAT+ simulation over the basin.

2. To evaluate the performance of CORDEX dataset in reproducing the historical climate over the IRB and study the role of bias correction in improving the quality of climate data and the simulated hydrological variables.

3. To study the characteristics of projected future climate change in climate and hydrological variables (and the associated extreme events) under the Representative Concentration Pathways (RCP) 8.5 scenarios at various global warming levels.

CHAPTER 2: Literature Review

This chapter reviews previous studies on the Incomati river basin and on how to model climate change impacts over river basins. The chapter starts by reviewing past hydroclimatic research activities over the Incomati River Basin and exposes the research gaps and challenges. It then reviews past work on climate and hydrological modelling, showing the state-of-the-art tools and techniques used to quantify future climate change scenarios and model hydrological impacts over river basins.

2.1 Hydroclimatic research activities over the Incomati River Basin

Past studies on IRB climate and hydrology have discussed the problem of hydrological extremes (droughts and floods) in IRB (*e.g.* Van der Zaag and Carmo Vaz, 2003; Schulz, 2006; Slinger et al., 2010; Gallego-Ayala and Juízo, 2014). While some of the discussion focused on the management of IRB hydrological resources among the three riparian countries (South Africa, Mozambique, and Swaziland), other studies focused on causes of IRB streamflow variability. On the management of hydrological resources, several studies (*e.g*. Van der Zaag and Carmo Vaz, 2003; Schulz, 2006; Slinger et al., 2010; Gallego-Ayala and Juízo, 2014) have reported on how to integrate river basin water resource management and planning across the countries to minimize impacts of droughts over the basin. For example, Gallego-Ayala and Juízo (2014) found heterogeneities in stakeholder management preferences and suggested a methodological framework to encompass involvement and participation in decision-making processes. Only a few studies (*e.g.* Van Ogtrop et al., 2005; Sengo et al., 2005; Gallego-Ayala and Juízo, 2014) have considered how to manage floods over the basin. Even so, the few studies have focused on lower Incomati. For example, Van Ogtrop et al. (2005) only investigated floods on the lower Incomati (in Mozambique). Hence, there is a dearth of information on how to manage flooding in IRB. The present study will improve knowledge on future characteristics of extreme streamflow that usually induce flooding in the basin.

Numerous studies have suggested climatic and oceanic drivers as the main cause of water stress in the basin (*e.g.* Sunday, 2013; Sunday et al., 2014) and linked hydrological drought over the

basin to climatological drought (*e.g.* Sifundza et al., 2019). For example, Sunday (2013) showed that the streamflow over the Crocodile catchment in the IRB has a significantly strong 0.265 correlation with ENSO, -0.239 correlation with sea surface temperature (SST) (both significant at 95% over the Atlantic and Indian Ocean), and the strongest 0.487 correlation with precipitation at a confidence level of 99%. Similarly, Sunday et al. (2014) found the correlation of ENSO, SST and precipitation to streamflow to be of statistical significance at a 95% confidence level. Studies that have focused on drought in the basin have mainly been over the South African part of the basin. For example, Sifundza et al. (2018) observed the occurrence of a climatological drought a month before hydrological drought in the basin during the 2015-2016 drought event over the Komati and Crocodile sub-catchments. Furthermore, Sifundza et al. (2019) related the drought event in the Komati sub-catchment to the El Niño event.

On the contrary, some studies have argued that climatic drivers have less impacts on the changes in streamflow in the basin. For example, Mussa (2013) showed that although precipitation is the main factor to changes in discharge, hydrological and meteorological droughts follow different patterns. The study also showed that despite the general clear negative trend (*i.e.* reductions) in discharge in the basin, there was no trend in the precipitation over the basin in the period 1940-2011. Hence, some studies have attributed changes in the Incomati river flow to human intervention instead of meteorological forces. For example, Mussa (2013) related the changes to increases in forestry, irrigation, and domestic use. Macuácua (2012) attributed the reduction in streamflow in the basin to changes in land use and increases in agricultural abstraction. Okello et al. (2015) suggested that a general decline in flow trends across the basin is a result of land use changes and flow regulations. However, the emphasis of these studies has been on impacts of climate variability and change in the past and present-day climates. The present study will consider impacts of future climate on the hydrology of basin, with emphasis on hydrological extremes that can lead to flooding.

2.2 Future climate projection tools

2.2.1 Global climate model projections

Several studies have established global climate models (GCMs) as essential tools for projecting future climate and for studying climate change impacts on hydrological extremes (*e.g.* Müller-Wohlfeil et al., 2000; Milly et al., 2002). Nonetheless, the credibility of GCMs to project future climate is dependent on the capability of the model to mimic past and present climate at a regional and global scale (Nyeko-Ogiramoi et al., 2010). Numerous shortcomings in GCMs have thus been identified and discussed over the years. While GCMs perform best in projecting climate at a global scale, their performance is rather unsatisfactory on a regional scale. For example, the Intergovernmental Panel on Climate Change (IPCC, 1992) indicated that using GCMs to simulate precipitation extremes that produce flooding is problematic at a local scale. Whetton et al. (1993) showed that there are large uncertainties in using GCMs to project daily rainfall patterns, because of coarse vertical and horizontal resolutions of the models. In recent times, Chen and Knutson (2008) found that most of the (IPCC) Fourth Assessment Report (AR4) underestimated the observed daily rainfall dataset over the United States. Similarly, Davis et al. (2017) further showed that GCMs tend to under-capture important local and regional climate determinants such as physical processes and landscape features. Despite the shortcoming, some studies have analysed GCM projections over southern Africa (*i.e.* Joubert et al., 1996; Mason, 1996; Joubert and Hewitson, 1997; Mason and Joubert, 1997) and showed that there is a lower confidence in the extreme rainfall projections than on temperature projections over the sub-continent. For example Shongwe et al. (2011) projected severe deficits in the southern African precipitation but cautioned on the usage of the projections for impact studies at local scale because of the uncertainties in their projections. To address these shortcomings of GCMs, GCM simulations are usually downscaled to regional and basin scales. All the GCM simulations used in the present study are downscaled to regional scale.

2.2.2 Downscaling of Global climate model projections

Past studies have adopted two approaches in downscaling GCM projections: the dynamic downscaling method and statistical downscaling method (Watson and Team, 2001; Pielke and Wilby, 2012; Tang et al., 2016). The two approaches use different techniques in adding regional

or local information to larger-scale climate signals from GCM projections. While the dynamic downscaling approach uses regional climate models (RCMs) to create higher resolution simulations over a region, the statistical downscaling approach utilizes statistical equations to establish relationships between observational atmospheric variables at global and local scales. Past studies have shown that each of the approaches have its merits and demerits. For example, Chen et al. (2013) and Li et al. (2013) highlighted that the dynamic downscaling approach is computationally expensive, while Zhang and Huang (2013) revealed that the statistical downscaling approach produces less detailed spatial information. Nonetheless, both approaches have been reported to produce enhanced and finer spatial and temporal resolution outputs for representing climate variables over regions comprising complex land and sea characteristics (*i.e.* Brown et al., 2005; Teutschbein and Seibert, 2012; Cortés-Hernández et al., 2016). Both approaches have been applied to downscale multi-GCMs in global experiments. For instance, Giorgi et al. (2009) reported application of the dynamic downscaling approach in the CO-ordinated Regional Downscaling Experiment (CORDEX; Jones et al., 2011) to produce regional climate simulations worldwide. On the other hand, Bokhari et al. (2018) reported the adoption of the statistical downscaling approach in the NASA Earth eXchange Global Daily Downscaled Projections experiment (NEX-GDDP; Thrasher and Nemani, 2015). The datasets produced in CORDEX and NEX can be easily accessed and have thus been widely applied in climate change related studies at regional scales. The present study utilized the CORDEX dataset over the study area. This is mainly due to the accessibility of the CORDEX dataset. More importantly, the dataset contains downscaled climate data for present-day and future climates.

2.2.3 CORDEX Climate Change Projections

Multiple studies have applied the CO-ordinated Regional Climate Downscaling Experiment (CORDEX) datasets with RCMs in conducting regional climate change projections worldwide (*e.g.* Pinto et al., 2016; Park et al., 2016). As a result, these high-resolution climate simulations have become the main tools for producing more reliable future extreme hydrological projections. For example, the overestimated precipitation simulations over the Tibetan Plateau using coarse GCMs resolutions were removed by RCMs in a study by Gu et al. (2018) using RCMs. Similarly, Cortés-Hernández et al. (2016) established satisfactory model performance as the model was

predominantly consistent with the observations. Numerous studies have reported satisfactory simulation projections using CORDEX datasets in Africa. For example, Pinto et al. (2016) found RCMs to generally capture the spatial pattern of observed precipitation. Similarly, Nikulin et al. (2018) also found robust increases in regional warming over most parts of Africa that exceed global mean warming. Some studies have analysed the CORDEX dataset over southern Africa (*e.g.* Kalognomou et al., 2013; Favre et al., 2016; Déqué et al., 2017; Maure et al., 2018; Abiodun et al., 2019b; Kisembe et al., 2019). Kalognomou et al. (2013) found all CORDEX RCMs to generally represent the characteristics of the rainfall in the region both spatially and temporally. Similarly, Abiodun et al. (2019b) found that the CORDEX datasets performed well in capturing the southern African rainfall indices climatology, with simulation errors falling within the uncertainties in the observation datasets. Furthermore, analysing the CORDEX dataset, Déqué et al. (2017) projected the precipitation days over tropical southern Africa to be less frequent but more intense. Hence, the CORDEX models have been used for further climate projections over the region. For example, Maúre et al. (2018) projected up to 0.1 mm rainfall increases over the southern Namibia and western and mid-South Africa, as well as 0.2 to 0.4 mm decreases over the northern part of Mozambique and most subcontinent regions per day. In addition, Abiodun et al. (2019b) projected increases in future extreme rainfall intensity and frequency over the northern part and decreases over the southern part of the region. Nevertheless, no study has analysed CORDEX datasets to study hydro-climatological extremes over the IRB. The present study is in this direction.

2.3 Future climate projection scenarios

As a means to understand complex interactions between future climate change impacts coupled with human interactions, different scenarios have been developed and applied in many studies (Nakicenovic et al., 2000; Moss et al., 2010; Van Vuuren et al., 2011; Pedersen et al., 2021). Furthermore, the development of climate change mitigation and adaptation policies requires careful consideration of a wide range of assumptions.

2.3.1 Special Report Emissions Scenarios (SRES)

The development of the different emission scenarios owing to future greenhouse gas (GHG) emission levels is discussed and used by multiple studies (*e.g.* Morita et al., 2000; Nakicenovic et

al., 2000; Van Vuuren et al., 2011; Pedersen et al., 2021). Nakicenovic et al. (2000) on Special Report on Emissions Scenarios (SRES) reported the development of three climate change emission scenarios: the high (SRES-A2), medium (SRES-A1B) and low SRES-B1 emissions. Even so, Morita et al. (2000) developed 40 scenarios based on various modelling approaches, assessment of literature and the "open process". The scenarios were based on family grouping and characteristic similarities. However, only four SRES storylines generally exist (*i.e.* A1, A2, B1 and B2), describing the evolving of economies, populations, lifestyles and political structures in future (Arnell, 2004). Several studies in the past have used these SRES emission scenarios to quantify impacts of future climate change (Nakicenovic et al., 2000). For example, Su et al. (2015) found a variation of tendencies in seasonal precipitation and streamflow over the Songhuajiang River basin under three emission scenarios. Arnell (2004) studied the climate change impact on global hydrological resources and found minimal differences between emission scenarios and a clear effect from different population assumptions.

2.3.2 Representative Concentration Pathways scenarios (RCPs)

In 2011, the IPCC released new greenhouse gas emission scenarios named the Representative Concentration Pathways scenarios (RCPs; Van Vuuren et al., 2011). RCPs are the 21st century greenhouse gas (GHG) concentration pathways that correspond to a variation of radiative forcing stabilization levels by the year 2100. Stocker et al. (2014) and Van Vuuren et al. (2011) reported that the development of RCP scenarios generally replaced SRES emission scenarios as SRES scenarios only incorporated non-intervention scenarios. Hence, recent studies have generally applied RCP scenarios. For example, Su et al. (2015) applied three RCP scenarios (*e.g.* RCP8.5, RCP4.5 and RCP2.6) and found that precipitation and streamflow exhibit obvious increasing tendencies under different RCPs than SRES. Multiple studies have applied the highest GHG emission scenario, RCP8.5, with roughly 8.5 W/m^2 radiation forcing by 2100 (*i.e.* Van Vuuren et al., 2011; Pinto et al., 2016; Su et al., 2015) followed by the middle level scenario, RCP4.5, with about 4.5 W/m^2 by 2100. The present study examines future climate projection under RCP8.5.

2.3.3 Global Warming Levels (GWLs)

As part of the efforts to reduce global warming and strengthen the actions towards a sustainable low carbon, the Paris Climate Agreement was made by the United Nations Framework Convention on Climate Change (UNFCCC) (Rogeli et al., 2016). The aim of the agreement is to keep global warming lower than 2°C above pre-industrial levels and to put attempts in place to reduce the increase to 1.5°C. Studies such as Rogelj et al. (2016) and Hulme (2016) have argued that the GWL 1.5 and 2°C may comprise limited differences in the climate change. Hence, a focus towards a 2.5°C warming level has also become another fundamental focus. Multiple studies around the world have computed the impact of climate change at the three global warming levels (*i.e.* Donnelly et al., 2017; Kumi and Abiodun, 2018; Gudoshava et al., 2020). In southern African river basins for instance, Beck and Bernauer (2011) projected maximum temperatures to reach 2.9°C over the Zambezi Basin, while Graham et al. (2011) projected 3°C increases over the Thukela Catchment, South Africa, and Mujere and Mazvimavi (2012) projected an increase of 3°C over the Mazoe catchment, Zimbabwe. Nonetheless, to date, no study has examined GWLs over the Incomati River basin. The present study projects the impacts of climate change on hydrological extremes at four global warming levels (1.5^{o}C, 2.0^{o}C, 2.5^{o}C and 3.0^{o}C).

2.3.4 Shared Socioeconomic Pathways (SSPs)

SSPs are newly developed climate change research scenarios. O'Neill et al. (2014) reported that four SSPs storylines (*i.e.* SSP1, SSP3, SSP4 and SSP5) describe low and high adaptation and mitigation challenge combinations while SSP2 only describes medium level challenges. Van Vuuren et al. (2014) reported that the SSP framework comprises several assumptions. The key assumption from O'Neill et al. (2014) being that SSPs were coupled with RCPs to meet socioeconomic scenarios with climate scenarios to facilitate impacts, adaptation and vulnerability research. Furthermore, Van Vuuren et al. (2014) expressed that this assumption would be achieved with SSPs defined as reference pathways in hypothetical cases where new climate mitigation and adaptation policies and future climate change impact are prohibited. Van Vuuren et al. (2014) noted the second key assumption to be that similar radiative forcing outputs can be achieved from varying development pathways. The second assumption is in relation to the conclusions from SRES that identifies multiple socio-economic scenarios from each forcing

level (Nakicenovic et al., 2000). The assumption was thus confirmed by Van Vuuren et al. (2012) who found minimal correlation between individual population and economic assumptions and different levels of forcing. Van Vuuren et al. (2014) further advised that SSPs be used as mitigation and adaptation policy analysis boundary conditions. Numerous studies have applied SSPs in their work (Dellink et al., 2017; Cuaresma, 2017; Leimbach et al., 2017). For example, Fujimori et al. (2017) confirmed the consistency of the SSP3 scenario with its narrative. However, SSP scenarios were not used in the dissertation because the CORDEX simulation datasets for SSPs were not available at time of the study.

2.4 Hydrological projection techniques

2.4.1 Hydrological models

Hydrological models are fundamental for the effective management of hydrological systems. As a result, several studies have used various models around the world to evaluate hydrological extremes (Bergström et al., 2001; Arnell, 2003; Laio et al., 2009). According to Sorooshian et al. (2008), hydrological modelling is a representation of complex realistic hydrology using simplified mathematical equations. Several studies have identified detailed precipitation and drainage datasets as the key input information in hydrological modelling, followed by different watershed characteristics (Karlsson and Arnberg., 2011; Devia et al., 2015; Abdulkareem et al., 2018). For example, Karlsson and Arnberg (2011) emphasized the importance of having accurate digital elevation models (DEM) for the revelation of relevant information on the topography, location of occurrence and visual past and future extents. Tarek et al. (2020) on the other hand identified precipitation and temperature as critical variables for the development of hydrological models for the description of water movement. Devia et al. (2015) further highlighted that hydrological models are not only developed for predicting and understanding hydrological processes but for studying climate change impact and the impact of changes in soil and land use on hydrological resources. Hence, it is important to incorporate adequate watershed characteristics for more realistic outputs. Singh and Woolhiser (2002) highlighted the importance of increasing hydrological predictivity in hydrological models using other climate variables (*i.e.* temperature, wind speed and relative humidity). Nonetheless, the hydrological modelling of extremes such as floods and drought are critical for mitigation and adaptation planning and management, input

data limitations and uncertainties inhibits the outcome of hydrological modelling. A coarse spatial resolution of rainfall for instance, creates a control run that is unrealistic, further producing unrealistic hydrological model outputs (Graham, 2000). For instance, Prudhomme et al. (2002) reanalysed a study on future flood projections previously done by Reynard et al. (2001) using new sets of climate scenarios over the United Kingdom. Contrary to Reynard et al. (2001), they found evidence of future flood peak reductions. Hence this underscores the significance of applying high spatial resolution climate model outputs as inputs in hydrological modelling.

2.4.2 Hydrological model classifications

Multiple hydrological models are continuously developed to simulate different hydrological behaviours over the years. As a result, multiple studies have attempted to classify hydrological models (*i.e.* Legesse et al., 2003; Brown et al., 2005; Yang et al., 2012). Over the years, hydrological models have generally been classified based on input variables, different parameters, and in accordance with their physical structures (Devia et al., 2015). For example, Moradkhani and Sorooshian (2009) and Krysanova et al. (2018) classified hydrological models as lumped or distributed, while Sorooshian et al. (2008) classified hydrological models to either be event-based or continuous. Refsgaard (1996) classified them as deterministic, stochastic, or joint stochastic-deterministic, while Devia et al. (2015) classified them to be either empirical, conceptual, or physical. Krysanova et al. (2018) further classified models based on scale (*i.e.* global or regional), resolution, conceptual or process based. Nevertheless, the most extensive classification of hydrological models by far comprises three classes, namely, empirical, conceptual, and physically based models (Sorooshian et al., 2008), which Abdulkareem et al. (2018) further classified as sub-divisions of the deterministic models which describe hydrological processes.

2.4.2.1 Empirical models

Empirical models are often referred to as data driven models due to them being developed from existing observation data. The development of these models encompassed mathematical equations that are derived from simultaneous input and output time series instead of hydrological features and processes of a catchment (Abdulkareem et al., 2018). Abdulkareem et

al. (2018) categorised empirical models into three, based on hydro informatics, hydrological and statistical methods. In the past, empirical models were well known and mostly referred to as black box models (Sherman, 1932; Nash,1959). The models were widely used for simulating and predicting streamflow (Sivakumar et al., 2002; Cheng et al., 2005). Although empirical models comprise shortcomings, the models are still being applied in recent times. For example, Guo et al. (2014) applied empirical models with multiple objectives for predicting streamflow. Moreover, empirical models are mostly incorporated into comprehensive models such as conceptual models.

2.4.2.2 Conceptual models

Conceptual models have been largely applied in hydrological modelling. According to Refsgaard and Knudsen (1996), most conceptual models comprise lumped model characteristics. The complexities of hydrological model calibration have directed the development of many conceptual models. For instance, Pitman (1973) developed the well-known PITMAN model. Similarly, Beven and Kirby (1979) developed the TOPMODEL, while Refsgaard et al. (2010) developed the SHE conceptual model. Nonetheless, Abdulkareem et al. (2018) emphasized the importance of having large time series datasets availability when using conceptual models. This is because conceptual models apply semi-empirical equations and are physically based, thus the assessment of model parameters occurs in field data as well as calibration (Abdulkareem et al., 2018). Even so, calibration is complex in conceptual models since it involves curve fitting. As a result, the models produce land use change impact simulations that are of low confidence. Nonetheless, several studies have applied conceptual models around the world (*i.e.* Hartmann and Bárdossy, 2005; Chiew et al., 2009; Fowler et al., 2016). For example, Coron et al. (2012) compared three conceptual models over 216 catchments in Australia and found the models to either overestimate or underestimate mean runoff.

2.4.2.3 Physical models

Physically based models generally apply mathematical equations to represent real life phenomena. According to Abdulkareem et al. (2018), physical models constitute an ability to

physically represent hydrological processes. Furthermore, although the models require extensive amounts of datasets for the representation of a catchment's physical characteristics (topography, topology, soil moisture, initial depth of water, river network information, *etc.*) minimal meteorological and hydrological datasets are however required (Abdulkareem et al., 2018). As a result, these models produce more comprehensive and accurate outputs better than empirical and conceptual models (Abdulkareem et al., 2018). Hence, multiple studies have developed and applied physically based models (*e.g*. ACRU, HEC-HMS, SWAT, and WRF-Hydro) in simulating hydrological extremes (*e.g.* Arnold et al., 1993; Schulze, 1995; Bieger et al., 2017; Silver et al., 2017). In recent times, several studies have highlighted the successful application of the newly released version of SWAT called SWAT+, and its model performance (*i.e.* Bieger et al., 2017; Yen et al., 2019; Wu et al., 2020). For example, a recent study by Wu et al. (2020) expressed high confidence in SWAT+ simulating reservoirs at a daily scale. Nonetheless, more studies need to be done in this context, especially at the watershed scale and vulnerable river basins. Hence, this research thesis will apply SWAT+ to simulate streamflow over the Incomati River Basin.

2.5 Future climate change impact on hydroclimatic extremes

Several studies have projected increases in largescale floods associated with future climate change impact on hydrological extremes predominantly over major river basins around the world (Alfieri et al., 2017; Hirabayashi et al., 2008; Hirabayashi et al., 2013). For example, Alfieri et al. (2017) projected a large number of global river basins may experience significant (exceeding 95%) increases in rainfall extremes and increased durations of extreme floods. Similarly, Hirabayashi et al. (2008) projected that river basins in high latitudes would experience future increase in daily rainfall compared to low latitude river basins, except for the Brahmaputra River basin. Furthermore, Hirabayashi et al. (2013) established more frequent flood occurrences in most of the major river basins over south and east Asia, and Africa. Nevertheless, river basin studies need to be downscaled in order to achieve extra accurate and precise regional projections.

Regional studies in this context have mostly been done over Europe, North America, and Asia. For instance, Pall et al. (2011) projected increased flood related risks associated with increasing global emissions of greenhouse-gases and the displacement of the North Atlantic jet stream in various river basins in England. Gutowski et al. (2008) also revealed projected increased intensification of rainfall extremes over the Upper Mississippi River Basin region. Additionally, Kundzewicz et al. (2014) projected increases in extreme rainfall events over Bangladesh and the Yangtze River basin. Lastly, Musselman et al. (2018) established 55% increases in runoff over North American river basins, with 20-200% rises in flood risks due to the snow and rainfall shifts. Very limited studies have been done in southern Africa. Nonetheless, Adrianne (2003) reported a 10-20% drop in expected rainfall and a below 50% drop in river levels over southern Africa by 2070. Alfieri et al. (2017) also revealed significant decreases in rainfall extremes in the Okavango and Orange Rivers, in Southern Africa. Consequent flood projections were however not performed in this regard. Smaller river basins are consequently neglected in such studies. For instance, Kusangaya et al. (2014) highlighted the importance of incorporating climate change information over the southern African river basin but fails to do so. Nevertheless, no study has projected impacts of climate change on hydrological extremes over the Incomati River Basin.

CHAPTER 3: Methodology

This chapter provides a description of the methodology used in the study. The chapter provides a physical and climatological description of the IRB study domain, as well as detailed information on the relevant datasets (data sources and resolutions). Three types of data were analysed for this study, namely: QGIS data, climate data and hydrological data. Thereafter, a thorough description of the SWAT+ hydrological model is given, and the procedure followed for the model setup over the Incomati River Basin.

3.1 The study domain

The Incomati River basin (IRB), as used in this study, is shown in Figure (3.1). The basin, which is in the eastern part of is a southern African (*i.e.* between latitudes 24°S and 26° 30´S and longitudes 29° 70´E and 33° 35´E), is shared among Swaziland, Mozambique and South Africa. The catchment covers an area of approximately 46,800 km^2 (Riddell et al., 2014; UNEP, 2010) with a predominant 61.3% over South Africa, 33.2% over Mozambique, and 5.5% in Swaziland (ICMA, 2010; Riddell et al., 2014). The headwaters of the basin occur south west of the basin along the high western mountains and plateau area (approximately 2000 m above sea level). The river continues its flow across the north-western part of Swaziland and the Great Escarpment, before it rapidly descends through the middleveld and lowveld, across the Lebombo mountains and into the coastal plain of Mozambique through significant ephemeral tributaries leading to the mouth (Riddell et al., 2014). The IRB lies within a semi-arid sub-tropical region of southern Africa, with mean annual temperatures of 17°C, with its hottest mean temperatures reaching 21°C in January and the coldest temperatures averaging 11.5°C during the month of June (Riddell et al., 2014). The basin further experiences rainfall that increases westward in summer (October - March) averaging approximately 740 mm annually. Contrary to precipitation, evaporation in this region decreases westwards with potential evaporation reaching annual averages of 1900 mm (Leestemaker, 2000; JIBS, 2001).

3.2 Data

This study analysed different observation and simulation datasets. The datasets can be classified into three groups, namely: Quantum Geographic Information System (QGIS) data, climate data and hydrological data.

3.2.1 QGIS data

Three types of the QGIS dataset were used in this study. They are the digital elevation model (DEM), land cover and soil type datasets. The DEM comprises important topographic attributes of a basin such as the surface area, slope, width and depth of the channel. The IRB DEM data was obtained from the Shuttle Radar Topography Mission (SRTM) downloaded from the Consortium for Spatial Information of the Consultative Group of International Agricultural Research (CGIAR–CSI; website; Jarvis et al., 2008) at 90 x 90 metre resolution. The DEM was used in the hydrological model to characterize the topography of the IRB. Digital land use and land cover maps were obtained from the USGS Global Land Cover Characterization (GLCC; United States Geological Survey National Center for Earth Resources) database website. The land use information maps for the different basins were all acquired from the United States Geological Survey Global Land Cover Characterization (USGS-GLCC) database website at a 400 m resolution and varying land cover classifications. The soil information maps which comprised key soil properties for each river basin were obtained from the FAO-UNESCO Digital Soil Map of the World website covering Africa at a scale of 1:5 000 000.

3.2.2 Climate data

The study employed two types of climate datasets, namely: the Global Meteorological Forcing Dataset (GMFD) and CO-ordinated Regional Downscaling Experiment (CORDEX) dataset.

3.2.2.1 GMFD datasets

The GMFD is a combination of global observational dataset and National Centers for Environmental Prediction–National Center for Atmospheric Research (NCEP/NCAR) reanalysis dataset. The dataset was developed for global land surface modelling at 1.0° high spatial resolution and a 3-hourly time step between 1948 and 2000 (Sheffield et al., 2006). The dataset

was established by the Terrestrial Hydrology Research Group at the Princeton University (Sheffield et al., 2006) and is widely used as an observational dataset (*i.e.* Diaconescu et al., 2018). GMFD observation climate data for six climate variables (minimum and maximum temperature, precipitation, solar radiation, relative humidity, and wind speed) was used to force hydrological simulations during calibration and validation periods. It was also used for the bias correction and evaluation of the climate simulation dataset (CORDEX).

3.2.2.2 *CORDEX datasets*

The CO-ordinated Regional Downscaling Experiment (CORDEX) is a global database developed by the World Climate Research Program (WCRP) to produce regional climate simulations worldwide (Giorgi al., 2009). The CORDEX model simulation datasets used in this study comprise a 50 km resolution (Nikulin et al., 2018) from seven RCMs (*i.e.* RCA_CCCma, RCA_CNRM, RCA_MIROC, RCA_MPI, RCA_NCC, RCA_IPSL and RCA_CSIRO) that were dynamically downscaled from GCM simulations. This study utilized CORDEX dataset to reproduce past climate (*i.e.* 1971 to 2005) and project future climate (*i.e.* 2005 to 2098), which were used in forcing the hydrological simulations over the IRB for the past and future climates, respectively. Although CORDEX archives future climate simulations under various future climate scenarios, only the future climate simulations for the Representative Concentration Pathway (RCP) 8.5 were utilized for the present study due to its relevance in light of current emissions trajectory as well as computational constraint. The RCP8.5 represents current high greenhouse gas emission trajectories that have led to highest concentration levels (~1370 ppm CO_2) by the end of the 21st century (Moss et al., 2010). The study selected these datasets due to their accessibility and large usage by researchers around the world and in southern Africa. The datasets also have all the climate variables needed as input for the SWAT+ simulation.

3.2.3 Hydrological data

Daily streamflow data were collected from the Department of Water Affairs (DWA) for calibration and validation of the hydrological model results. The datasets are limited to South Africa due to limited access to station datasets over Mozambique and Swaziland. Even so, large

inconsistencies, discrepancies and gaps in the datasets influenced the number of stations chosen for a detailed analysis in this study. Further investigation done by Okello et al. (2015) revealed that many of these datasets contain major data gaps and missing data are a consequence of hydrological disturbances and alterations associated with infrastructure developments such as the building of dams *etc.* Hence, only four stations (*i.e.,* X1H003, X2H016, X2H036 and X3H015) were chosen for calibration (between 1988 and 1990) and validation (between 1991 and 1995) based on the dataset availability, their proximity to the river basin mouth and being located in the three river catchment areas in South Africa (*i.e.,* Komati, Crocodile and Sabie). Detailed information about the four stations is shown in Figure 3.1.

Table 3.1: Descriptions of the four streamflow gauge stations.

Station	Location	Latitude (°S)	Longitude (°E)	Catchment area (km^2)
X1H003	Komati River	-25.348889	31.781944	8 785
X2H016	Crocodile River	-25.363889	31.955833	10 365
X2H036	Komati River	-25.436667	31.9825	21 652
X3H015	Sabie River	-25.149444	31.940556	5 715

3.3 Methods

3.3.1 Description of hydrological model (SWAT+)

The study applied a hydrological model called SWAT+ model. The SWAT+ is an improved version of the Soil and Water Assessment Tool (SWAT; Arnold, 2012). SWAT is a well-known river basin model used to simulate hydrological processes over complex basins like the IRB. It has components for weather, surface runoff, ground and return water flow, percolation, evapotranspiration, decreases in transmission, storage in ponds and reservoirs, growth and irrigation of crops, reach routing, loading of nutrient and pesticide, as well as the transfer of water (Wu et al., 2020). The structure of the model has been shown in (Figure 3). The improvement of SWAT+ over SWAT includes representation flexibilities towards the interconnection of varying landscapes such as riparian upslope wetlands and floodplains, rivers, and groundwater resources (Van Griensven et al., 2018). SWAT+ was also built to overcome present-day and future water related modelling and management challenges, and subsequently meet the needs of all the model users (Bieger et al., 2017). SWAT+ also contains independent

modules for easier model maintenance as well as corresponding developments. It further sustains the availability of data, its analysis and visualization. Reservoir functions were identified as a primary setback in SWAT. SWAT+ thus contains enhanced functions that accommodate their significance in watershed responses (Yen et al., 2019). In addition to the new reservoir functionalities, SWAT+ comprises exclusive aquifer controls for flexible boundary definition without hydrological response unit (HRU) limitations. The fundamental improvement of SWAT+ over SWAT includes the spatial representation of watershed processes and elements, model flexibility, and interconnectivity. Hence, the SWAT+ is more efficient and was used to conduct watershed simulations over the Incomati River Basin.

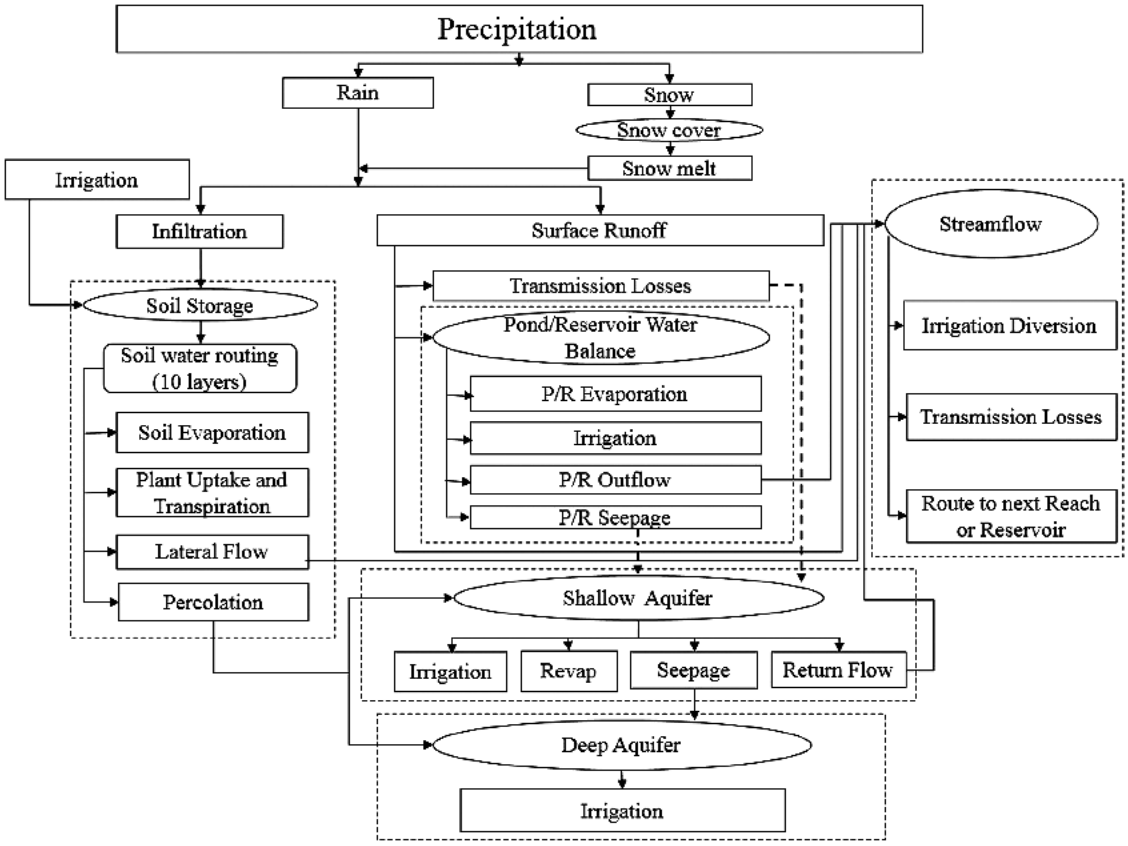

Figure 3: The structure of SWAT model (Zhang et al., 2016).

3.3.2 SWAT+ setup over the Incomati River Basin

The IRB SWAT+ model was set up using the latest version of QGIS (QGIS 3.4 Madeira long term release version) and QGIS interface for SWAT+ called, QSWAT+ version 1.2.2 (Bieger et al., 2017). The required input information (pre-processed data including the basin DEM, soil characteristics,

and land cover data) were first clipped and merged to IRB domain and then reprojected into raster format. The model setup consisted of three main steps.

Step 1: Delineate watershed

In the model delineation step, QSWAT+ applied the IRB DEM input information to automatically delineate the IRB to 23 sub-basins (by default). The default option was chosen to be consistent with the choice of default values in other model parameters. The model aggregated a burn in of an existing Incomati river network as streamflow information and reclassified it into sub-basin level by rerouting the river channels in accordance with the model database codes. During the delineation, default threshold definition and sub basins were used, and no existing inlets/outlets or reservoirs were assumed. The IRB DEM and SWAT+ classified watershed are represented in Figure 3.1 and 3.2 below.

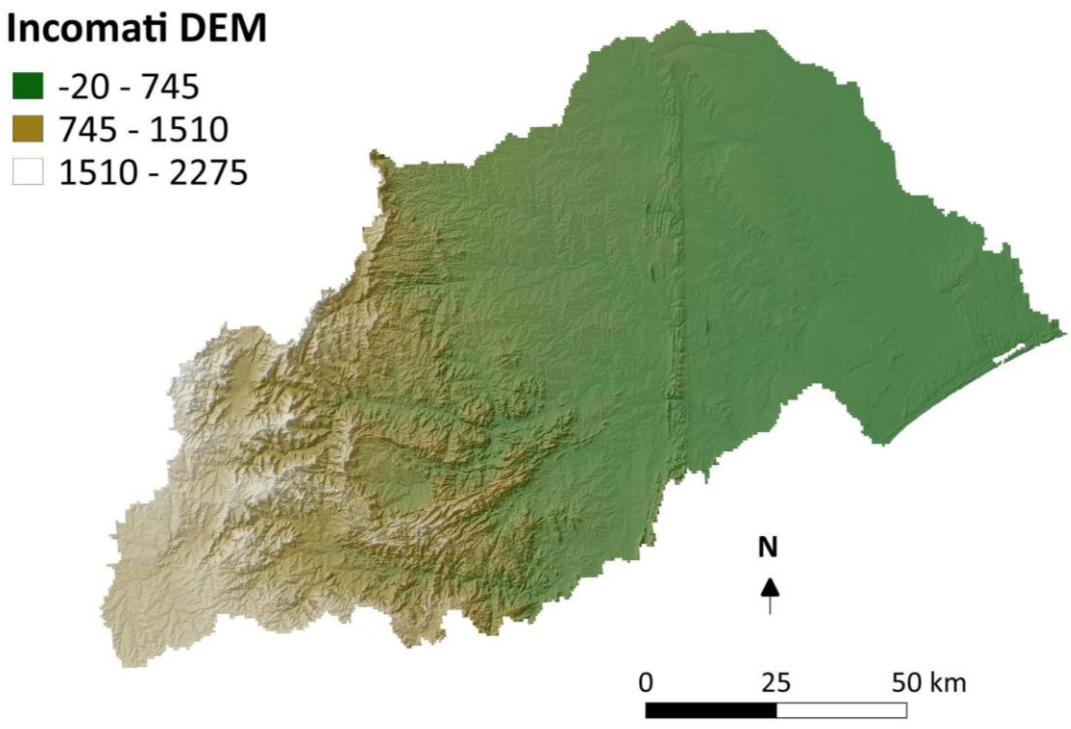

Figure 3.1: The topography of the Incomati river basin (DEM).

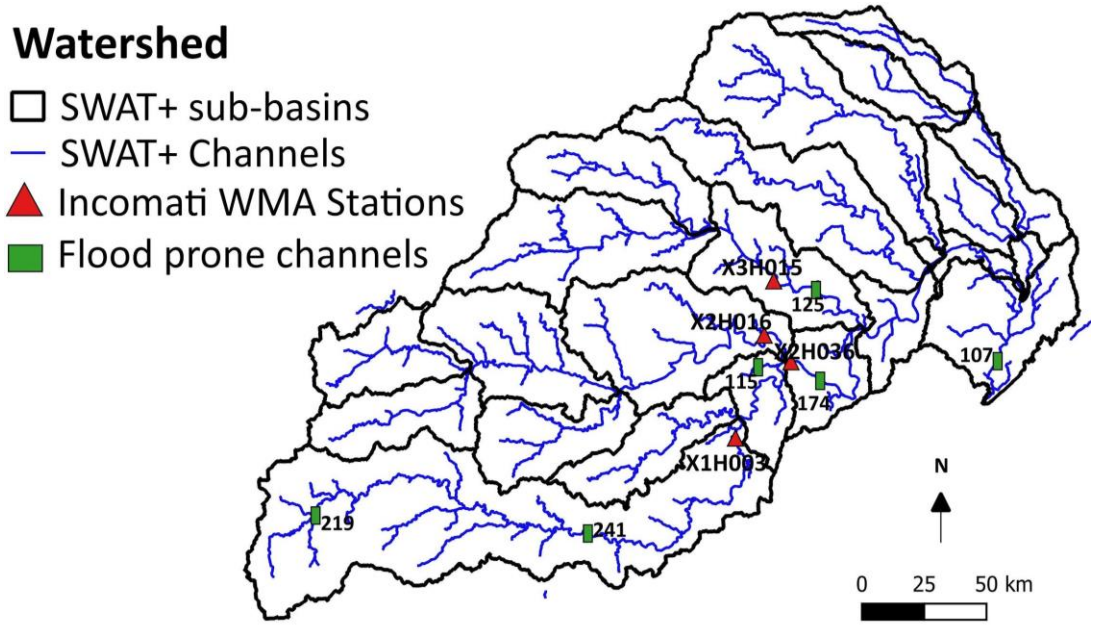

Figure 3.2: Spatial distribution of the IRB watershed, streams and sub-basins classified by QSWAT+ and point locations of the 4 streamflow gauge stations (*i.e.* X1H003, X2H016, X2H36 and X3H015) and 6 flood-prone river channels (*i.e.* channel 107, 115, 125, 174, 219 and 241) in the basin.

Step 2: Create Hydrologic Response Units (HRUs)

Hydrologic Response Units (HRUs) are units of the basins. The units comprise a mixture of distinctive soil, land use and slope properties. In this step, the land use, soil and slope input information (using the global land use, soils and user-soil tables) were reclassified in accordance with the SWAT+ database codes in order to be used as inputs in the model. In doing so, the sub basins were then split into 241 HRUS. The HRUs were filtered by land use, soil, and slope at a 10% threshold. The spatial representation of the SWAT+ reclassified land use and soil datasets, as well as thorough description of the land use and soil classes are demonstrated in Figure 3.3 and 3.4 and tables 3.2 and 3.3.

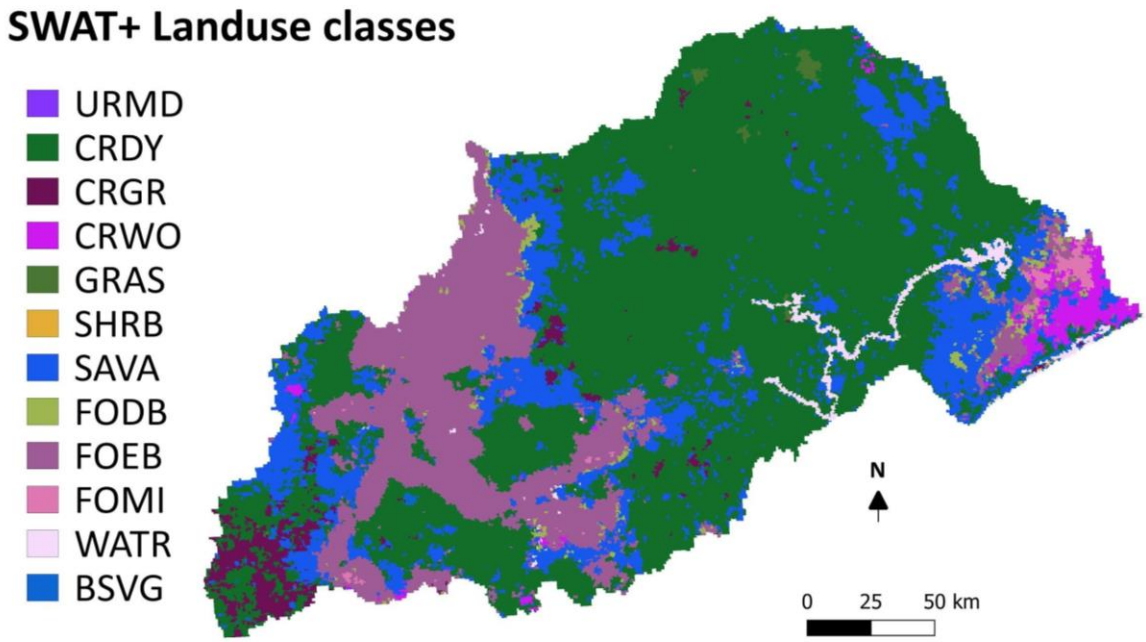

Figure 3.3: The land use classification of the Incomati river basin as seen by QSWAT+.

Table 3.2: SWAT+ land use classes.

SWAT+ land use class code	**Land use type**
URMD	URBAN MEDIUM DENSITY
CRDY	DRYLAND CROPLAND AND PASTURE
CRGR	CROPLAND/GRASSLAND MOSAIC
CRWO	CROPLAND/WOODLAND MOSAIC
GRAS	GRASSLAND
SHRB	SHRUBLAND
SAVA	SAVANNA
FODB	DECIDUOUS BROADLEAF FOREST
FOEB	EVERGREEN BROADLEAF FOREST
FOMI	MIXED FOREST
WATR	WATER
BSVG	BAREN OR SPARSLY VEGETATED

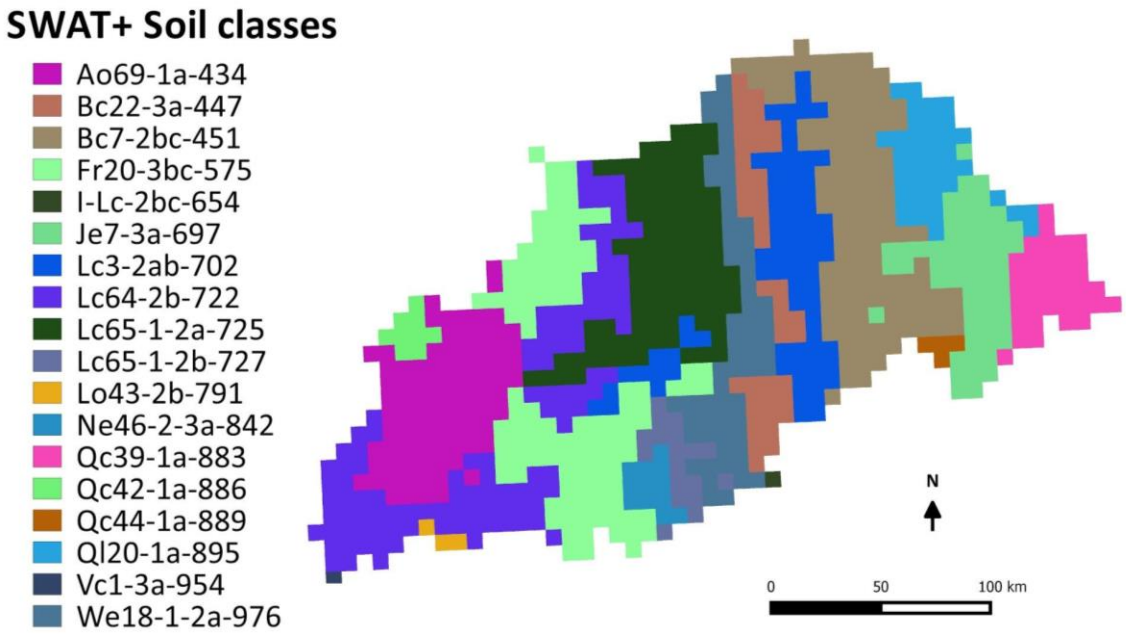

Figure 3.4: Spatial distribution of the Incomati River basin soil classification as seen by QSWAT+.

Table 3.3: Description of the QSWAT+ soil classes.

Swat+ Soil class code	Soil texture
Ao69-1a-434	SANDY_LOAM
Bc22-3a-447	CLAY
Bc7-2bc-451	SANDY_CLAY_LOAM
Fr20-3bc-575	CLAY
I-Lc-2bc-654	LOAM
Je7-3a-697	CLAY
Lc3-2ab-702	SANDY_CLAY_LOAM
Lc64-2b-722	SANDY_CLAY_LOAM
Lc65-1-2a-725	SANDY_LOAM
Lc65-1-2b-727	SANDY_LOAM
Lo43-2b-791	LOAM
Ne46-2-3a-842	CLAY_LOAM
Qc39-1a-883	SANDY_LOAM
Qc42-1a-886	SANDY_LOAM
Qc44-1a-889	SANDY_LOAM
Ql20-1a-895	SANDY_LOAM
Vc1-3a-954	CLAY
We18-1-2a-976	SANDY_LOAM

Step 3: Edit inputs and run SWAT+

This step first imports and edits the QGIS datasets from QSWAT+ in SWAT+ editor. The input datasets become regenerated according to the SWAT+ database code using the weather generator software tool. From there, long term observed daily GMFD climate datasets including precipitation, minimum and maximum temperature, solar radiation, relative humidity and wind speed were read into the model. The input data files were then saved, and the model was run using SWAT+ rev. 59.3 executable. The model output datasets were saved and analysed.

3.3.3 Model Calibration

Model calibration is an effort to enhance the parameterization of a model to a specified group of localized conditions, subsequently lowering the level of uncertainty in predictions. Available daily observed streamflow datasets between 1988 and 1990 from four gauging stations (namely, X1H003, X2H016, X2H036 and X3H015; Table 3.2 above) were used to perform efficient calibration. The study calibrated SWAT+ over the basin, using a selection of eight sensitive model parameters (shown in Table 3.6 below). The structure of the model (Figure 3) includes hydrological processes (i.e. runoff, evaporation, etc) that have been represented in the parameters selected for model sensitivity in order to enhance the model's efficiency in simulating the hydrological processes over the IRB. To achieve best calibration results over the IRB, four objective functions (*i.e.,* 1-NSE, 1-R^2, PBIAS and RMSE) were used to estimate the performance of SWAT+. Several simulation iterations were performed (1000 simulations in each run) to determine convergence for the four objective functions over the IRB. The sensitivity of each objective function to changes in the parameter values were analysed and presented in a form of scatter plots. From there, calibration of the IRB streamflow was computed across the four stations using the four objective functions. The overall performance of the different objective functions was then compared, and the best objective function was selected and applied for further analysis. Detailed descriptions of the four objective functions are given in 3.3.3.1 below. The results were displayed in a form of line graphs comparing the SWAT+ best simulation with the observation. Furthermore, a plume was incorporated in the plot to show the simulation ensemble spread.

Table 3.4: Description of parameters used over the IRB.

Parameter	Description
CN_2	Curve number for soil water condition 2
ESCO	Soil evaporation compensation factor
EPCO	Plant uptake compensation factor
K	Saturated hydraulic conductivity
AWC	Available water capacity of the soil layer
SURLAG	Surface runoff lag time
DELAY	Groundwater delay
FLOW_MIN	Minimum aquifer storage to allow return flow
REVAP_CO	Groundwater 'revap' coefficient
REVAP_MIN	Threshold depth of water in the shallow aquifer required for return flow to occur

3.3.3.1 Description of the four objective functions

The four selected objective functions for the calibration and validation processes have been chosen based on information from previous studies (e.g., Gassman et al., 2007; Moraisi et al., 2007; Niraula et al., 2012; Yen et al., 2019).

1. 1-NSE

The Nash–Sutcliffe Efficiency coefficient (NSE; Nash and Sutcliffe, 1970) is a statistical measure that is extensively used for quantifying the performance of a model (Servat and Dezetter, 1991). In general, NSE is designed to emphasize and catch peaks (e.g., flood, concentration, loads, etc) to evaluate how well a simulation fit observation. NSE measures the level at which the observed and modelled flow values agree with each other in a catchment by normalizing errors between the observed and modelled against the observation mean (Yen et al., 2016). NSE =1 indicates a perfect agreement between the two variables. Poor performance is represented by a negative or small value of NSE. Calibration thus targets an objective value of 1-NSE = 0 (Yen et al., 2016). Equation (3.1) represents the formula of NSE:

$$NSE = 1 - \frac{\sum_{i=1}^{N}\left(y_i^{obs} - y_i^{sim}\right)^2}{\sum_{i=1}^{N}\left(y_i^{obs} - y_i^{obs,mean}\right)^2} \qquad \text{Equation (3.1)}$$

where, y_i^{obs} is a record of the observed response at time step i; y_i^{sim} is simulation response at time step i; and $y_i^{obs,mean}$ is the mean of the observed record at timestep i; N represents the total number of simulation time steps.

2. 1-R^2

The coefficient of determination (R^2) is a measure of the correlation coefficient squared. It measures how well the simulated and the observed flow regression line reaches an ideal match ranging between 0 and 1. An R^2 value of 0 signifies zero correlation between the two variables while a value of 1 suggests an equal dispersion between the variables (Krause et al., 2005). A perfect fit is specified by a regression slope that is equal to 1 while the intercept is 0 (Gassman et al., 2007). In calibration, the targeted objective value is thus for 1-R^2 to be equal to zero. Equation (3.2) represents the formula for calculating R^2:

$$R^2 = \left[\frac{\sum_{i=1}^{N}(O_i - O^{mean})\,(P_i - P^{mean})}{\sqrt{\sum_{i=1}^{N}(O_i - O^{mean})^2}\sqrt{\sum_{i=1}^{N}(P_i - P^{mean})^2}}\right]^2 \qquad \text{Equation (3.2)}$$

with O_i representing the observed values at time step i; O^{mean} representing the observed mean; P_i represents the model simulation at time step i; and P^{mean} representing the simulation mean at timestep i; n represents the total number of simulation time steps.

3. PBIAS

Percent bias (PBIAS) is an objective function that calculates the mean tendency of the simulated datasets to be less or greater than the observed dataset of flow (Niraula et al., 2012). The perfect PBIAS value is 0, hence, values closest to zero represent minimal error in the model simulations. Furthermore, a negative PBIAS value indicates that a model is underestimating, while a positive value shows that a model is overestimating the observed. Equation 3 below shows the formula

for calculating PBIAS, with representing the simulated and o representing the observed dataset values.

$$PBIAS(\%) = \frac{(\sum S - \sum O)}{\sum O} * 100 \qquad \text{Equation (3.3)}$$

4. RMSE

The Root Mean Square Error (RMSE) as an objective function measures the general standard deviation of the observed and simulated watershed response such as flow. The errors in RMSE values normally follow a normal distribution and are unbiased (Chai and Dexlar, 2014). RMSE is primarily expressed as shown in Equation 3.4:

$$RMSE = \sqrt{\frac{1}{N} * \sum_{j-1}^{N} (O_j - S_j)^2} \qquad \text{Equation (3.4)}$$

where *Oj* represents the observed watershed response, and *Sj* represents the simulated response, and *N* is the total number of simulation datasets. A perfect RMSE value is equal to 0, showing that the observed and simulated assume the same value (Bekele and Nicklow, 2007).

3.3.3.2 IPEAT+ Automatic Calibration Algorithm

The study employed the Uncertainty Analysis Tool (called IPEAT+) framework to calibrate SWAT+ over the IRB. IPEAT+ is an automatic calibration tool which accommodates the conduction of model calibration and evaluates model uncertainty from multiple sources such as parameters (Yen et al., 2019; Wu et al., 2020). The SWAT+ output files (under TxtInOut) were imported into the Linux project directory and run. The algorithm was coupled with the SWAT+ manual calibration feature that allows users to change parameter values (calibration.cal file). Model calibration was done for a period of three years (1988-1990) while validation was done for five years (1991-1995). The simulation was however started in 1984 to accommodate a five-year

warm up period. The periods used for calibration and validation were selected based on the available observed data with less data missing gaps.

3.3.4 Model validation

Model validation is a process that aims to diagnose the strengths and weaknesses in the behaviour of the model, and in doing so, provides an accurate representation of the model's ability to be applied in future projections. Similar to the process of model calibration, the validation of a model requires the assessment of observed and simulated values. This process applies the same set of parameters, objective functions (1-NSE, 1-R^2, PBIAS and RMSE), and streamflow stations (X1H003, X2H016, X2H036 and X3H015) used in calibration to simulate the observed flow over the IRB. However, a different set of daily data that is selected from the four stations (starting from 1991 to 1995) was used. Furthermore, the process validates the performance of the model using four statistical metrics (NSE, R^2, PBIAS and RMSE) explained previously in equation 3.1 to 3.4. The results of validation are then compared with those of calibration.

3.3.5 Bias correction of climate datasets (CORDEX)

Bias correction is a process of identifying likely biases within the observed and modelled climate variables with the aim to correct systematic errors in climate variables by employing various transformation algorithms (Teutschbein and Seibert, 2013). Various bias correction approaches have initially been created to downscale climate variables in GCM datasets. Over time, more sophisticated bias corrections were developed to also downscale RCM datasets (*i.e.,* temperature and precipitation) and hydrological model outputs in order to correct systematic and random errors (Chen et al., 2011). Such methods generally employ weather generators or probability mapping (Teutschbein and Seibert, 2013). These methods include, quantile mapping, delta-change correction, linear transformation, histogram equalisation, local intensity scaling, precipitation threshold, distribution mapping, nonparametric methods, empirical method, power transformation, variance scaling, etc. Quantile mapping approaches have however been recommended in literature for hydroclimatic modelling (Teutschbein and Seibert, 2012; Meyer

et al., 2019). Hence, this study employed the Quantile Delta Mapping (QDM) method. QDM is a univariate bias correction algorithm that has been largely applied in climate change impact studies. This method was designed to preserve relative changes in the simulated climate variable quantiles (*e.g.* precipitation) (Cannon et al., 2015). QDM further reduces systemic biases and uncertainty in raw simulation datasets. This study employed the QDM algorithm in R software (website) for the bias correction of the CORDEX dataset using the GMFD dataset as the reference.

3.3.6 Identification of extreme events

The present study defined an extreme event based on the 95th percentile threshold over the IRB. The percentile, which was calculated by multiplying the standard deviation of different hydroclimate variable annual mean by 1.645, computed the intensity of the extreme event. The number of events above the threshold defined the frequency of the extremes. The historical occurrence of these extreme events was simulated across six hydrological variables (*i.e.* streamflow, surface runoff, soil moisture, percolation, evaporation and water yield) using the four objective functions (1-NSE, 1-R2, PBIAS, and RMSE) between 1971 and 2000. For future projections, the intensity and frequency of extreme events in the basin were computed (between 2005 and 2098) based on both the intensity and frequency of extreme precipitation and channel flow at the four GWLs and plotted in the form of spatial variation plots.

3.3.7 Future projections of climate and hydrological variables

The study projected the future impacts of climate change on mean climate variables (temperature, precipitation, potential evapotranspiration and evapotranspiration), hydrological variables over land (soil moisture, runoff, and water yield) and hydrological variables in the river channel (streamflow evaporation and river flow) over the IRB. The projections were done using CORDEX model simulation datasets from seven RCMs (*i.e.* RCA_CCCma, RCA_CNRM, RCA_MIROC, RCA_MPI, RCA_NCC, RCA_IPSL and RCA_CSIRO) from 2005 to 2098. The datasets served as input into the SWAT+ hydrological simulations over the IRB for the future climates at the four global warming levels (GWL1.5, GWL2.0, GWL2.5 and GWL3.0). Each GWL period (Table 3.4 below) was defined in accordance with Nikulin et al. (2018), such that each GWL (level 1.5,

2.0, 2.5 and 3.0°C) is a climatology (30-year period) of the global temperature averages that exceeds the pre-industrial standard period that is between 1861 and 1890 at the four global warming values (1.5°C, 2.0°C, 2.5°C and 3.0°C). The results were analysed in two ways. Firstly, to assess if there is any trend in the variability of the projected hydroclimate variables, and secondly, to assess the spatial variation of the hydroclimatic variables at the four GWLs. The results were then represented in the form of spatial distribution plots. From there, future climate change impact was projected specifically on the intensity and frequency of extreme precipitation and channel flow across six flood prone river channels (channels 107, 115, 125, 174, 219 and 241; Figure 3.2) at the four global warming levels in the IRB. The results were presented in the form of box plots so as to illustrate the spread of the projected changes (minimum, median and maximum).

Table 3.5: The seven RCMs at corresponding 30-year periods for the four global warming levels (1.5, 2, 2.5 and 3.0°C) under RCP8.5 scenario.

RCM	Period of global warming levels (GWLs)			
	1.5 ºC	2.0ºC	2.5 ºC	3.0 ºC
RCA_CCCma	01-JAN-1999:31-DEC-2028	01-JAN-2012:31-DEC-2041	01-JAN-2024:31-DEC-2053	01-JAN-2034:31-DEC-2063
RCA_CNRM	01-JAN-2015:31-DEC-2044	01-JAN-2029:31-DEC-2058	01-JAN-2041:31-DEC-2070	01-JAN-2052:31-DEC-2081
RCA_MIROC	01-JAN-2019:31-DEC-2048	01-JAN-2034:31-DEC-2063	01-JAN-2047:31-DEC-2076	01-JAN-2058:31-DEC-2087
RCA_MPI	01-JAN-2004:31-DEC-2033	01-JAN-2021:31-DEC-2050	01-JAN-2034:31-DEC-2063	01-JAN-2046:31-DEC-2075
RCA_NCC	01-JAN-2019:31-DEC-2048	01-JAN-2034:31-DEC-2063	01-JAN-2047:31-DEC-2076	01-JAN-2059:31-DEC-2088
RCA_IPSL	01-JAN-2002:31-DEC-2031	01-JAN-2016:31-DEC-2045	01-JAN-2027:31-DEC-2056	01-JAN-2036:31-DEC-2065
RCA_CSIRO	01-JAN-2018:31-DEC-2047	01-JAN-2030:31-DEC-2059	01-JAN-2040:31-DEC-2069	01-JAN-2050:31-DEC-2079

CHAPTER 4: Calibration and validation of SWAT+ simulations on the Incomati River Basin

Before applying any hydrological model for studies over a basin, model calibration and validation over the basin is vital. This chapter presents and discusses the results of calibration and validation of SWAT+ over the IRB. The calibration employs four objective functions, ten model parameters, and 1000 iterations (or simulations) in obtaining the best simulation, while the validation utilises four statistics metrics to quantify the performance of the best simulation over four stations in the basins. The information about the four objective functions (*i.e.* 1-NSE, 1-R^2, PBIAS and RMSE), ten model parameters (*i.e.* CN_2, ESCO, EPCO, AWC, K, SURLAG, DELAY, FLOW_MIN, REVAP_CO and REVAP_MIN), four statistics metrics (NSE, R^2, PBIAS and RMSE), and the four stations (*i.e.* X1H003, X2H016, X2H036 and X3H015) are provided in the Chapter 3. The present chapter shows how the choice of an objective function influences the convergence of the model iteration, the model's sensitivity to the parameters, and the best simulation performance in reproducing the observed streamflow over the four stations.

4.1 Convergence of model iterations

Figure 4.1 shows that the speed at which SWAT+ simulations converge over the Incomati River Basin (IRB) in the calibration varies among the four objective functions (*i.e.* 1-NSE, 1-R^2, PBIAS and RMSE). The calibration converges fastest with 1-NSE and RMSE (*i.e.* less than 300 iterations) and slowest in 1-R^2 and PBIAS (*i.e.* more than 600 iterations) (Figure 4.1). The simulations convergence obtained with 1-NSE and RMSE in this calibration are very fast, compared to those previously reported in other studies using IPEAT+ algorithm (*e.g.* Yen et al., 2015). This may be due to two possible reasons. This may be due to the fact that the present calibration uses only ten model parameters while other studies used more than ten parameters. For example, using RMSE and 1-NSE as objective functions, Yen et al. (2015) performed calibration with 30 model parameters and obtained convergence after 500 iterations. Secondly, although the IRB comprises a larger surface area of 46,800 km^2, its convergence speed exceeds that of Yen et al. (2015), that employed a basin with a 248 km^2 surface area. Limited studies have computed the

simulation convergence speed using PBIAS and 1-R^2 as objective functions (Singh et al., 2004; Moriasi et al., 2007). Nonetheless, the results of the present study suggest that using 1-NSE or RMSE for SWAT+ calibration over IRB is more computationally efficient than using PBIAS and 1-R^2.

However, while achieving fast iteration convergence is important, the convergence of the iteration converging to a reasonable objective function value is also crucial. In any calibration, the targeted objective value is zero (*i.e.* NSE and R^2 will be equal to 1 for 1-NSE and 1-R^2 objective functions, respectively; Yen et al., 2016). Figure 4.1 shows that none of the objective function values attains zero after the convergence of the iterations: 1-NSE = 1.17 (*i.e.* NSE = -0.17), 1-R^2 = 0.51 (R^2 = 0.49), PBIAS = 19.8% and RMSE = 35.7 m^3/s. As presented in the methodology chapter, the reasonable values suggested in literature are > 0.5 for NSE (Moriasi et al., 2007), > 0.5 for R^2 (Van Liew et al., 2003) and ± 25% for PBIAS (Moriasi et al., 2007). A comparison of results of this study to these reasonable values indicates that the calibration with objective function 1-NSE (which converges at NSE = -0.17) performed poorly, while the calibrations with objective function 1-R^2 (which converges at 0.49) and objective function PBIAS (which converges at 19.8%) perform reasonably well. The relatively poor performance of calibration with objective function 1-NSE here may be due to the complexity and stringiness of the NSE criteria. Several calibration studies have reported worse values over different basins. For example, McCuen et al. (2006) achieved relatively high 1-NSE values between 0.63 and 0.97 (i.e. NSE = 0.37 and 0.13). Similarly, Schaefli et al. (2005) achieved a 1-NSE value of 0.85. Muleta (2012) also found unsatisfactory 1-NSE performance (1-NSE = 0.73). However, the present results indicate that while the calibration with 1-NSE converges fastest over the IRB, the convergence may be poor.

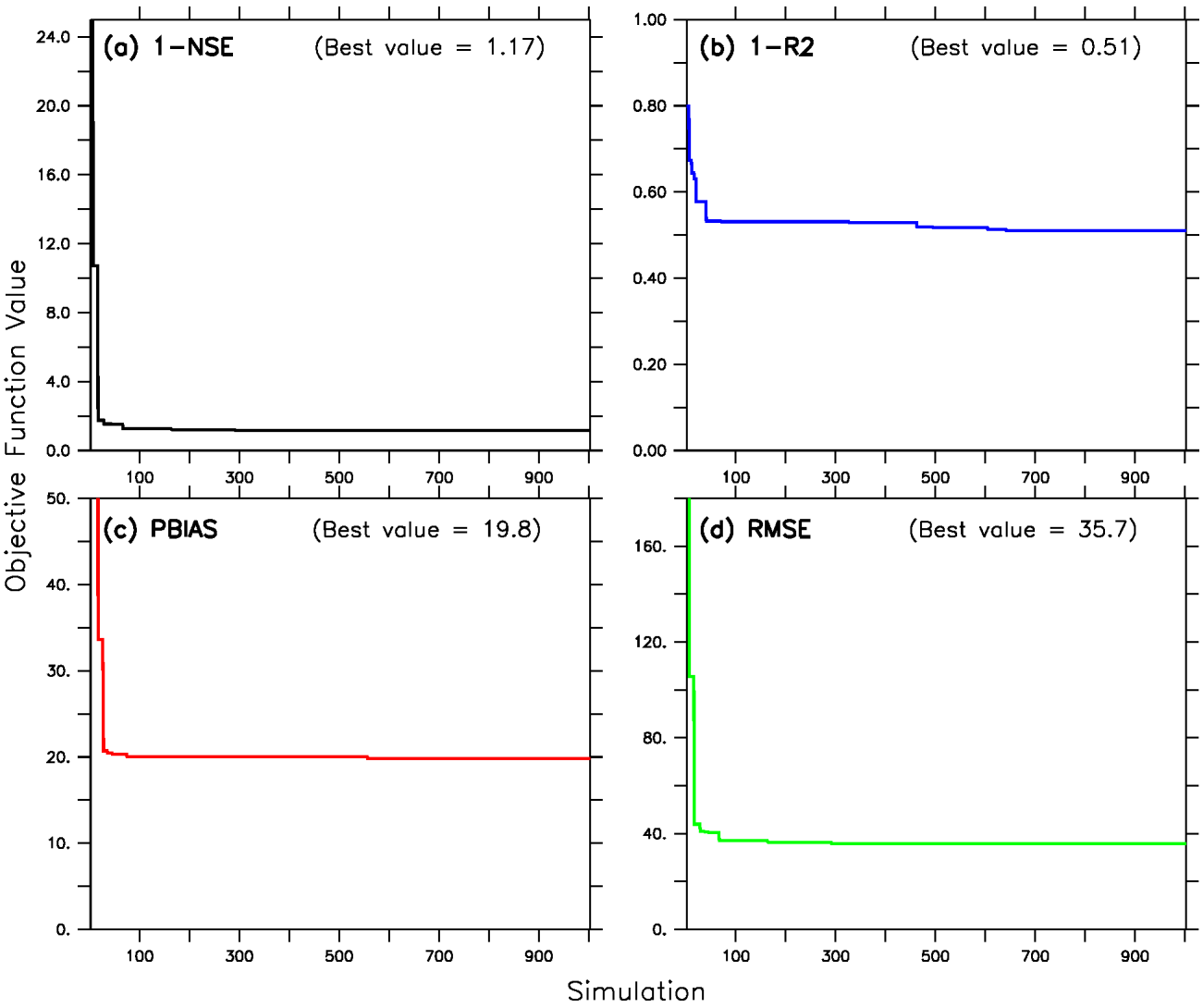

Figure 4.1: The convergence of 1000 model iterations during calibration using the four objective functions for (a) 1-NSE,(b) 1-R^2,(c) PBIAS and (d) RMSE.

4.2 Sensitivity of the SWAT+ simulations to calibration parameters

The SWAT+ simulation over the IRB has different sensitivity to the selected model parameters (*i.e.* CN2, ESCO, EPCO, AWC, K, SURLAG, DELAY, FLOW_MIN, REVAP_CO and REVAP_MIN; Figure 4.2). Figure 4.2 shows that, for all the objective functions, the simulation is most sensitive to CN_2. However, the shape of the sensitivity (*i.e.* relationship between CN_2 and the objective functions) varies. With 1-NSE, PBIAS and RMSE, a change in CN_2 between -30% and -10% produces relatively small changes in the objective functions (1-NSE < 10 and RMSE < 10 m^3/s), but with a change in CN_2 between 0% and 30% the value of the objective functions rises exponentially (1-NSE > 40,

PBIAS > 50 and RMSE > 200 m^3/s, respectively). However, the exponential increase in RMSE appears to be more gradual than that of PBIAS and 1-NSE. Although PBIAS also features an exponential increase with changes in CN_2 (0 - 10%), the pattern and the relationship become more linear from a 10% change. A different relationship pattern is however observed between 1-R^2 and CN_2 (Figure 4.2b). In this case, the sensitivity of the objective function to CN_2 exhibits a positive linear relationship. However, all calibrations with the objective functions agree that the default values of CN_2 in the current version of SWAT+ are too high over the IRB. While the calibration with PBIAS suggests that a decrease of 14.1% is needed for the iteration to converge, 1-NSE, 1-R^2 and RMSE indicated a decrease of at least 30% is needed to attain convergence. Given that changes in CN_2 have implications for land use characteristics over the basin, a decrease of -30% is usually considered to be high (Eckhardt and Arnold, 2001). Hence, there is a need for further development of SWAT+ over the basins, focusing on improving basin land use characteristics in the model. Similar to this study, Yen et al. (2019) used 1-NSE in calibrating SWAT+ over a basin and obtained a reduction of 30% CN_2 in order to achieve the best simulation. However, the authors cautioned that 30% reduction may be considered as an over-calibration of the model.

Although the sensitivity of the model simulation to other model parameters is very weak (*i.e.* in comparison to that of CN_2), the calibrations suggest changes in the parameter values in obtaining best simulations over the basin. Similar to CN_2, however, the simulation is also sensitive to changes in the value of ESCO when using PBIAS and RMSE. The similarities occur both in the shape of the sensitivity (*i.e.* exponential relationship) and the suggested value change for iteration convergence (*i.e.* approximately -30% change). For some parameters, the direction of change is similar regardless of the objective function used, while for some parameters, the direction of change differs among the objective functions. For example, to obtain the best simulations, all the calibrations with the different objective functions agree on an increase in AWC, K, SURLAG, and DELAY, and a decrease in ESCO, REVAP_CO, and REVAP_MIN. However, while 1-R^2 and PBIAS suggest an increase in EPCO to obtain the best simulation, 1-NSE and RMSE suggest a decrease. A summary of the suggested parameter changes (in percentage values) by four objective functions 1-NSE, 1-R^2 PBIAS and RMSE) to different calibration parameters is presented in Table 4. Nevertheless, given that the sensitivity of a simulation is dominated by CN_2,

which is a key parameter to hydrological processes, a better adjustment of CN_2 in the model may potentially enhance the model's efficiency in simulating the hydrological processes over the IRB.

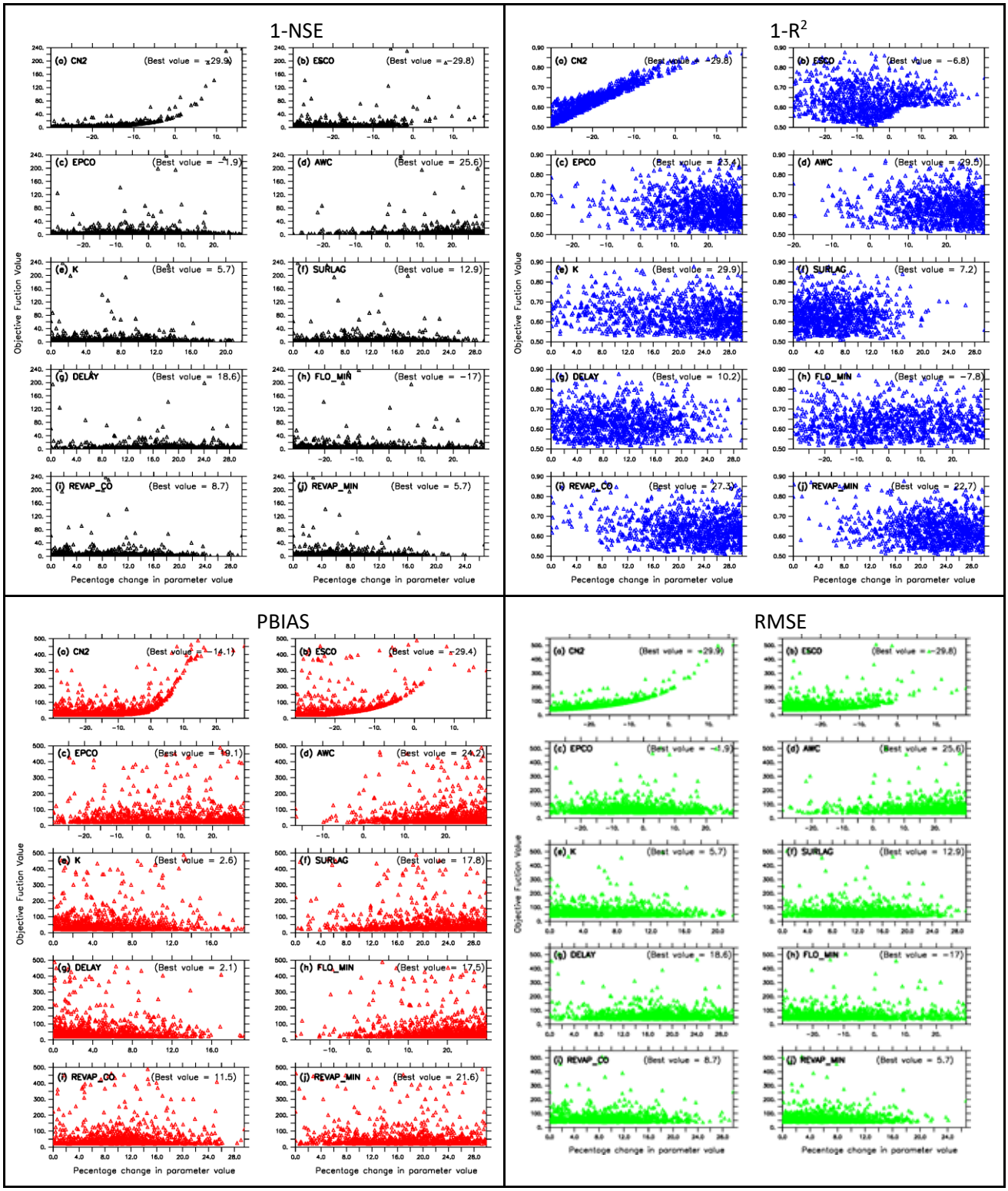

Figure 4.2: Scatter plots of the sensitivity of four objective functions (1-NSE, 1-R^2 PBIAS and RMSE) to different calibration parameters.

Table 4: Table of the suggested changes in the SWAT+ parameters (in % of the default values) as obtained from the model calibration over the Incomati River basin using four objective functions (1-NSE, 1-R^2 PBIAS and RMSE)

	Suggested changes (% of the default values):			
Parameter	1-NSE	1-R^2	PBIAS	RMSE
CN_2	-29.9	-29.8	-14.2	-29.9
ESCO	-29-8	-6.8	-29.4	-29.8
EPCO	-1.9	23.4	19.1	-1.9
K	25.6	29.5	24.2	25.6
AWC	5.7	29.9	2.6	5.7
SURLAG	12.9	7.2	17.8	12.9
DELAY	18.6	10.2	2.1	18.6
FLOW_MIN	-17	-7.8	17.5	17
REVAP_CO	8.7	27.3	11.5	8.7
REVAP_MIN	5.7	22.7	21.6	5.7

4.3 Evaluation of best simulations over selected stations

Figure 4.3 compares the performance of the best SWAT simulations obtained using the four calibration functions (1-NSE, 1-R2, PBIAS, and RMSE) over the four selected stations (X1H003, X2H016, X2HO36 and X3H015) during the calibration period (1988-1990) and evaluation period (1991-1995). The performance of the simulations are quantified with four evaluation metrics (NSE, R^2, PBIAS, and RMSE). The figure shows that the performance of the best simulations vary with the objective functions, the station and the evaluation metrics, and differ during the calibration and evaluation periods. With NSE as the performance evaluation metric, SWAT+ performs poorly during calibration and validation when using the 1-NSE calibration function as it produced extremely low NSE values (*i.e.* NSE<0). For instance, the model performed worse during the validation period (*i.e.* station X1H003 NSE= -0.08, X2H036 NSE= -0.1 and X3H015 NSE= -0.3) than during calibration (*i.e.* station X1H003 NSE= -0.1, X2H036 NSE= -0.05 and X3H015 NSE= -0.07) except for station X2H016 (*i.e.* NSE= -0.07 3 during both calibration and validation). Even though the model slightly underestimates daily streamflow peaks during calibration (especially over stations X3H015 (Figure 4.3d), higher levels of overestimation occur during validation (*i.e.* especially over stations X2H036 (Figure 4.3b). Nonetheless, this performance is still better than those reported in some studies over other basins. For example, Abbaspour et al. (2015) found

an NSE value of 0.03 and 0.26 over some stations during calibration. Thavhana et al. (2018) also experienced a deterioration of the NSE value during validation (*i.e.* NSE = 0.66 during calibration to 0.48 during validation). In contrast, better performance is shown by the positive R^2 values ($0.008 \leq R^2 \geq 0.3$ during calibration and $0.03 \leq R^2 \geq 0.3$ during validation). Even so, similar to NSE, the model performed poorly since the values are below the suggested reasonable value of 0.5 (Van Liew et al., 2003). The PBIAS values indicate better model performance during validation with values within reasonable range (*i.e*. values below 20% along stations X1H003, X2H016, and X2H036) except for station X3H015 where the model drastically underestimates the observed (*i.e.* approximately -77% during calibration and validation). Similarly, RMSE values show improvement during validation over stations X1H003, X2H016, and X2H036 and is worse over station X2H036 (*i.e.* values>30 m^3/s during both calibration and validation).

The performance of the model in calibrating and validating daily streamflow over the IRB, using RMSE as an objective function, is similar to when using 1-NSE (*i.e.* Figure 4.3a and d). The values of three performance metrics (*i.e.* NSE, RMSE and R^2) during both calibration and validation are identical to that of 1-NSE objective functions at all the four stations. On the contrary, employing the objective functions 1-R^2 and PBIAS exhibited the worst model performance as they significantly over-exaggerated the daily streamflow during both calibration and validation. Although the NSE and R^2 performance metrics of these objective functions have better performance than 1-R^2 as an objective function, the values of their PBIAS and RMSE are worse over the stations. Unfortunately, no studies have calibrated and validated observed streamflow using PBIAS, 1-R^2 or RMSE as objective functions. However, the results of this study thus find calibration and validation to be best performed by 1-NSE and RMSE. Nonetheless, the model still performed poorly when using these objective functions (1-NSE and RMSE) because their performance metric values are extremely below the suggested reasonable values.

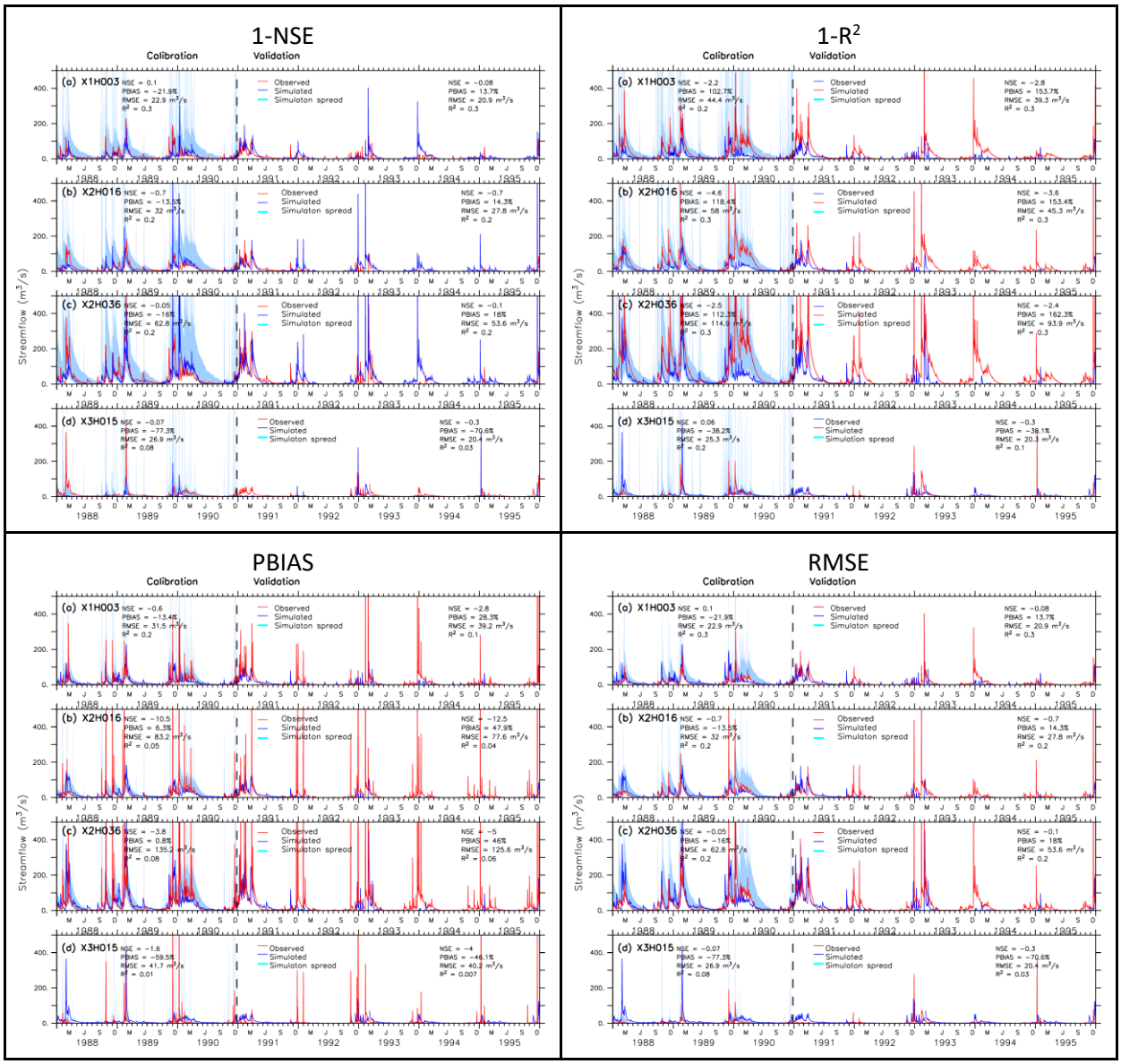

Figure 4.3: Comparison of the best simulated daily streamflow against the observed streamflow during calibration period (1988-1990) and validation period (1991-1995) with the objective function NSE.

4.4 Spatial distribution of hydro-climatological variables over Incomati River Basin.

4.4.1 GMFD Climate variables

Figure 4.4 presents the spatial distribution of temperature (TMP), precipitation (PRE), potential evapotranspiration (PET) and climate water balance (CWB: PRE minus PET) over the Incomati River Basin between the year 1971 and 2000. The temperature field shows an increase in temperature from about 22^{o}C over the south-west mountain range to about 30^{o}C in the north-east plain lands (Fig. 4.4a). The lowest temperature over the mountain range can be attributed to the general decrease in temperature as the altitude increases. However, the precipitation distribution has an opposite pattern to the temperature distribution. It features the highest precipitation (> 70 mm month^{-1}) over the mountain range and the lowest over north-east plain lands. The highest precipitation over the mountain range can be attributed to orographic lifting of the warm Atlantic and Indian Oceans moisture by the Drakensberg and Lebombo mountains. The local peak in precipitation (about 65 to 75mm) along the lower Incomati (25-25.6^{o}S and 32.5-33^{o}E) may be due to the coastal extreme precipitation systems such as tropical cyclones (Vaz, 2000; Van Ogtrop et al., 2005; Davis et al., 2017). The spatial distribution PET over the basin is consistent with that of the mean temperature (*i.e.* low temperature and PET occur along the high escarpment and vice versa; Figure 4.5a and c; 24.5-26.2^{o}S and 30.3-31.6^{o}E). This is because the atmospheric demand for moisture (PET) increases with temperature. The spatial distribution of climate water balance (CWB = PRE - PET) shows that the annual PET is higher than the annual PET over the basin. This is typical of a basin in the semi-arid region. The highest deficit (*i.e.* negative value about -80 mm month^{-1}) in CWB occurs over the northern part of the basin where the TMP and PET features the maximum values (> 30^{o}C and > 135 mm month^{-1}, respectively) and the PRE shows the lowest values (< 135 mm month^{-1}).

All these results (Figure 4.4) are consistent with those in several studies. For example, Okello et al. (2015) reported the basin's high escarpment (24.5-26.2^{o} S and 30.3-31.6^{o}E) to experience the highest rainfall amounts (800 to 1600 mm), lowest temperatures (10 to 16°C) and potential evaporation (1600 to 2000 mm), and the lower Incomati to experience lower rainfall amounts (400 to 800 mm) coupled with high mean temperatures (20-26°C) and potential evaporation rates (2200 to 2400 mm) annually. Similarly, Van Eekelen al. (2015) identified the high escarpment region to also experience maximum rainfall (*i.e.,* 1250mm/a) while the north eastern

tip experiences the lowest amounts (<575 mm/a). Tauacale et al. (2007) identified this region (25-25.6S and 32.5-33E) to experience annual mean rainfall ranging between 651 and 760 mm. In terms of the basin's water balance, several studies (Sengo et al., 2005; Okello, 2019) have reported the difference in precipitation and potential evapotranspiration, and some of the studies even highlighted the high demand of irrigation water along the eastern part of the basin owing to the large deficit in CWB.

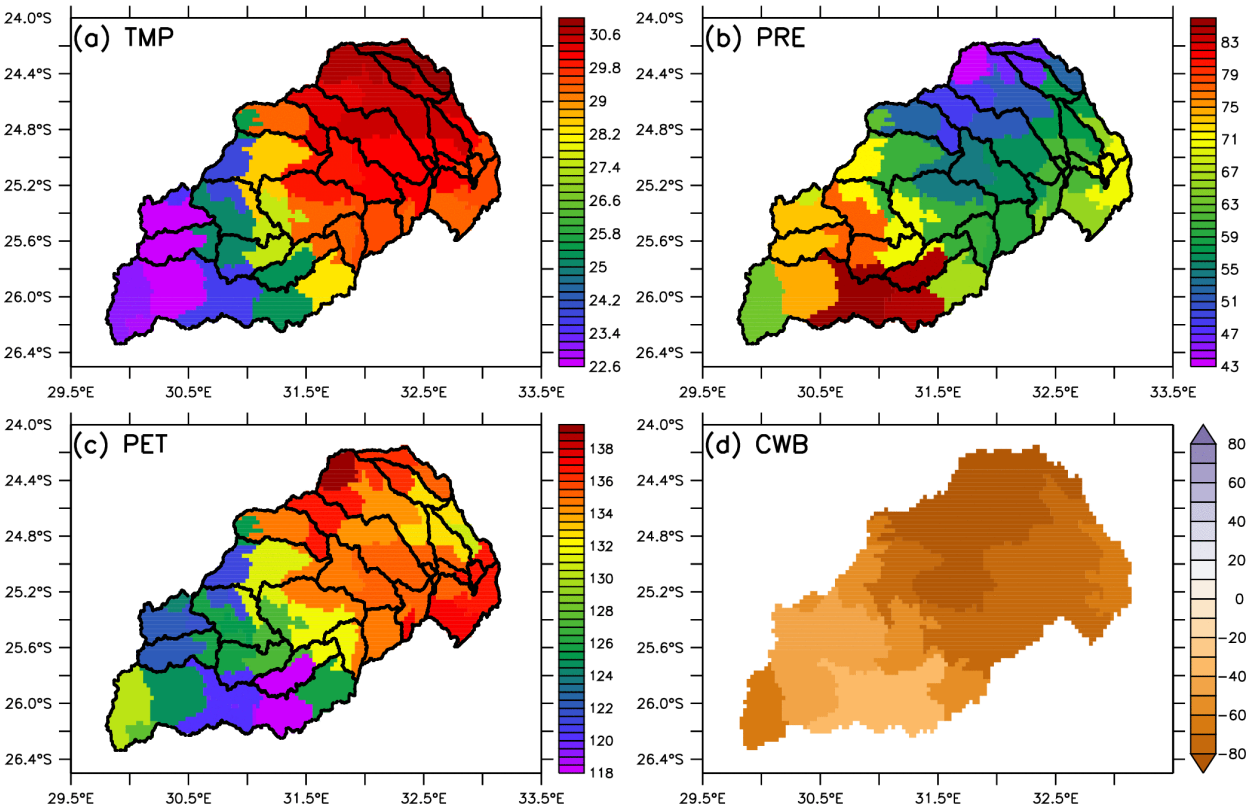

Figure 4.4: Spatial distribution of climate variables: (a) temperature (TMP), (b) precipitation (PRE), (c) potential evapotranspiration (PET) and (d) climate water balance (CWB: PRE-PET) over the Incomati River Basin (1971-2000) as depicted by GMFD dataset.

4.4.2 SWAT simulated hydrological variables

Figure 4.5 presents the spatial distribution of seven hydrological variables (*i.e.* evapotranspiration, soil water, percolation, water yield, runoff, streamflow and channel evapotranspiration) over the IRB in 1971 and 2000 as simulated by SWAT+ using the four objective functions (1-NSE, 1-R2, PBIAS, and RMSE). These variables were selected based on their significant role in influencing flooding in river basins. Variations are observed across the different

objective functions and in relation with the previously observed spatial distribution of temperature and precipitation (*i.e.* Figure 4.4) of the basin. The simulated distributions of the hydrological variables show a general consistency with the observed temperature, PRE, PET and CWB over the IRB (Figure 4.5 above). For example, the mean evaporation features the maximum values over the south-west of the basin (*i.e.* over the high escapement), where the maximum PRE occurs. The discrepancy between spatial distribution of evaporation and PET highlights the fact that annual PRE has a higher influence evaporation than PET does, because PRE determines the amount of water available for evaporation. The evaporation pattern is consistent across the four objective functions, except that model calibration with $1\text{-}R^2$ features the lowest evaporation, especially over the escapement. In agreement with the pattern of precipitation, the soil moisture and water yield distributions also feature the maximum values over the escapement. However, the simulation that used $1\text{-}R^2$ (as the calibration objective function) features higher values of soil moisture and water yield than other simulations. This is because this simulation evapotranspires less soil moisture than other simulations. For the same reason, the simulation also produces higher percolation than the other three simulations. The spatial distribution of evapotranspiration and soil moisture simulated here (using the objective functions 1-NSE, RMSE and PBIAS; Fig 4.5) are consistent with the observed evapotranspiration and soil water distribution reported Van Eekelen et al. (2015), who also found the highest values of these two variables over the high escarpments and over lower Incomati and attributed spatial distribution of precipitation over the basin.

In contrast to the soil moisture pattern, the simulated spatial distribution of the runoff is similar for objective functions 1-NSE and RMSE, and similar for objective functions $1\text{-}R^2$ and PBIAS. while the first pair (*i.e*. 1-NSE and RMSE) features a runoff of more 4 $m^3\ s^{-1}$ less one-third of the basin, the other pair ($1\text{-}R^2$ and PBIAS) features it over more than two-third of the basin. As a result, although all the simulation features the highest streamflow values over the eastern path of the domain, the simulated streamflow in the channels is generally higher for the first pair (*i.e.* 1-NSE and RMSE) than for the second pair ($1\text{-}R^2$ and PBIAS). However, the simulation with objective function $1\text{-}R^2$ features the higher streamflow (up to 4,096 $m^3\ s^{-1}$) than other objective functions (about 2,404 $m^3\ s^{-1}$ for 1-NSE and RMSE; about 2905 $m^3\ s^{-1}$ for PBIAS). This is because the evapotranspiration of soil moisture is less in the simulations than the other. However, despite

the discrepancy among the simulation on the magnitude of evapotranspiration, soil moisture and streamflow, all the simulations agree on the spatial distribution and magnitude of channel evaporation over the basin (Fig 4.5). All the simulations feature the high evaporation rates over the channels with high streamflow and large water bodies (*e.g.* Curumana and Moamba dams).

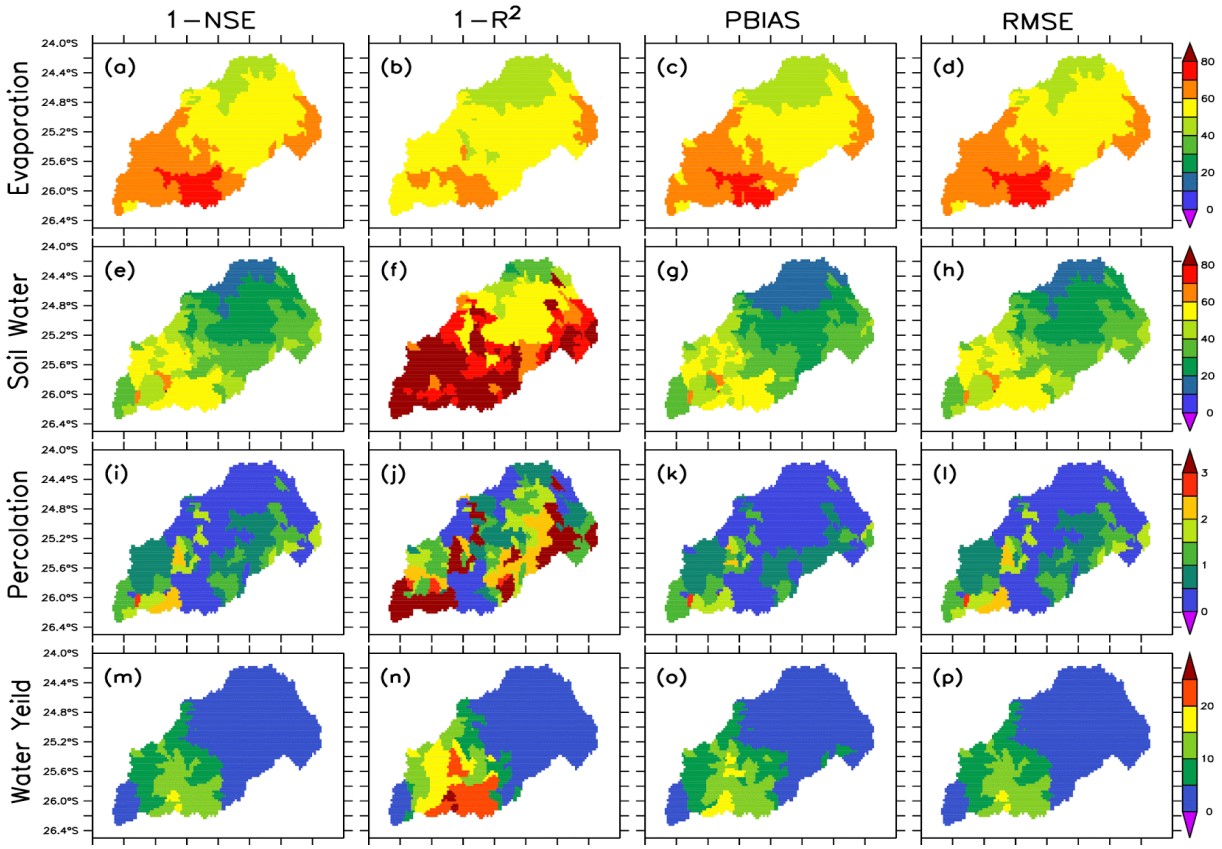

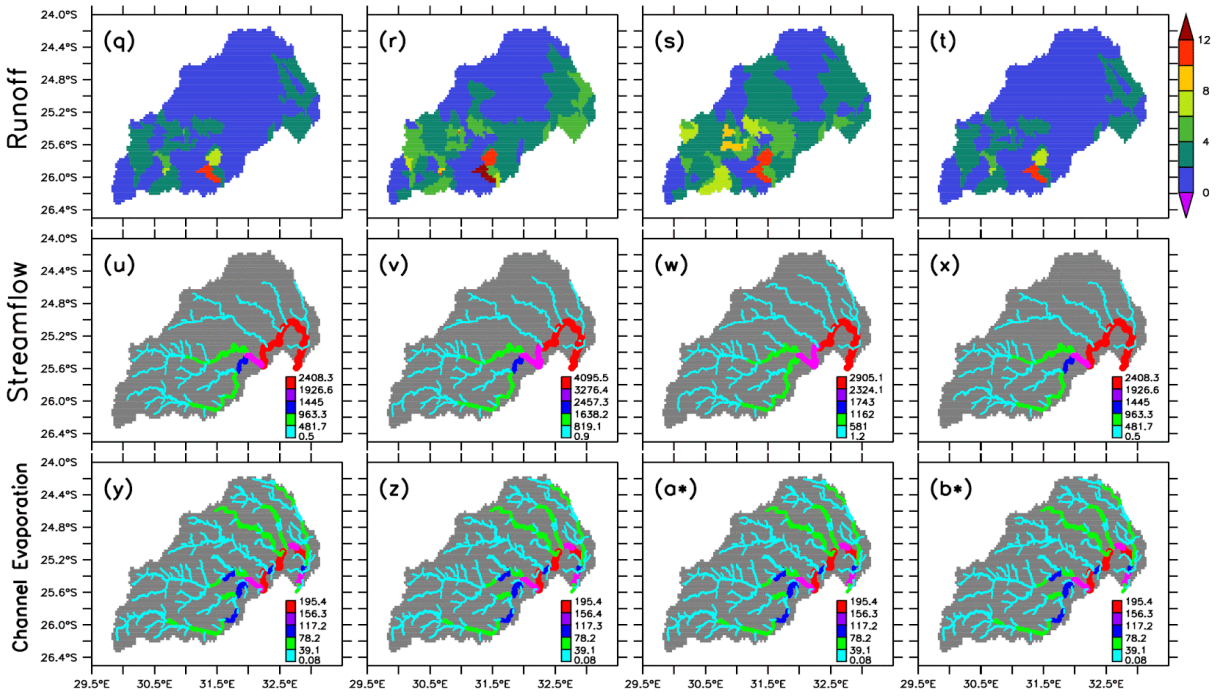

Figure 4.5: The spatial distribution of hydrological variables over the Incomati River Basin (1971-2000) as simulated by SWAT+ using four calibration objective functions (1-NSE, 1-R^2, PBIAS, and RMSE).

CHAPTER 5: Influence of bias correction of climate variables on hydrological simulations

Regional climate model (RCM) simulation outputs usually comprise large systemic biases in relation to observational datasets. These biases need to be corrected before using the climate model outputs as input into data hydrological models. This chapter reports how the bias correction of the RCM climate datasets influence the simulated hydrological variables in the Incomati River Basin. To study the influence, one of the most common bias correction methods (called the quantile delta mapping, QDM) was applied on the CORDEX climate simulation dataset. Then original and bias-corrected CORDEX climate datasets were separately used as input SWAT+ hydrological simulation, and the results compared. The QDM method and CORDEX dataset have already been discussed in Chapter 3. The chapter reports the capability of the QDM to reduce simulation biases in annual cycle and spatial distribution of seven climate variables (*i.e.*, minimum, maximum, and mean temperatures; precipitation; potential evapotranspiration; evapotranspiration and channel evapotranspiration) and five hydrological variables (soil moisture, surface runoff, channel flow, percolation and water yield) is discussed. The GMFD climate datasets and GMFD-forced SWAT+ simulation described in the previous chapter (Chapter 4) are used as reference.

5.1 Temporal distribution of hydroclimate variables

The annual variation of CORDEX simulated hydroclimate variables before and after the bias correction are presented in Figure 5.1 and Figure 5.2, respectively. Prior to bias correction, the models generally underestimate the annual cycle of Tmax, Tmin, Tmean, PET and ET (Figure 5.1a, b, c, f, and h) while overestimating PRE and ET (Figure 5.1e and g). In addition, strong agreement exists among the models with inconsistencies occurring predominantly in the captured magnitude of precipitation cycle exist (*i.e.* Figure 5.1e). The abovementioned climate variables play a fundamental role in hydrological modelling (*i.e.* precipitation is a main source of surface hydrology). Hence, their uncertainty will impact hydrological model outputs (Li et al., 2013). Consequently, the incorporation of these climate variables in SWAT+ generally amplified

the uncertainty in the simulated hydrological variables (soil water, runoff, channel flow, percolation, and water yield; Figure 5.1d, i, j, k and l) and variability amongst the simulations. For example, the models significantly overestimate the magnitude of the hydrological conditions experienced in the annual cycles (*i.e.* the models captured >1.4mm in runoff to occur in January instead of approximately 0.1 mm GMFD). Hence the importance of reducing uncertainties in CORDEX climate variable outputs before incorporating them in hydrological simulations.

The benefits of bias correcting climate variables on the simulated hydrological modelling are shown in Figure 5.2 below. The bias correction algorithm QDM significantly reduced the biases and uncertainties that were previously simulated in the climate variables (Figure 5.1a, b, c, e, g, and h above). For instance, the models now strongly capture the annual cycle of the climate variables over the IRB (*i.e.* the models no longer over- or under-estimate the climate variables cycles). These results are consistent with some that have confirmed the effectiveness of QDM in removing systemic model biases and preserving signal changes in climate variables like temperature and precipitation (*i.e.* Fauzi et al., 2020; Heo et al., 2019; Tong et al., 2020). However, the models performed well in simulating temperature and precipitation with QDM in comparison with Meyer et al. (2019) who experienced overestimations and Heo et al. (2020) who found significant model simulation variations. According to Cannon (2018), a correction procedure that shows evidence of preserved hydroclimatic variable interdependency may be deemed suitable for further application in impact analyses. Hence the willingness to apply QDM bias corrected outputs in simulating hydrological variables over the IRB. As a consequence of using bias corrected climate variables to simulate these hydrological variables, systemic biases and ensemble spread variabilities were removed, preserving the variable trends, and showing agreement amongst 5 hydrological variables (*i.e.,* Figure 5.1d, i, j, k and l). Nonetheless, the models still failed to capture the trend and patterns of the hydrological variables during the summer months (*i.e.* variabilities exist between January and March across the variables). Limited studies have used QDM corrected climate variables to model hydrological variables. Nonetheless, this study has indicated the importance of bias correcting climate variables before using them in hydrological simulations.

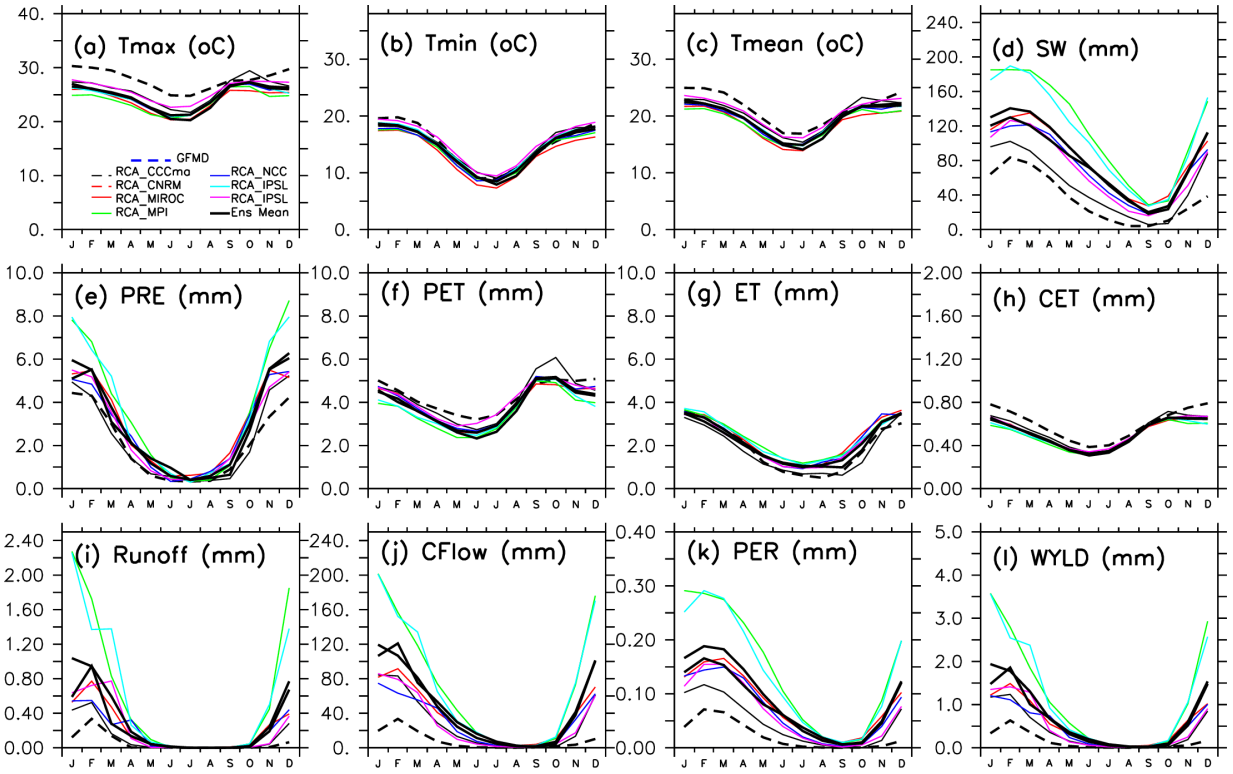

Figure 5.1: Annual cycle of hydroclimate variables as depicted by GFMD and original CORDEX datasets in the period 1971 - 2000.

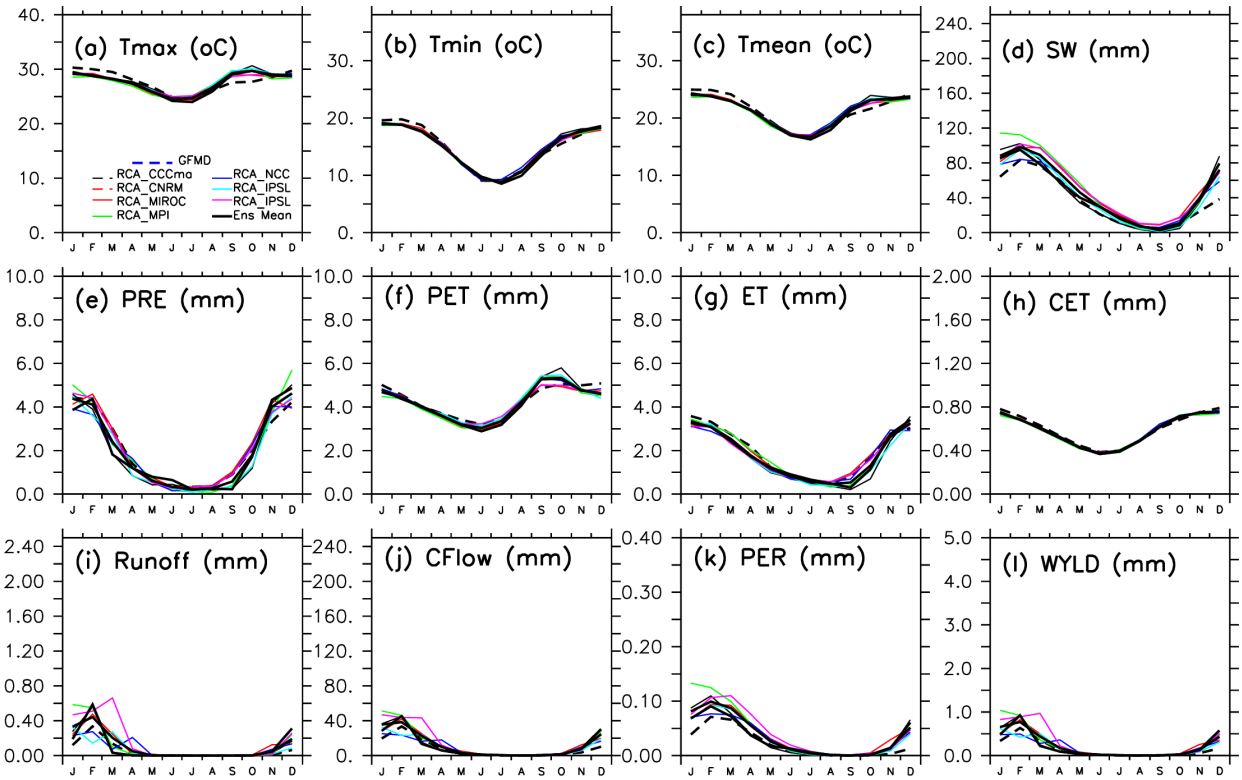

Figure 5.2: Same as Figure 5.1, but for the bias corrected CORDEX datasets.

5.2 Spatial distribution of hydroclimate variables

5.2.1 Climate variables

The spatial distribution of CORDEX simulated climate variables (*i.e.* mean temperature (Tmean), precipitation (PRE), potential evapotranspiration (PET) and evapotranspiration (ET)) before and after bias correction, as well as the biases, are presented in Figure 5.3. The original CORDEX (CORDEX ORG) simulations generally underestimated Tmean and PET (Figure 5.3b and q, and overestimated ET and PRE (Figure 5.3g and l) especially over the upper Incomati (*i.e.* 25.2-26.3^{o}S and 29.9-37^{o}E). For example, minimum mean temperatures (16oC ≤ Tmean ≤ 18^{o}C) experienced over the south-western part of upper Incomati (25.3-26.8^{o}E and 28.5-30.5^{o}S) were underestimated by more than 2^{o}C, especially at the tip (*i.e.* 12^{o}C ≤ Tmean ≤ 14^{o}C at 25.7-26.8^{o}E and 28.5-30.2^{o}S). On the other hand, the model overestimated the evapotranspiration (ET) by approximately 0.2 mm over the entire upper Incomati. The biases were further quantified in Figures 5.3 d, i, n and s, confirming the occurrence of large biases, especially in the simulation of Tmean and ET (*i.e.* Tmean bias ≤ -1^{o}C and ET bias -1 mm). Similar discrepancies have also been observed in other studies over southern Africa. For instance, Nikulin et al. (2012) found biases in the CORDEX ensembles which underestimated precipitation over parts of Tanzania by 3mm/day. Nonetheless, the presence of biases within modelled climate outputs increases discrepancies in further applications studies (Choudhary and Dimri, 2019; Tong et al., 2020). Hence, large efforts to enhance spatial resolutions and simulation skills for better quality of projections have been continuously implemented through various bias correction methods (Mpelasoka and Chiew, 2009; Ryu et al., 2009; Abiodun et al., 2019b).

The QDM bias corrected CORDEX simulations provide a more realistic illustration of the observed climate variables over the IRB, thus emphasizing the importance of bias correction. The models predominantly captured the spatial variation of Tmean, PRE and PET; over the basin (Figure 5.3c, h, and m). Similarly, evidence of the reduced model bias is represented in Figure 5.3e, j, o, and t, indicating the capability of QDM. For example, Figure 5.3j indicates that the biases in Tmean and PRE were significantly minimized to approximately zero. However, some discrepancies in the bias corrected model simulations still exist. For example, the model generally failed to capture some locations that experience high conditions (*i.e.* high Tmean, PET and ET especially over lower Incomati). However, the models captured the mean temperature and precipitation spatial

distributions in accordance with the topography of the basin. For example, the influence of the high Drakensberg mountain escarpments in upper Incomati is reflected by the precipitation amounts in that region (*i.e.* PRE > 2mm/day; 25.6-26.2°E and 33-33.7°S). Large complexities associated with local, global, temperate, and tropical atmospheric dynamics highly influence climate variables (Reason et al., 2006). Hence, models that are able to capture essential climate dynamics of a region are fundamentally important for further application in hydrological modelling.

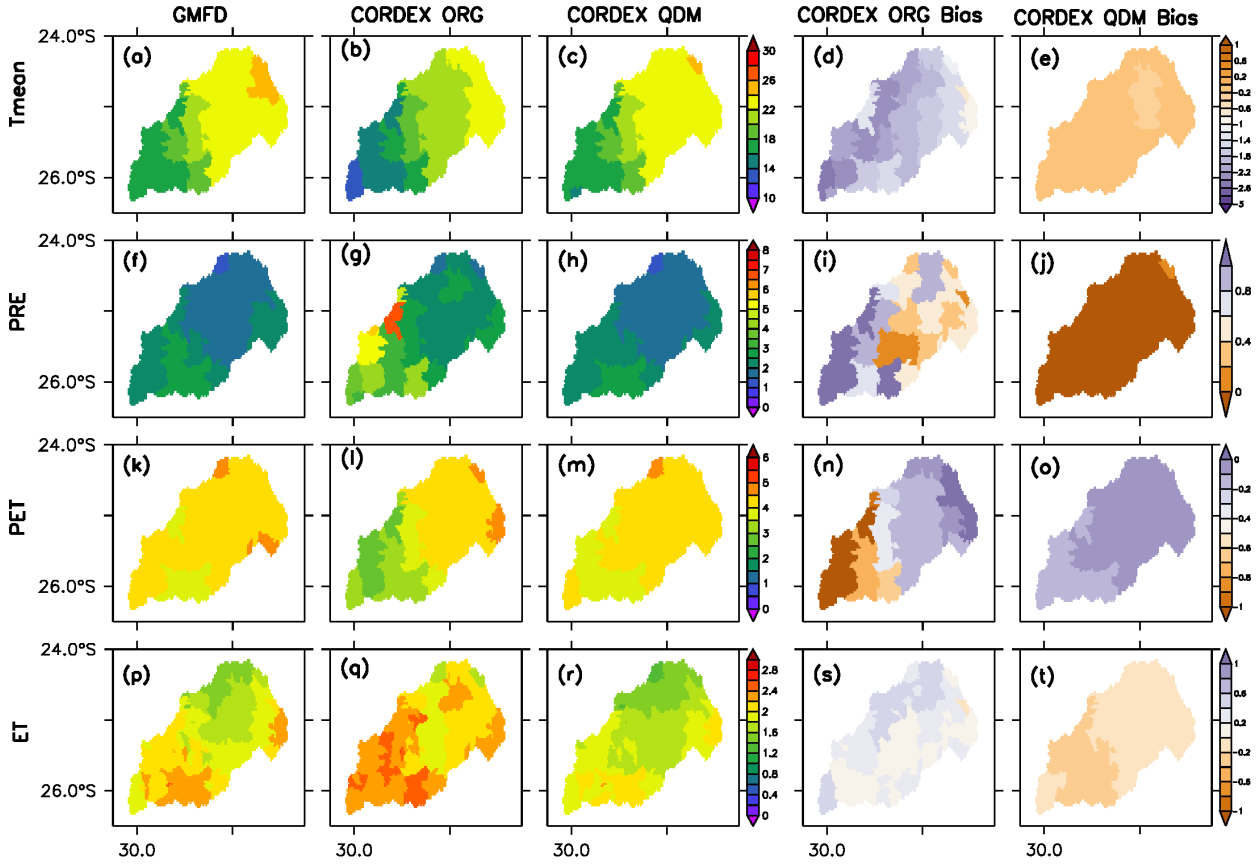

Figure 5.3: Spatial distributions of climatic variables over the Incomati River Basin as depicted by CORDEX original and QDM modelled ensemble datasets between 1971 and 2000.

5.2.2 Land unit hydrological variables

Figure 5.4 below represents the spatial distribution of CORDEX simulated hydrological variables (soil moisture (SW), percolation (PERC), runoff and water yield (WYLD)) before and after bias correction, as well as the biases. As a consequence the raw climate dataset inputs (discussed previously in Figure 5.3), the original CORDEX (CORDEX ORG) simulations failed to adequately

capture the spatial distribution of hydrological variables over the Incomati River Basin. For example, the models significantly overestimated the variability of all the hydrological variables especially over the upper Incomati (*i.e.* SW> 90 mm, PERC >0.1mm, runoff > 0.3mm and WYLD> 1mm; 25.2-26.3°S and 29.9-37°E) disagreeing with the observed spatial distributions (Figure 5.4a-b, f-g, k-l, and p-q). This is further validated by the bias plots (Figure 5.4d, i, n and s) which indicate soil water to constitute the highest bias (*i.e.* up to 100mm biases). Hence the importance of bias correction. Post bias correction, evidence of the systemic biases and uncertainties being significantly removed are observed in Figures 5.4c, h, m and r and bias plots Figure 5.4e, j, o, and t (i.e. CORDEX QDM adequately simulated the spatial distributions of the variables in accordance with GFMD). Comparable results over southern Africa (*i.e.* Li et al., 2013) agree that bias correcting climate variables such as precipitation enhances hydrological simulations of runoff. Hence, this further underscores the importance of bias correction.

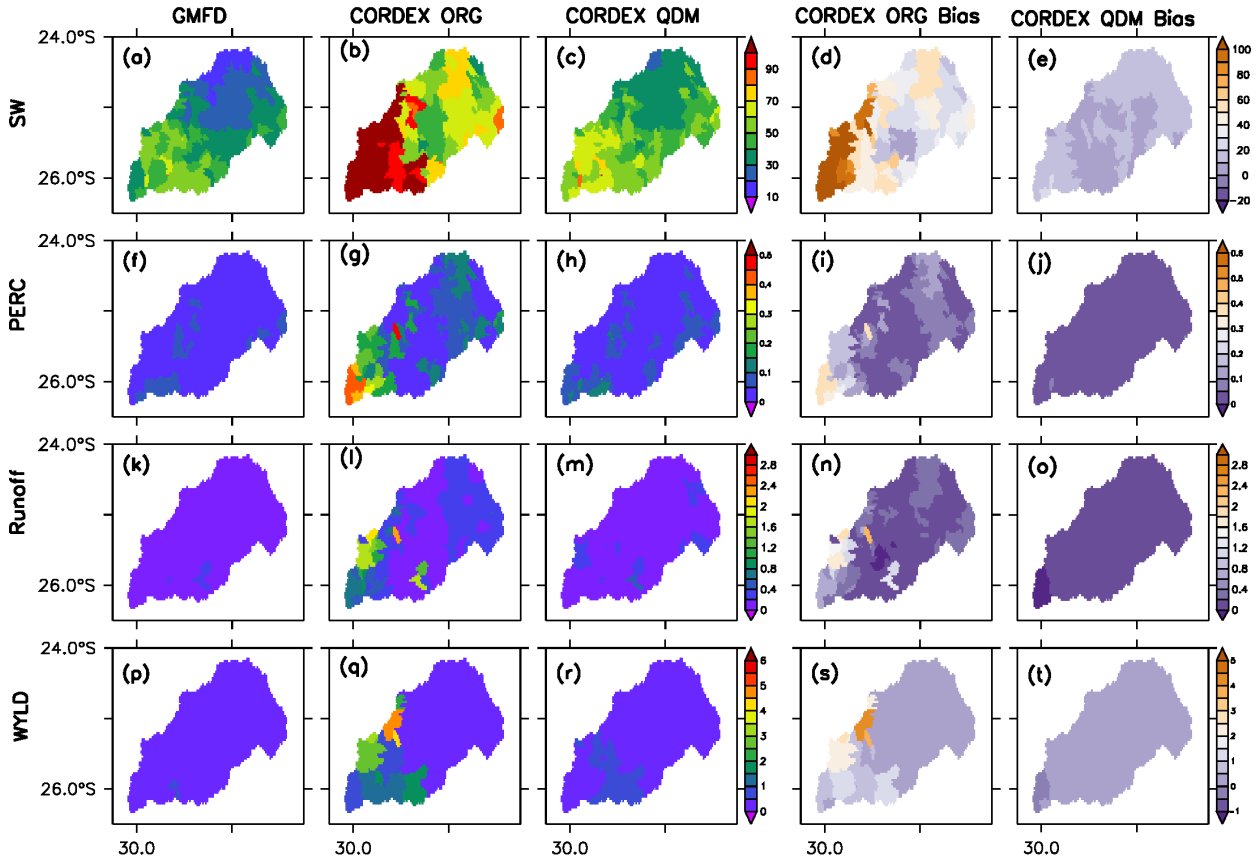

Figure 5.4: Spatial distributions of hydrological variables over the Incomati River Basin as depicted by CORDEX original and QDM modelled ensemble datasets between 1971 and 2000.

5.2.3 River channel hydrological variables

Figure 5.5 below shows the spatial distribution of CORDEX simulated river channel hydrological variables (channel precipitation (CPRE), channel evapotranspiration (CEP) and channel flow (Cflow)) before and after bias correction, as well as the biases. The CORDEX simulations prior bias correction (*i.e.* CORDEX ORG) generally overestimated the river channel precipitation and flow (*i.e.* Figure 5.5b and l) while underestimating some parts of the channel evapotranspiration over the IRB. Conversely, the CORDEX simulations post bias correction (CORDEX QDM) adequately captures the basin's CEP, overestimates the CPRE and underestimates the Cflow (*i.e.* Figure 5.5c, h and m). Nonetheless, the model simulations are consistent with the basin's natural streams and topography (*i.e.* the channels connect and broaden east of the basin, flowing from towards the mouth, south east). Even so, the bias plots depict that CORDEX ORG simulations constitute larger biases (*i.e.* Figure 5.5 d, i and n) in comparison to bias corrected simulations (CORDEX QDM) (*i.e.* Figure 5.5e, j and o). Hence, bias correction is important in hydrological modelling.

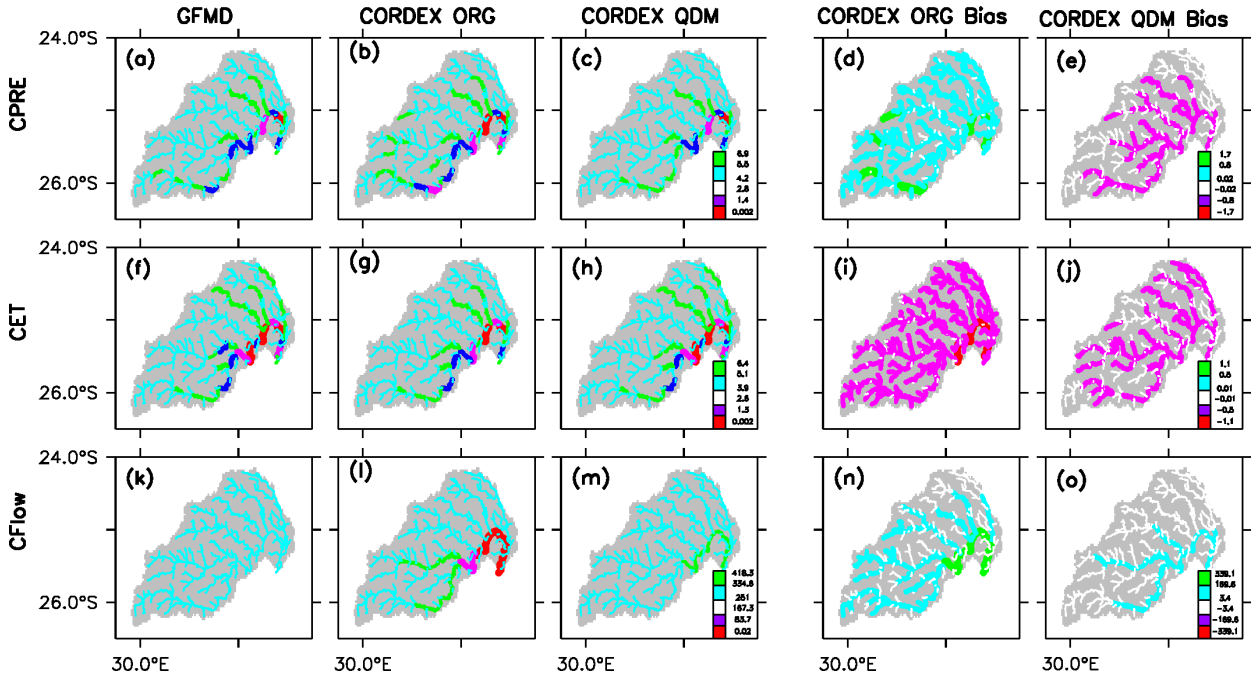

Figure 5.5: Spatial distributions of the Incomati River Basin channels as depicted by CORDEX.

CHAPTER 6: Potential impacts of global warming on atmospheric and hydrological variables in Incomati River basin

Global warming is expected to contribute to large scale changes in atmospheric and hydrological variables that influence extreme rainfall and flooding events. As part of ongoing efforts to provide information for managing the future risks and vulnerabilities in the flood prone Incomati River Basin, this chapter presents the potential impacts of climate change and extreme hydroclimate variables over the basin. To put the results in the context of the Paris agreement, the projected impacts are presented at four global warming levels (*i.e.* GWL: 1.5, 2.0, 2.5 and 3.0) under the RCP8.5 future climate scenario. The impacts are first projected for four climate variables that contribute to the hydrology processes in any basin (temperature, precipitation, potential evapotranspiration, and evapotranspiration) and four hydrological variables over land (soil water, surface runoff, percolation and water yield) and three river channel variables (channel precipitation, channel evapotranspiration, and channel flow). Then, the impacts are examined on two characteristics of extreme precipitation and channel flow (*i.e.* the intensity and frequency), using the 95th percentile of the daily values for these variables as the threshold for their extremes.

6.1 Climate change impacts on mean hydroclimatic variables

6.1.1 Climate variables

Figure 6.1 presents the spatial distribution of the projected changes in the climate variables at four global warming levels (*i.e.* GWL1.5, GWL2.0, GWL2.5 and GWL3.0). The figure shows that as the global warming levels increase, there is a general increase in the projected mean temperature (Tmean) and potential evapotranspiration (PET), and a decrease in precipitation (PRE) and evapotranspiration (ET). For Tmean, the quasi-uniform increase is indicated over the basin at each GWL, except that the magnitude of the increase becomes higher as the global warming level increases. However, there are indications that at GWL3.0, the warming may be higher at the south-western tip of the basin than at the remaining part of the basin. In contrast

to Tmean, PRE changes are projected to vary in the basin. At GW1.5, increased PRE (<2 mm/month) is projected at the south-western tip while decreased PRE (2-6 mm month) is projected in the remaining part of the basin. However, as the GWL increases, the increase in PRE over the south-western tip turns to a decrease of the same magnitude while the magnitude of the rainfall deficit over the remaining part of the basin increases. While the projected increase in PET is consistent with the Tmean (because warming increases the capacity of air to contain water vapour), the spatial distribution of the PET differs from that of Tmean (possibly because PET is calculated from Tmax and Tmin and not from Tmean). However, the projected changes in Tmean, PRE and PET obtained here is consistent with those reported in other studies over southern Africa (*i.e.* Tadross et al., 2005; Andersson et al., 2011; Li et al., 2015; Abiodun et al., 2019a).

The projected changes in ET differs from that of PET, both in direction and magnitude. With the increase in PET, ET is expected to increase in order to fulfil the atmospheric demands for moisture. But, at GWL1.5, a decrease in ET (about 2 mm/month) is projected in most parts of the basin, except in the south-western area where an increase in ET (<2 mm/month) occurs. As the warming level increases, the area of increased ET decreases such that, at GWL3.0, a decrease in ET dominates the whole basin. This implies that projected changes in ET are limited by the amount of water available at the surface regardless of the projected increase in PET. With the projected decrease in PRE, less water will be available for ET. This is in line with study by Li et al (2015) that projected a PET increase of +2.3% over the IRB riparian countries (*i.e.* South Africa, Mozambique, and Swaziland) in conjunction with the projected increases in mean temperatures.

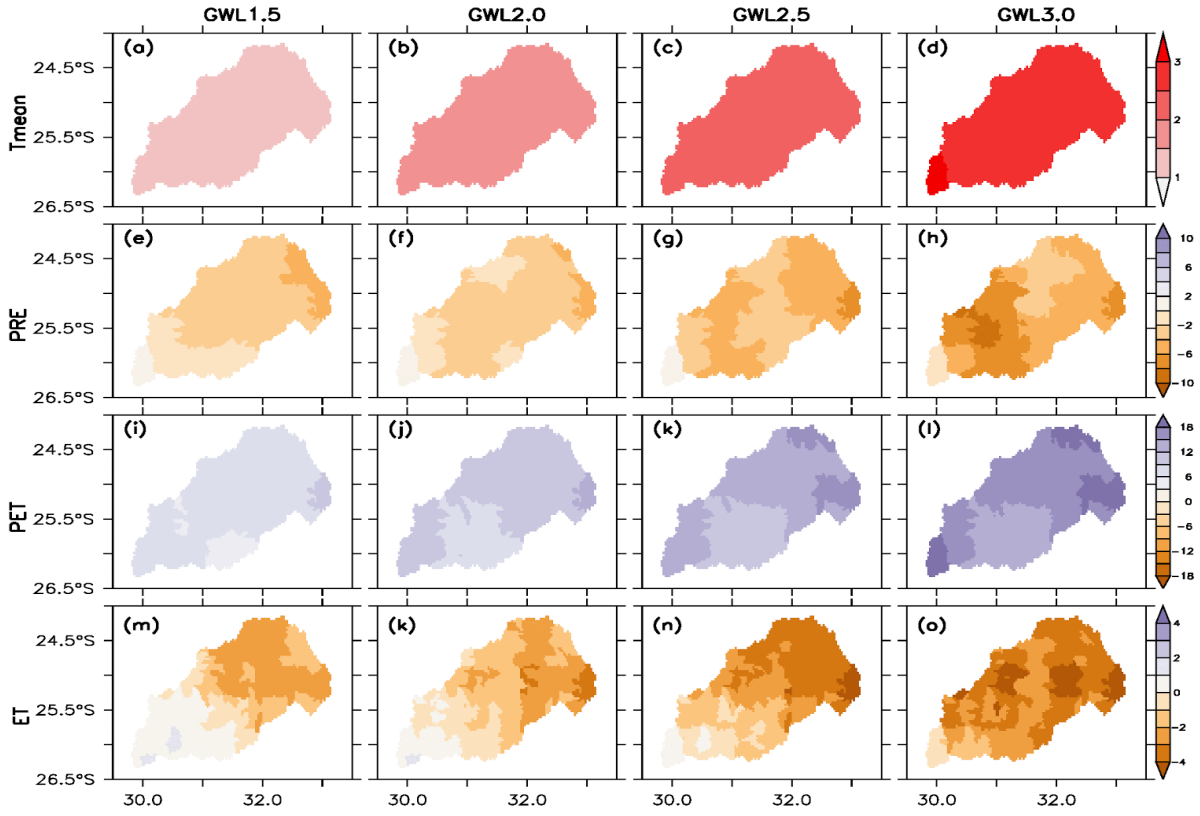

Figure 6.1: Spatial distributions of future projected changes in climate variables (i.e. mean temperature (Tmean; Figure 6.1a-d), precipitation (PRE; Figure 6.1e-h), potential evapotranspiration (PET; Figure 6.1e-h) and evapotranspiration(ET; Figure 6.1m-o) at four global warming levels over the Incomati River Basin.

6.1.2 Hydrological variables over land

Figure 6.2 presents the spatial distribution of the projected changes in hydrological variables over land: soil moisture (SW), percolation (PERC), surface runoff (runoff) and water yield (WYLD). While a general decrease is projected for all the variables, there are variations in the spatial patterns of the changes across the variables and across the GWLs. Even so, the projected changes are consistent with the climate variable projections (in Figure 6.1). The SW is projected to decrease over the whole basin with the highest decrease at GWL3.0. The increase in the PRE over the south-eastern tip of the basin at GWL1.5 does not result in increased SW, because the additional moisture has gone for ET following the increased PET (Figure 6.1.1). PERC is projected to decrease over the whole basin (by more up to 0.8 mm month). This has a huge implication on underground water recharge in the basin.

Although there is a general decrease in runoff with increasing GWLs, some areas of the basin (especially over the south-western tip of the basin) are projected to experience increases. The projection is consistent with the slight increases in precipitation seen in the area (Figure 6.1e-g). However, the decreased PERC with increased runoff over the south-western part basin suggests that additional water from PRE goes for runoff rather than for moistening the soil or for changing the groundwater. While WYLD is projected to decrease over the basin, the largest decrease is projected over the mountainous escarpments of the basin where the magnitude of the decrease grows with the increase in the warming levels. These results are consistent with the 16% decrease in streamflow projected over the Zambezi River basin (Hamududu and Killingtveit, 2016). Similarly, Sood et al. (2013) projected similar future significant drops in soil moisture, groundwater recharge, and water yield reaching 40% over the between 2071 and 2100 in west Africa. Nevertheless, the results of this study raise serious concern for future increases in water resources stress. Hence, management and mitigation plans are of great importance.

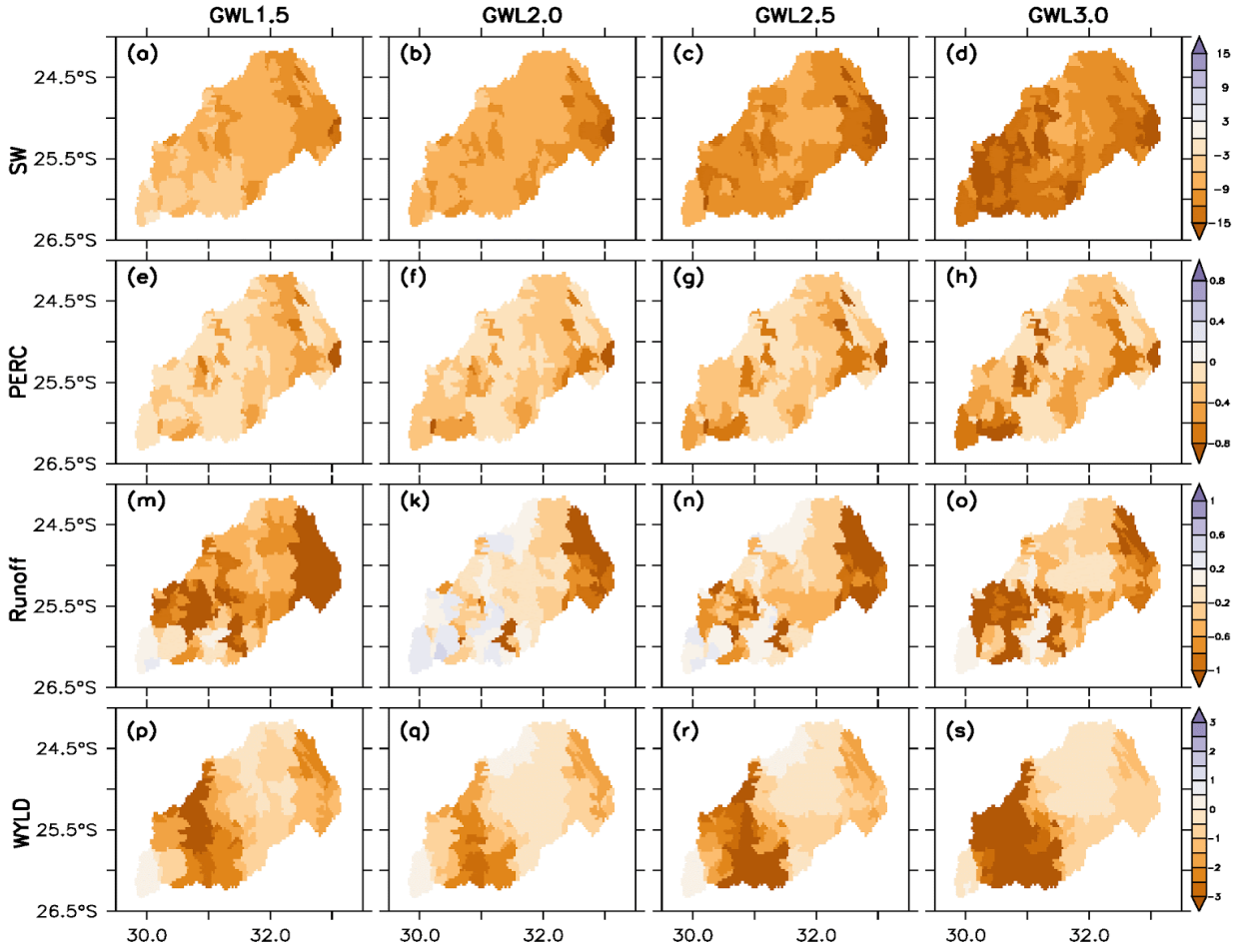

Figure 6.2: Spatial distribution of the projected changes in hydrological variables over land: soil moisture (SW), percolation (PERC), surface runoff (runoff) and water yield (WYLD) at four global warming levels (GWL1.5, GWL2.0, GWL2.5, and GWL3.0) over the Incomati River Basin.

6.1.3 River channel variables

Figure 6.3 shows projected changes in the river channel variables: channel precipitation (CPRE), channel evapotranspiration (CET), and channel flow (CFlow). In accordance with the changes in PRE over land, CPRE is projected to decrease over most parts of the basin and increase over the south-west tip of the basin. However, in contrast to changes in ET over land, increased CET (up to 16 mm/day) is indicated over the channels. The reason for this discrepancy is that, over the channels, the increase in CET (due the increased PET) may not be limited by the projected decreased PRE as long as there is water in the channels. However, the magnitude of the increase in CET depends on the volume of water in the channel and on the warming levels. The downstream channels with larger volume of water (especially near the river mouth) experience higher CET than those with smaller volume of water. The higher the warming level, the higher the increase in CET. In accordance with a decrease in CPRE and increase PET, a decrease in CFlow is projected along major river channels where the majority of the river channel tributaries join and expand as they lead to the river mouth.

In contrast, the river channels in the south-western tip of the basin are generally projected to experience negligible changes in CFlow, possibly because the increase in PRE compensates the impacts of increased CET on CFlow in these channels. Other inconsistencies in these future projections also exist. For example, over the northern Incomati, the projected changes in CFlow are insignificant (especially at GWL2.0 and about), despite the projected decreased CPRE and increased CET over the area. Nevertheless, projected decreases in CFlow following the general increase in temperature and precipitation (PRE and CPRE) are consistent with some previous studies. For example, Hamududu and Killingtveit. (2016) projected 2.7°C increases in temperature and -8 to -19% changes in precipitation over the Zambezi River Basin that could lead to increased river channel evaporation and 14 - 26% reductions in river flow by 2080. Similarly, Sood et al. (2013) projected up to 3.6°C increases in temperature, approximately 20% decrease in precipitation, consequent 25% increase in PET, 14% decrease in ET, and a 40% decrease in water yield over the Volta River Basin between 2071 and 2100. However, the

projected future reduction in the streamflow over the IRB indicated in the present study should be a concern. This is because reduced future streamflow will have implications on the availability of water in the basin that will negatively affect the livelihoods of people and farmers in the basin. Consequently, food security and water related sectors of the economy in the riparian countries will be at risk. Hence, the need to include such findings in future mitigation and adaptation plans over this basin.

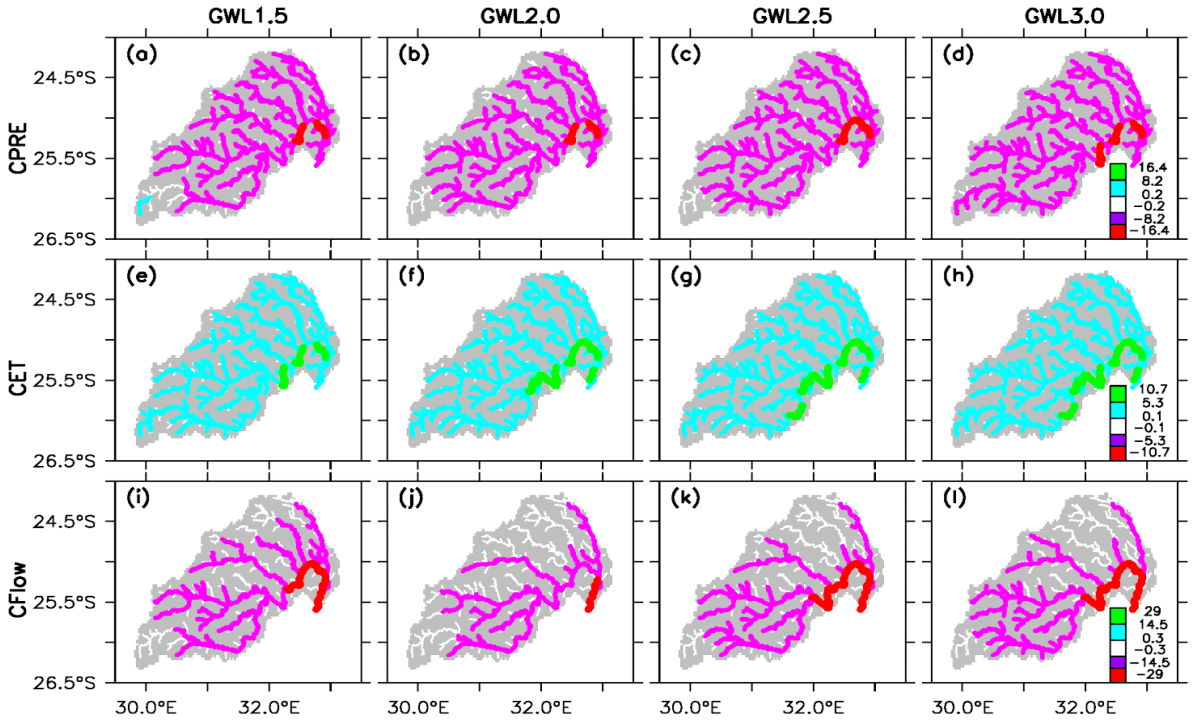

Figure 6.3: Spatial distributions of future change in river channel variables (*i.e.* precipitation [CPRE; Figure 6.3a-d), evapotranspiration (CET; Figure 6.3e-h) and channel flow (CFlow; Figure 6.3i-l) at four global warming levels over the Incomati River Basin.

6.2 Climate change impacts on extreme precipitation and streamflow events

Figure 6.4 shows the spatial distribution of the simulated intensity and frequency of extreme precipitation and extreme stream flow over the Incomati River basin in the present-day climate and the projected changes in the future climate at the for GWLs (*i.e*. GWL1.5, GWL2.0, GWL2.5 and GWL3.0). In the present-day climate, the maximum extreme precipitation intensity (> 50 mm/day) occurs along steep slopes of the mountain range while the maximum frequency of extreme precipitation occurs over the peak of the mountain range. These can be attributed to the mountain induced deep convection. Several studies have documented how mountain ranges

drive initial deep convection, storms, and extreme precipitation by lifting moist air parcels to the level of free convection (Roe et al, 2003; Cooley et al., 2007; Huang et al., 2020). In Figure 6.4, the maximum extreme rainfall intensity occurs over the slope and not over the mountain peak, possibly because when the slope triggers a deep convection in a flow, most of the moisture in the flow will be released as heavy precipitation over the slope, reducing the availability of moisture for precipitation over the mountain peak. However, the mountain peak experiences the highest frequency of extreme precipitation events because there may be some cases when the moist-laden flow may not reach its level of free convection until it reaches the peak of the mountain. As anticipated, the highest magnitude of extreme streamflow intensity does not occur in the channels over the mountain peak or along the slope, but in the plain towards the mouth of the river where the streamflow from the channels converges. The pattern is consistent with the reported extreme river flooding events along the Mbabane, Mlambothwala and Mlumati Rivers in Hhohho, Swaziland that led to eight deaths and flood damages in Kaaprivier influenced by the Dieskkopies dam (25.6-25.8^{o}S and 31.3-31.5^{o}E) (Hill, 2014). In contrast to the extreme streamflow intensity, the extreme streamflow frequency features its maximum values in the channels along the slopes.

There is no consistent pattern in the spatial distribution of the projected changes in the intensity and frequency of extreme precipitation at different GWLs (Figure 6.4). Figure 6.4 demonstrates that an increase in the intensity of extreme precipitation is projected over some parts of the basin and a decrease over others. It also shows an increase in the precipitation frequency over the mountain peak but a decrease over the slope and the plain. At GWL3.0, the increase in extreme precipitation is up to 2% while the magnitude of the decrease is up to 4%. These findings are consistent with extreme precipitation projections over southern Africa by several studies (e.g. Abiodun et al., 2017; Abiodun et al., 2019b). In response to the precipitation projection, an increase in extreme streamflow is projected in some channels while a decrease is projected in other channels. The number of the channels that feature the increase in extreme streamflow increases with the GWLs, such that, at GWL3.0, all the channels report an increase in the extreme streamflow intensity. The projected changes in frequency of extreme streamflow agree with that of extreme precipitation to an extent. For example, it shows an increase in the frequency of extreme streamflow (>87%) over the mountain peak, where extreme precipitation is projected

to be more frequent, and less frequent over the slopes and the plains, especially at the GWL3.0. The results suggest that while the frequency of extreme streamflow may decrease over the basin, the intensity of the event may increase. The projected increases in streamflow are in agreement with a global study by Asadieh and Krakauer (2017). Moreover, Abiodun et al. (2019a) also projected increases in the frequency and intensity of drought over the IRB basin in a study over southern Africa at different GWLs.

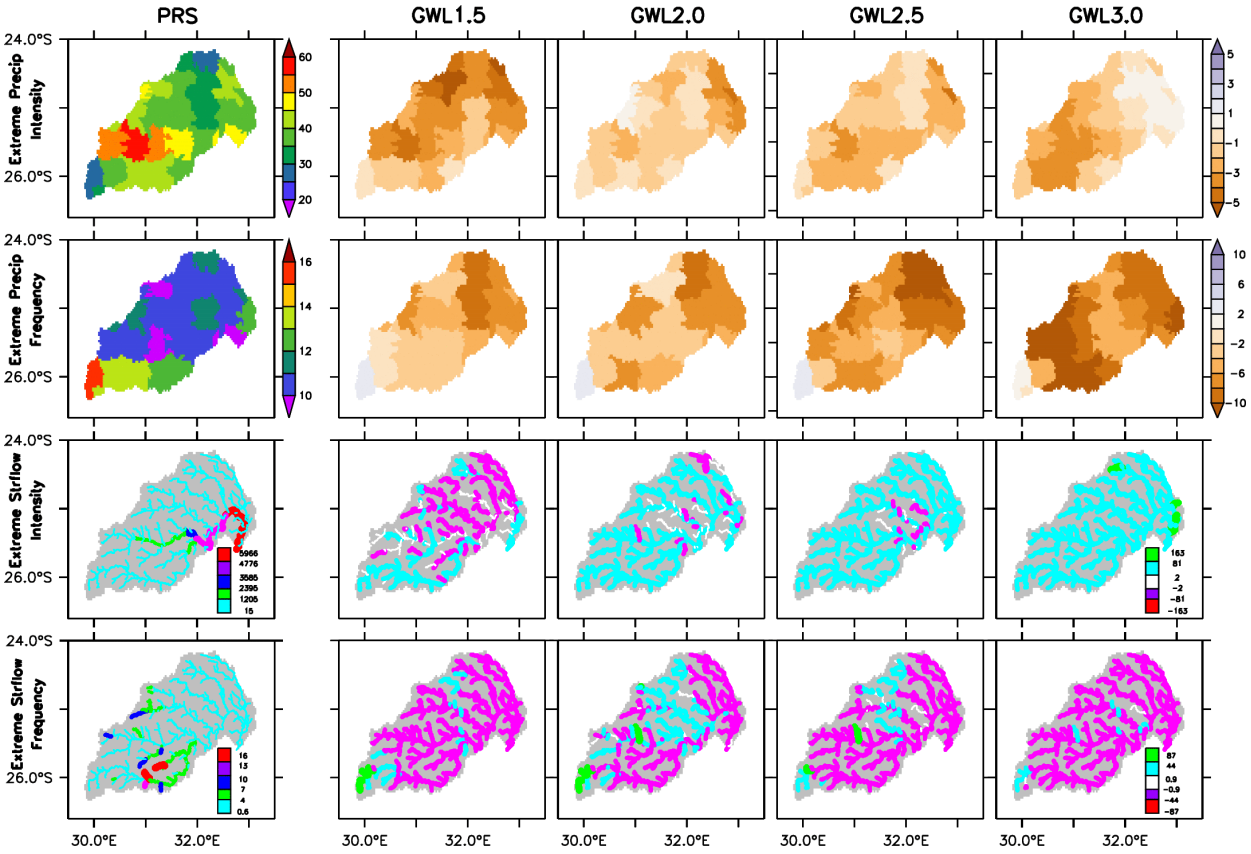

Figure 6.4: Spatial distributions of the intensity and frequency of extreme precipitation (Extreme precip) and extreme streamflow (Extreme Strflow) during the present-day climate and the projected changes in the future climate (PRS) at four global warming levels (GWLs: GWL1.5, GWL2.0, GWL2.5, and GWL3.0) over the Incomati River Basin.

Figure 6.5 presents the projected future climate change impact on the intensity and frequency of precipitation and streamflow over 6 reportedly flood prone river channels (*i.e.* channel 107, 115, 125, 172, 219 and 241) in the IRB at four global warming levels (GWL1.5, GWL2.0, GWL2.5 and GWL3.0). For precipitation, the river channels generally agree on a potential negative

percentage change in both the intensity and frequency of the events (*i.e.* over 60% of the simulations projected between 0 and 30% decline in the intensity and frequency of extreme precipitation events; Figure 6.5a and b). The river channels exhibit their best agreement at GWL3.0 whereby 100% of the simulations projected that extreme precipitation in this basin will be less intense and frequent along river channels 125 and over 50% agree along channels 107, 115, 174, 219 and 241). Nevertheless, while the direction of the projected change in the frequency of extreme precipitation is generally consistent with increasing GWLs across the different river channels, the projected change in intensity is not. Hence, the inconsistencies in the two projections over some channels. For example, the direction of the future projected change in the frequency of extreme precipitation events over all river channels is negative (Figure 6.5b). With regard to intensity however, the direction of change over channel 107, 115, 174 and 219 becomes positive as the GWLs increase, while a general negative change in direction occurs along channel 125 and 241 (Figure 6.5a). Although no study has projected extreme precipitation intensity and frequency over these particular channels, some projections have taken place over regions close to these channels. For example, these projections are consistent with those of Abiodun et al. (2017) over Maputo, Davis (2010) and Schulze (2011) over Mpumalanga, as well as New et al. (2006) over southern Mozambique.

The projected intensity and frequency of extreme streamflow events over the IRB are generally inconsistent with the extreme precipitation projections along all river channels except channel 241 (*i.e.* there is a general increase in the projected change as the GWLs increase across all river channels and a general decrease at channel 241; Figure 6.5c and d). The projected changes along channel 241 may be linked to the channel being the only one located along high mountainous escarpments in the basin (*i.e.* 25.8-28^{o}E and 30-30.7^{o}S). On the other hand, channel 219 is projected to experience the most intense positive changes in streamflow events that slightly decrease as the GWLs increase (*i.e*. 75% of the projected changes lie in the positive spectrum at different GWLs with projected changes exceeding 200%). Nevertheless, all projections generally lie on both sides of the spectrum, suggesting an almost equal percent chance of the channels experiencing either more or less intense extreme streamflow events (Figure 6.5c). In terms of frequency, however, more than 60% of the simulations projected a general decrease, suggesting an over 50% negative percentage change in future events, except for channel 219 where more

than 100% positive percentage change is projected at different GWLs (Figure 6.5d). Notably, the projections along channel 219 are logical and consistent with the general projections in Figure 6.1 because it is located in the south-west part of the basin, along the hazard prone Nooitgedacht Dam. Hence, the importance of applying these findings in future climate change mitigation strategies on hydrological impact over these presently flood prone parts of IRB.

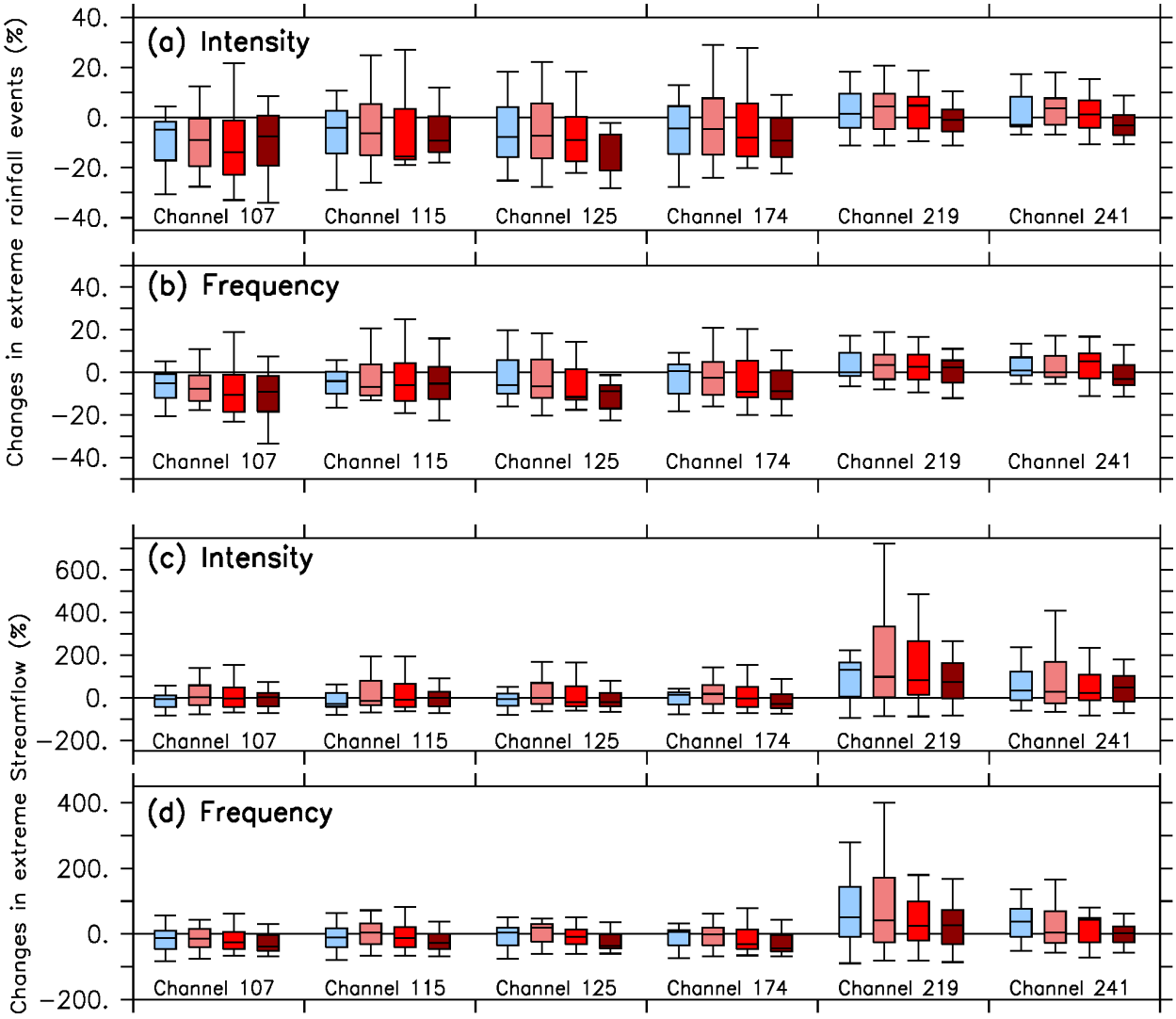

Figure 6.5: Boxplots showing the spread of the projected changes (*i.e.* minimum, median, and maximum) in the intensity and frequency of precipitation and streamflow at four global warming levels over the Incomati River Basin.

CHAPTER 7: Conclusions

This chapter offers the main conclusions from this study, the limitations of the research findings and the major sources of uncertainty. Thereafter, it offers recommendations for future research avenues. By recognizing the limitations of this study, more realistic and robust conclusions may be achieved. This is important as the findings from this study may influence policy making and seek implementation in the climate change impact mitigation strategies and efforts towards preserving hydrology over the Incomati River basin and other southern African basins.

7.1 Summary

As part of the efforts to investigate and mitigate the potential impacts of global warming on extreme precipitation and hydrological events over vulnerable river basins in southern Africa, this dissertation has studied the impacts of climate change on extreme hydrological events over the basin. In Chapter 2, it provided a comprehensive review and reflection on past and present fundamental studies at a global and regional scale. In Chapter 3, the methodology used in this study as well as the study area, the Incomati River Basin (IRB), were thoroughly described and explained in Chapter 3. In Chapter 4, it calibrated and evaluated the hydrological model SWAT+ by investigating the role of objective functions (1-NSE, 1-R^2, RMSE and PBIAS) in calibrating SWAT+. Based on the best calibration results, the study further applied 1-NSE as the best objective function in further studies. In Chapter 5, it showed the extent to which the quantile delta mapping algorithm (QDM) bias correction can improve quality and uncertainty of the datasets used as inputs in hydrological modelling. Chapter 6 projected the future impacts of climate change on the mean hydroclimate variables and on the characteristics of extreme hydrological events, as well as the potential changes in the intensity and frequency of extreme precipitation and streamflow events (using the 95th percentile to define an extreme event) at four global warming levels (*i.e.* GWL1.5, GWL2.0, GWL2.5, GWL3.0) under the RCP8.5 future climate scenario.

The results of this study can be summarised as follows:

- Using 1-NSE or RMSE as the objective function in the IPEAT+ algorithm to calibrate SWAT+ over IRB is computationally efficient; the results converge faster than using 1-R^2 or PBIAS as the objective function. However, the convergence value is generally poor for all the objective functions.
- The calibration of SWAT+ is most sensitive to the curve number (CN_2), which proves to be the most dominant parameter controlling the magnitude of simulated streamflow during the calibration period. The best simulation requires a 30% in the original values CN_2 with 1-NSE, 1-R^2 and RMSE as objective functions and -14.1% with PBIAS as the objective functions.
- The performance of SWAT+ in simulating the streamflow over the basin depends on the statistical metrics used in the evaluation; while the NSE of the model SWAT+ simulation is poor (*i.e.* NSE ≈ -0.08) over all the stations, the PBIAS is very good (*i.e.* PBIAS ≈ 13.7%) at some stations.
- The best SWAT+ simulation obtained with 1-NSE gives better simulation of daily stream flow and more realistic spatial distribution of the hydrological variables over the basin than the best simulation obtained with the other objection functions.
- Prior to bias correction, the models generally underestimated the annual cycle and spatial distributions of climate variables over IRB. The QDM bias correction algorithm reduced the biases and uncertainties that were previously observed in the climate variables.
- The uncertainty in climate variables amplified the uncertainty in the simulated hydrological variables. Correcting bias and uncertainty in the climate data consequently reduced the biases and uncertainties in the hydrological variables.
- While future increase in temperature is projected over the basin with increasing GWLs, a decrease in annual precipitation is predicted over the basin except at the south-west tip of the basin. Hence, streamflow is projected to experience decrease across the basin except at the south-western area.
- PET is projected to increase due to the increasing Tmean. However, ET over land is projected to generally decrease in accordance with the projected decrease in PRE,

resulting in less water available for ET. Since CET depends on the volume of water in the channel instead of CPRE, it is projected to increase due to the increasing PET.

- While the maximum extreme precipitation intensity occurs along steep slopes of the mountain range in the present-day climate, the maximum frequency of extreme precipitation occurs over the peak of the mountain range.
- The present-day highest magnitude of extreme streamflow intensity occurs in the plain towards the mouth of the river where the streamflow from the channels converges, while the extreme streamflow frequency features its maximum values in the channels along the slopes.
- At all the GWLs, there is no consistent pattern in the spatial distribution of the projected changes in the intensity and frequency of extreme precipitation. There is an increase in frequency of the precipitation over the mountain peak but a decrease over the slope and the plain.
- Future projections of extreme streamflow are consistent with the precipitation projections to an extent, such that, the mountain peaks are also projected to experience more frequent streamflow events while decreases are projected over the slopes and the plains.
- There is an inconsistent direction of projected changes in precipitation intensity with increasing GWLs across the different river channels and a clear tendency towards a negative change in precipitation frequency.
- There is a strong agreement on a general increase in future projected intensity and frequency of extreme streamflow across 5/6 river channels with increasing global warming levels in the Incomati River Basin.

The thesis has successfully accomplished its three objectives outline in Chapter 1. In Chapter 4, it has examined how SWAT+ simulates the hydrology of the IRB. This was done by first calibrating and evaluating the hydrological model. The influence of different objective functions (1-NSE, 1-

R^2, RMSE and PBIAS) in obtaining the best SWAT+ simulation over the basin was investigated and 1-NSE gave the best calibration results. The calibrated SWAT+ captured the daily streamflow over the basin and produced the realistic spatial distribution of the hydrological variables over the basin. Hence, the model is found suitable for hydrological modelling over the IRB.

In Chapter 5, the study evaluated the performance of CORDEX dataset in reproducing the historical climate over the IRB by comparing how well the dataset reproduce the hydroclimatic variables of the IRB with the GMFD results. After bias-correcting the dataset using the algorithm (QDM) technique, it showed that the bias-corrected dataset enhanced the quality and CORDEX datasets and the hydrological simulation produced with the dataset. Hence, the study shows the extent to which bias corrected CORDEX data can improve hydrological simulation over the Incomati river basin.

In Chapter 6, the thesis studied the characteristics of projected future climate change in climate and hydrological variables (and the associated extreme events) by applying different GWLs to project the impact of climate change on the hydroclimatic variables over the basin. It projected an increase in temperature and a general decrease in precipitation, leading to general decrease in streamflow over the basin except the south-western area. It showed that extreme streamflow projections are consistent with the precipitation projections.

7.2 Implications for policy

The results of this thesis have several implications for future climate change impact related mitigation strategies for policy relating to extreme climate and hydrological events over the IRB. Since the results of this study revealed that the impact of climate change on extreme precipitation and streamflow varies across the different parts of the IRB, there is a need for policy makers to formulate relevant adaptation and mitigation strategies that will accommodate the impacts over the different parts of the basin. For example, future plans and strategies to address flood related risks associated with more intense and frequent extreme precipitation and streamflow events as a result of climate change in the basin should focus mainly over channel 219 and the rest of the south-west area of the basin, as well as river channel 241 due to projected increases. Many strategies for controlling and containing flood related extremes have been established in recent years. For example, several studies around the world have found land-use

modifications as suitable strategies of mitigating climate change impact on extreme flooding events over river basins (International Commission for the Protection of the Rhine (ICPR), 2001; Zhang et al., 2016). Land cover changes such as forestation, grasslands and some measures of agricultural planting (*i.e.* intercropping), are amongst those that were identified to best mitigate flooding in river basins. However, the application of such strategies may need further study focusing on the IRB. This would enable relevant policy making that would also account for factors like population growth and infrastructure development and currently ongoing activities in IRB.

Government and other policy makers need to focus on the implications of the projections over areas of the IRB which are anticipated to become drier with increasing GWLs. As previously discussed, temperatures are projected to increase while precipitation decreases. There is high atmospheric demand for evaporation (increased PET) and low precipitation, soil moisture, percolation and runoff, that may create a significant stress on the basin's water resources. For example, increased river channel evapotranspiration (CET) may have devastating consequences on agricultural activities (which are mostly rain-fed) since the soil may be unsuitable for both crop and livestock farming due to the irrigation demands on drier soils. Overtime, this may threaten food security and the economy across the three riparian countries. Furthermore, increased reduction in percolation with increasing GWLs may threaten underground water levels, thus affecting the extraction of water through boreholes by farmers and dwellers. In addition, increasing human populations will not only exacerbate water demand but will increase the demand for electricity. Reduced availability of water in the basin will severely affect hydroelectric power generation. Since the basin is shared amongst the three countries, severe economic consequences may be felt in all three countries. Hence, a more integrated approach to formulate strategic river basin plans to manage and mitigate these implications is of fundamental importance in policy making. These may include (1) strategic land use changes that may control loss of water through evapotranspiration in the basin, (2) decentralizing techniques used for harvesting precipitation in the entire basin (UNEP, 2010), (3) conserving soil moisture through mulching and tillage (Sood et al., 2013), (4) development and management of groundwater irrigation systems (Dillon, 2009), and (5) the use of other sources of energy such as wind and solar for generating electricity. Subsequently, future climate change impacts in IRB may be better managed.

Nevertheless, the above-mentioned mitigation strategies for policy making can only be successful if the climate and hydrological datasets are robust and reliable. Owing to the vulnerabilities and low adaptive capabilities associated with climate and hydrological extremes as well as the process of acquiring the datasets in southern African river basins, there is an urgent need to resolve the quality and reliability of climate and hydrological datasets and simulations. Hence, the importance of calibrating hydrological model simulations and bias correcting climate simulation outputs. However, in terms of hydrological events for instance, the calibration of hydrological models to improve streamflow simulations is usually a challenge since large datasets are used, thus making the process more time consuming and tedious. This study not only revealed that using the IPEAT+ calibration algorithm is more efficient than performing manual calibration, but that calibration with SWAT+ is less sensitive too, and more computationally efficient when using 1-NSE and RMSE as objective functions in comparison to 1-R^2 or PBIAS. Hence, the study suggests that other SWAT+ users with limited computational resources should consider using the IPEAT+ calibration algorithm coupled with the 1-NSE or RMSE as the objective function in calibrating streamflow over the IRB (or other southern African basin). In doing so, tediousness and subjectivity of calibration would be reduced while achieving robust and reliable hydrological simulations especially in climate change impact studies associated with extreme hydrological events over vulnerable and dataset-scarce southern African river basins.

Similarly, the limited sources of observational climate datasets exist in southern Africa as station coverage is usually sparse and consists of large gaps (Dinku et al., 2018). Hence, different efforts to reduce the challenges associated with data accessibility and availability have been developed. For example, the CORDEX Africa programme produces climate model simulation datasets that can be widely used in future climate change related projections. However, due to large inherent uncertainties and biases in the CORDEX model output datasets, this study made use of the QDM bias correction algorithm, to make the datasets more useful over the IRB. As a result, important climate features were better captured and used as inputs in SWAT+ for hydrological modelling of future climate change impact. Hence, the climate and hydrological impacts obtained in this study may be used in climate change adaptation planning and mitigation strategies by government policy makers over the IRB.

7.3 Limitations of the study

Although the results of this study show that SWAT+ gives realistic simulations of hydrological processes in the IRB, notable biases in the simulated streamflow exist. Several factors could be responsible for this. For example, daily observation streamflow dataset used for calibration and validation were not accessible over stations in Mozambique and Swaziland. Hence, calibration and evaluation were performed over South African catchments only. Even so, the low quality and limited availability of the daily streamflow dataset further restricted the choice of stations and period used for calibration (1988-1990) and validation (1991-1995). This limited a more in-depth evaluation of the performance of SWAT+ in simulating streamflow over the basin. In addition, the inability to represent all the physical features in the basin (e.g. dams and reservoirs) as input data in the model delineation due to the unavailability of data could also be a limiting factor. Moreover, since no such study has been done over the river basin using SWAT or SWAT+, the parameters selected for the sensitivity analysis in this study were guided by previous studies done over South African river basins in close proximity to the IRB (*i.e.* Gyamfi et al., 2016 over Olifants basin). The overall biases that were found in the simulation of the basin's hydrology (*i.e.* streamflow, runoff) may have been attributed to the model's high sensitivity to CN_2, which regulates the magnitude of the flow in SWAT (Guse et al., 2014). Hence the need to enhance the sensitivity of the model outputs to required changes in CN_2 in order to produce more robust and realistic projections. The model failed to capture some streamflow peaks over the stations. This may have been attributed to heavy precipitation events and storms not being captured in the datasets. Hence, attention to the precipitation and streamflow data used in the simulations should be given and improved for better representation of the basin's extreme hydrological processes.

7.4 Suggestions for further studies

The results of this study have revealed the complexity of understanding hydrological processes such as soil moisture, percolation and evapotranspiration as well as their importance over the IRB. Consequently, further research should work towards improved representation of these variables in order to improve the simulation of hydrological processes in this basin. Hence, continued modifications of SWAT model structure and code need to be developed. This can be

done by adding new parameters in the model or adding more groundwater layers (Guse et al., 2014). In addition, since this study only made use of one bias correction method to reduce bias and uncertainty in the CORDEX simulation output datasets, we recommend that other studies investigate other bias correction algorithms and select the one with the best results for their basin. Most importantly, a further study to examine suitable land cover changes to mitigate the projected changes in extreme climate and hydrological events over the Incomati River Basin is recommended so as to increase the relevance of this study to policy makers and lean towards potential climate change mitigation options. The variety of approaches suggested in this study will therefore add significant contributions towards understanding climate and hydrologic processes and dynamics over the IRB. Hence the application of SWAT+ in similar studies is advised to better understand hydrological processes and make realistic resolutions.

REFERENCES

Abbaspour, K.C., Rouholahnejad, E., Vaghefi, S.R.I.N.I.V.A.S.A.N.B., Srinivasan, R., Yang, H. and Kløve, B., 2015. A continental-scale hydrology and water quality model for Europe: Calibration and uncertainty of a high-resolution large-scale SWAT model. *Journal of Hydrology*, *524*, pp.733-752.

Abdulkareem, J.H., Pradhan, B., Sulaiman, W.N.A. and Jamil, N.R., 2018. Review of studies on hydrological modelling in Malaysia. *Modeling Earth Systems and Environment*, *4*(4), pp.1577-1605.

Abiodun, B.J., Adegoke, J., Abatan, A.A., Ibe, C.A., Egbebiyi, T.S., Engelbrecht, F. and Pinto, I., 2017. Potential impacts of climate change on extreme precipitation over four African coastal cities. *Climatic Change*, *143*(3), pp.399-413.

Abiodun, B.J., Makhanya, N., Petja, B., Abatan, A.A. and Oguntunde, P.G., 2019a. Future projection of droughts over major river basins in Southern Africa at specific global warming levels. *Theoretical and Applied Climatology*, *137*(3-4), pp.1785-1799.

Abiodun, B.J., Mogebisa, T.O., Petja, B., Abatan, A.A. and Roland, T.R., 2019b. Potential impacts of specific global warming levels on extreme rainfall events over southern Africa in CORDEX and NEX-GDDP ensembles. *International Journal of Climatology*.

Adrianne, A., 2003. Global warming may dry up Africa's rivers. *Natural Geographical News*, *3*.

Akoon, I., Archer, E., Colvin, C., Davis, C., Diedericks, G.P.J. and Maherry, A., 2011. South African risk and vulnerability atlas. *Pretoria: Department of Science and Technology*.

Alfieri, L., Bisselink, B., Dottori, F., Naumann, G., de Roo, A., Salamon, P., Wyser, K. and Feyen, L., 2017. Global projections of river flood risk in a warmer world. *Earth's Future*, *5*(2), pp.171-182.

Andersson, L., Samuelsson, P. and Kjellstro¨ M, E., 2011. Assessment of climate change impact on water resources in the Pungwe river basin. *Tellus A: Dynamic Meteorology and Oceanography*, *63*(1), pp.138-157.

Arnell, N.W., Hudson, D.A. and Jones, R.G., 2003. Climate change scenarios from a regional climate model: Estimating change in runoff in southern Africa. *Journal of Geophysical Research: Atmospheres*, *108*(D16).

Arnell, N.W., 2004. Climate change and global water resources: SRES emissions and socio-economic scenarios. *Global environmental change*, *14*(1), pp.31-52.

Arnold, J.G., Engel, B.A. and Srinivasan, R., 1993. A continuous time, grid cell watershed model. *Application of advanced information technologies for management of natural resources*, pp.17-19.

Asadieh, B. and Krakauer, N.Y., 2017. Global change in streamflow extremes under climate change over the 21st century. Hydrology and Earth System Sciences, 21(11), p.5863.

Beck, L. and Bernauer, T., 2011. How will combined changes in water demand and climate affect water availability in the Zambezi river basin?. *Global Environmental Change*, *21*(3), pp.1061-1072.

Bekele, E.G. and Nicklow, J.W., 2007. Multi-objective automatic calibration of SWAT using NSGA-II. *Journal of Hydrology*, *341*(3-4), pp.165-176.

Benito, G., Díez-Herrero, A. and De Villalta, M.F., 2003. Magnitude and frequency of flooding in the Tagus basin (Central Spain) over the last millennium. *Climatic Change*, *58*(1-2), pp.171-192.

Bergström, S., Carlsson, B., Gardelin, M., Lindström, G., Pettersson, A. and Rummukainen, M., 2001. Climate change impacts on runoff in Sweden assessments by global climate models, dynamical downscaling and hydrological modelling. *Climate research*, *16*(2), pp.101-112.

Bernstein, L., Bosch, P., Canziani, O., Chen, Z., Christ, R. and Riahi, K., 2008. *IPCC, 2007: climate change 2007: synthesis report*. IPCC.

Beven, K.J. and Kirkby, M.J., 1979. A physically based, variable contributing area model of basin hydrology/Un modèle à base physique de zone d'appel variable de l'hydrologie du bassin versant. *Hydrological Sciences Journal*, *24*(1), pp.43-69.

Bieger, K., Arnold, J.G., Rathjens, H., White, M.J., Bosch, D.D., Allen, P.M., Volk, M. and Srinivasan, R., 2017. Introduction to SWAT+, a completely restructured version of the soil and water assessment tool. *JAWRA Journal of the American Water Resources Association*, *53*(1), pp.115-130.

Bokhari, S.A.A., Ahmad, B., Ali, J., Ahmad, S., Mushtaq, H. and Rasul, G., 2018. Future climate change projections of the Kabul River Basin using a multi-model ensemble of high-resolution statistically downscaled data. *Earth Systems and Environment*, *2*(3), pp.477-497.

Brown, D.G., Riolo, R., Robinson, D.T., North, M. and Rand, W., 2005. Spatial process and data models: Toward integration of agent-based models and GIS. *Journal of Geographical Systems*, *7*(1), pp.25-47.

Cannon, A.J., Sobie, S.R. and Murdock, T.Q., 2015. Bias correction of GCM precipitation by quantile mapping: How well do methods preserve changes in quantiles and extremes?. *Journal of Climate*, *28*(17), pp.6938-6959.

Cannon, A.J., 2018. Multivariate quantile mapping bias correction: an N-dimensional probability density function transform for climate model simulations of multiple variables. *Climate dynamics*, *50*(1), pp.31-49.

Chai, T. and Draxler, R.R., 2014. Root mean square error (RMSE) or mean absolute error (MAE)?–Arguments against avoiding RMSE in the literature. *Geoscientific model development*, *7*(3), pp.1247-1250.

Chen, C.T. and Knutson, T., 2008. On the verification and comparison of extreme rainfall indices from climate models. Journal of Climate, 21(7), pp.1605-1621.

Chen, H., Xu, C.Y. and Guo, S., 2012. Comparison and evaluation of multiple GCMs, statistical downscaling and hydrological models in the study of climate change impacts on runoff. *Journal of hydrology*, *434*, pp.36-45.

Chen, J., Brissette, F.P. and Leconte, R., 2011. Uncertainty of downscaling method in quantifying the impact of climate change on hydrology. *Journal of hydrology*, *401*(3-4), pp.190-202.

Chen, J., Brissette, F.P., Chaumont, D. and Braun, M., 2013. Finding appropriate bias correction methods in downscaling precipitation for hydrologic impact studies over North America. *Water Resources Research*, *49*(7), pp.4187-4205.

Cheng, C., Chau, K., Sun, Y. and Lin, J., 2005, May. Long-term prediction of discharges in Manwan Reservoir using artificial neural network models. In *International Symposium on Neural Networks* (pp. 1040-1045). Springer, Berlin, Heidelberg.

Chiew, F.H.S., Teng, J., Vaze, J., Post, D.A., Perraud, J.M., Kirono, D.G.C. and Viney, N.R., 2009. Estimating climate change impact on runoff across southeast Australia: Method, results, and implications of the modeling method. *Water Resources Research*, *45*(10).

Choudhary, A. and Dimri, A.P., 2019. On bias correction of summer monsoon precipitation over India from CORDEX-SA simulations. *International Journal of Climatology*, *39*(3), pp.1388-1403.

Cooley, D., Nychka, D. and Naveau, P., 2007. Bayesian spatial modeling of extreme precipitation return levels. *Journal of the American Statistical Association*, *102*(479), pp.824-840.

Coron, L., Andreassian, V., Perrin, C., Lerat, J., Vaze, J., Bourqui, M. and Hendrickx, F., 2012. Crash testing hydrological models in contrasted climate conditions: An experiment on 216 Australian catchments. *Water Resources Research*, *48*(5).

Cortés-Hernández, V.E., Zheng, F., Evans, J., Lambert, M., Sharma, A. and Westra, S., 2016. Evaluating regional climate models for simulating sub-daily rainfall extremes. Climate Dynamics, 47(5-6), pp.1613-1628.

CRIDF, 2018. Case study: Incomati Basin. INVESTING IN FLOOD RISK MANAGEMENT REDUCES FLOOD VULNERABILITY AND BUILDS CLIMATE RESILIENCE.

Cuaresma, J.C., 2017. Income projections for climate change research: A framework based on human capital dynamics. *Global Environmental Change*, *42*, pp.226-236.

Davis, C., 2010. *Climate change handbook for north-eastern South Africa*. Council for Scientific and Industrial Research (CSIR).

Davis, C.L., Engelbrecht, F.A., Tadross, M., Wolski, P. and Archer, E.R., 2017. Future climate change over Southern Africa. AFRICAN SUN MeDIA.

Davis, C.L. and Vincent, K., 2017. Climate risk and vulnerability: a handbook for Southern Africa.

DEA, 2010. Department of Environmental Affairs. Green economy summit report. Pretoria: DEA

Dellink, R., Chateau, J., Lanzi, E. and Magné, B., 2017. Long-term economic growth projections in the Shared Socioeconomic Pathways. *Global Environmental Change*, *42*, pp.200-214.

Déqué, M., Calmanti, S., Christensen, O.B., Aquila, A.D., Maule, C.F., Haensler, A., Nikulin, G. and Teichmann, C., 2017. A multi-model climate response over tropical Africa at+ 2 C. *Climate Services*, *7*, pp.87-95.

Devia, G.K., Ganasri, B.P. and Dwarakish, G.S., 2015. A review on hydrological models. *Aquatic Procedia*, *4*, pp.1001-1007.

Diaconescu, E.P., Mailhot, A., Brown, R. and Chaumont, D., 2018. Evaluation of CORDEX-Arctic daily precipitation and temperature-based climate indices over Canadian Arctic land areas. *Climate dynamics*, *50*(5), pp.2061-2085.

Dinku, T., Thomson, M.C., Cousin, R., del Corral, J., Ceccato, P., Hansen, J. and Connor, S.J., 2018. Enhancing national climate services (ENACTS) for development in Africa. *Climate and Development*, *10*(7), pp.664-672.

Donnelly, C., Greuell, W., Andersson, J., Gerten, D., Pisacane, G., Roudier, P. and Ludwig, F., 2017. Impacts of climate change on European hydrology at 1.5, 2 and 3 degrees mean global warming above preindustrial level. *Climatic Change*, *143*(1), pp.13-26.

DWAF, 2003. Department of Water Affairs and Forestry. Inkomati Water Management Area: Overview of Water Resources Availability and Utilisation. 2003. PWMA 05/000/00/0203

Eckhardt, K. and Arnold, J.G., 2001. Automatic calibration of a distributed catchment model. *Journal of hydrology*, *251*(1-2), pp.103-109.

Van Eekelen, M.W., Bastiaanssen, W.G., Jarmain, C., Jackson, B., Ferreira, F., Van der Zaag, P., Okello, A.S., Bosch, J., Dye, P., Bastidas-Obando, E. and Dost, R.J.J., 2015. A novel approach to estimate direct and indirect water withdrawals from satellite measurements: A case study from the Incomati basin. *Agriculture, Ecosystems & Environment*, *200*, pp.126-142.

Fauzi, F., Kuswanto, H. and Atok, R.M., 2020, May. Bias correction and statistical downscaling of earth system models using quantile delta mapping (QDM) and bias correction constructed analogues with quantile mapping reordering (BCCAQ). In *Journal of Physics: Conference Series* (Vol. 1538, No. 1, p. 012050). IOP Publishing.

Favre, A., Philippon, N., Pohl, B., Kalognomou, E.A., Lennard, C., Hewitson, B., Nikulin, G., Dosio, A., Panitz, H.J. and Cerezo-Mota, R., 2016. Spatial distribution of precipitation annual cycles over South Africa in 10 CORDEX regional climate model present-day simulations. *Climate Dynamics*, *46*(5-6), pp.1799-1818.

Fowler, K.J., Peel, M.C., Western, A.W., Zhang, L. and Peterson, T.J., 2016. Simulating runoff under changing climatic conditions: Revisiting an apparent deficiency of conceptual rainfall-runoff models. *Water Resources Research*, *52*(3), pp.1820-1846.

Fujimori, S., Hasegawa, T., Masui, T., Takahashi, K., Herran, D.S., Dai, H., Hijioka, Y. and Kainuma, M., 2017. SSP3: AIM implementation of shared socioeconomic pathways. *Global Environmental Change*, *42*, pp.268-283.

Gallego-Ayala, J. and Juízo, D., 2014. Integrating stakeholders' preferences into water resources management planning in the Incomati river basin. *Water resources management*, *28*(2), pp.527-540.

Gassman, P.W., Reyes, M.R., Green, C.H. and Arnold, J.G., 2007. The soil and water assessment tool: historical development, applications, and future research directions. *Transactions of the ASABE*, *50*(4), pp.1211-1250.

Giorgi, F., Jones, C. and Asrar, G.R., 2009. Addressing climate information needs at the regional level: the CORDEX framework. World Meteorological Organization (WMO) Bulletin, 58(3), p.175.

Graham, P.L., 2000. *Large-scale hydrologic modeling in the Baltic basin* (Doctoral dissertation, Institutionen för anläggning och miljö).

Graham, L.P., Andersson, L., Horan, M., Kunz, R., Lumsden, T., Schulze, R., Warburton, M., Wilk, J. and Yang, W., 2011. Using multiple climate projections for assessing hydrological response to climate change in the Thukela River Basin, South Africa. *Physics and Chemistry of the Earth, Parts A/B/C*, *36*(14-15), pp.727-735.

Gu, H., Yu, Z., Yang, C., Ju, Q., Yang, T. and Zhang, D., 2018. High-resolution ensemble projections and uncertainty assessment of regional climate change over China in CORDEX East Asia. *Hydrology and Earth System Sciences*, *22*(5), p.3087.

Gudoshava, M., Misiani, H.O., Segele, Z.T., Jain, S., Ouma, J.O., Otieno, G., Anyah, R., Indasi, V.S., Endris, H.S., Osima, S. and Lennard, C., 2020. Projected effects of 1.5 C and 2 C global warming levels on the intra-seasonal rainfall characteristics over the Greater Horn of Africa. *Environmental Research Letters*, *15*(3), p.034037.

Guo, J., Zhou, J., Lu, J., Zou, Q., Zhang, H. and Bi, S., 2014. Multi-objective optimization of empirical hydrological model for streamflow prediction. *Journal of Hydrology*, *511*, pp.242-253.

Guse, B., Reusser, D.E. and Fohrer, N., 2014. How to improve the representation of hydrological processes in SWAT for a lowland catchment–temporal analysis of parameter sensitivity and model performance. *Hydrological processes*, *28*(4), pp.2651-2670.

Gutowski Jr, W.J., Willis, S.S., Patton, J.C., Schwedler, B.R., Arritt, R.W. and Takle, E.S., 2008. Changes in extreme, cold-season synoptic precipitation events under global warming. *Geophysical Research Letters*, *35*(20).

Gyamfi, C., Ndambuki, J.M. and Salim, R.W., 2016. Application of SWAT model to the Olifants Basin: calibration, validation and uncertainty analysis. *Journal of Water Resource and Protection*, *8*(03), p.397.

Hamududu, B.H. and Killingtveit, Å., 2016. Hydropower production in future climate scenarios; the case for the Zambezi River. *Energies*, *9*(7), p.502.

Hartmann, G. and Bárdossy, A., 2005. Investigation of the transferability of hydrological models and a method to improve model calibration. *Advances in Geosciences*, *5*, pp.83-87.

Heo, J.H., Ahn, H., Shin, J.Y., Kjeldsen, T.R. and Jeong, C., 2019. Probability distributions for a quantile mapping technique for a bias correction of precipitation data: A case study to precipitation data under climate change. *Water*, *11*(7), p.1475.

Hirabayashi, Y., Kanae, S., Emori, S., Oki, T. and Kimoto, M., 2008. Global projections of changing risks of floods and droughts in a changing climate. *Hydrological sciences journal*, *53*(4), pp.754-772.

Hirabayashi, Y., Mahendran, R., Koirala, S., Konoshima, L., Yamazaki, D., Watanabe, S., Kim, H. and Kanae, S., 2013. Global flood risk under climate change. *Nature Climate Change*, *3*(9), pp.816-821.

Holbrook, E. 2010. Countries Most Vulnerable to Economic Losses. Risk Management Monitor. https://www.riskmanagementmonitor.com/countries-most-vulnerable-to-economic-losses/

Huang, X., Swain, D.L. and Hall, A.D., 2020. Future precipitation increase from very high resolution ensemble downscaling of extreme atmospheric river storms in California. *Science Advances*, *6*(29), p.eaba1323.

Hughes, D.A., Andersson, L., Wilk, J. and Savenije, H.H., 2006. Regional calibration of the Pitman model for the Okavango River. *Journal of Hydrology*, *331*(1-2), pp.30-42.

Hulme, M., 2016. 1.5 C and climate research after the Paris Agreement. *Nature Climate Change*, *6*(3), pp.222-224.

ICMA, 2010. The Inkomati Catchment Management Strategy: A First Generations Catchment Management Strategy for the Inkomati Water Management Area. Inkomati Catchment Management Agency, Nelspruit.

ICPR, 2001. Atlas on the Risk of Flooding and Potential Damage due to Extreme Floods of the Rhine.

IPCC, 1992: *Climate Change 1992. The Supplementary Report to the IPCC Scientific Assessment.* J. T. Houghton, B. A. Callander, and S. K. Varney, Eds., Cambridge University Press, 200 pp.

JIBS, 2001. Joint Incomati Basin Study Report. Phase 2. Consultec Report No: C14- 99MRF/BKS ACRES

Jongman, B., Ward, P.J. and Aerts, J.C., 2012. Global exposure to river and coastal flooding: Long term trends and changes. *Global Environmental Change*, *22*(4), pp.823-835.

Jones, C., Giorgi, F. and Asrar, G., 2011. The Coordinated Regional Downscaling Experiment: CORDEX–an international downscaling link to CMIP5. *CLIVAR exchanges*, *16*(2), pp.34-40.

Joubert, A.M., Mason, S.J. and Galpin, J.S., 1996. Droughts over southern Africa in a doubled-CO2 climate. *International Journal of Climatology*, *16*(10), pp.1149-1156.

Joubert, A.M. and Hewitson, B.C., 1997. Simulating present and future climates of southern Africa using general circulation models. *Progress in physical geography*, *21*(1), pp.51-78.

Jury, M.R., 2016. Summer climate of Madagascar and monsoon pulsing of its vortex. *Meteorology and Atmospheric Physics*, *128*(1), pp.117-129.

Kalognomou, E.A., Lennard, C., Shongwe, M., Pinto, I., Favre, A., Kent, M., Hewitson, B., Dosio, A., Nikulin, G., Panitz, H.J. and Büchner, M., 2013. A diagnostic evaluation of precipitation in CORDEX models over southern Africa. *Journal of climate*, *26*(23), pp.9477-9506.

Karlsson, J.M. and Arnberg, W., 2011. Quality analysis of SRTM and HYDRO1K: a case study of flood inundation in Mozambique. *International Journal of Remote Sensing*, *32*(1), pp.267-285.

Kay, G. and Washington, R., 2008. Future southern African summer rainfall variability related to a southwest Indian Ocean dipole in HadCM3. *Geophysical Research Letters*, *35*(12).

Kiersch, B. (2001). Land use impacts on water resources: a literature review. Food and Agriculture Organization (FAO) of the United Nations, Rome. Available from: http://www.fao.org/docrep/004/y3618e/y3618e07.htm

Kisembe, J., Favre, A., Dosio, A., Lennard, C., Sabiiti, G. and Nimusiima, A., 2019. Evaluation of rainfall simulations over Uganda in CORDEX regional climate models. *Theoretical and Applied Climatology*, *137*(1), pp.1117-1134.

Knebl, M.R., Yang, Z.L., Hutchison, K. and Maidment, D.R., 2005. Regional scale flood modeling using NEXRAD rainfall, GIS, and HEC-HMS/RAS: a case study for the San Antonio River Basin Summer 2002 storm event. *Journal of Environmental Management*, *75*(4), pp.325-336.

Knoesen, D., Schulze, R., Pringle, C., Summerton, M., Dickens, C. and Kunz, R., 2009. Water for the future: impacts of climate change on water resources in the Orange-Senqu River basin. *Report D*, *3*(7).

Krause, P., Boyle, D.P. and Bäse, F., 2005. Comparison of different efficiency criteria for hydrological model assessment.

Kruger, A.C. and Shongwe, S., 2004. Temperature trends in South Africa: 1960–2003. *International Journal of Climatology: A Journal of the Royal Meteorological Society*, *24*(15), pp.1929-1945.

Krysanova, V., Donnelly, C., Gelfan, A., Gerten, D., Arheimer, B., Hattermann, F. and Kundzewicz, Z.W., 2018. How the performance of hydrological models relates to credibility of projections under climate change. *Hydrological Sciences Journal*, *63*(5), pp.696-720.

Kundzewicz, Z.W., Kanae, S., Seneviratne, S.I., Handmer, J., Nicholls, N., Peduzzi, P., Mechler, R., Bouwer, L.M., Arnell, N., Mach, K. and Muir-Wood, R., 2014. Flood risk and climate change: global and regional perspectives. *Hydrological Sciences Journal*, *59*(1), pp.1-28.

Kumi, N. and Abiodun, B.J., 2018. Potential impacts of 1.5 C and 2 C global warming on rainfall onset, cessation and length of rainy season in West Africa. *Environmental Research Letters*, *13*(5), p.055009.

Kusangaya, S., Warburton, M.L., Van Garderen, E.A. and Jewitt, G.P., 2014. Impacts of climate change on water resources in southern Africa: A review. *Physics and Chemistry of the Earth, Parts A/B/C*, *67*, pp.47-54.

Laio, F., Di Baldassarre, G. and Montanari, A., 2009. Model selection techniques for the frequency analysis of hydrological extremes. *Water Resources Research*, *45*(7).

Leestemaker, J., 2000. The domino effect, a downstream perspective in water management in Southern Africa. *Green Cross International, Water for Peace in the Middle East and Southern Africa, Geneva*.

Legesse, D., Vallet-Coulomb, C. and Gasse, F., 2003. Hydrological response of a catchment to climate and land use changes in Tropical Africa: case study South Central Ethiopia. *Journal of hydrology*, *275*(1-2), pp.67-85.

Leimbach, M., Kriegler, E., Roming, N. and Schwanitz, J., 2017. Future growth patterns of world regions–A GDP scenario approach. *Global Environmental Change*, *42*, pp.215-225.

Li, L., Ngongondo, C.S., Xu, C.Y. and Gong, L., 2013. Comparison of the global TRMM and WFD precipitation datasets in driving a large-scale hydrological model in southern Africa. *Hydrology Research*, *44*(5), pp.770-788.

Li, L., Diallo, I., Xu, C.Y. and Stordal, F., 2015. Hydrological projections under climate change in the near future by RegCM4 in Southern Africa using a large-scale hydrological model. *Journal of Hydrology*, *528*, pp.1-16.

Macuácua, E.B.C., 2012. Impact of Land Use Change and Increased Agricultural Water Use on the Incomati River Flow Regime.

Maúre, G., Pinto, I., Ndebele-Murisa, M., Muthige, M., Lennard, C., Nikulin, G., Dosio, A. and Meque, A., 2018. The southern African climate under 1.5 C and 2 C of global warming as simulated by CORDEX regional climate models. *Environmental Research Letters*, *13*(6), p.065002.

Mason, S.J. and Joubert, A.M., 1997. Simulated changes in extreme rainfall over southern Africa. *International Journal of Climatology: A Journal of the Royal Meteorological Society*, *17*(3), pp.291-301.

Mason, S.J., Waylen, P.R., Mimmack, G.M., Rajaratnam, B. and Harrison, J.M., 1999. Changes in extreme rainfall events in South Africa. *Climatic Change*, *41*(2), pp.249-257.

McCuen, R.H., Knight, Z. and Cutter, A.G., 2006. Evaluation of the Nash–Sutcliffe efficiency index. *Journal of hydrologic engineering*, *11*(6), pp.597-602.

Meyer, J., Kohn, I., Stahl, K., Hakala, K., Seibert, J. and Cannon, A.J., 2019. Effects of univariate and multivariate bias correction on hydrological impact projections in alpine catchments. *Hydrology and Earth System Sciences*, *23*(3), pp.1339-1354.

Milly, P.C.D., Wetherald, R.T., Dunne, K.A. and Delworth, T.L., 2002. Increasing risk of great floods in a changing climate. *Nature*, *415*(6871), pp.514-517.

Monteiro, P.M.S. and Marchand, M. eds., 2009. *Catchment2Coast: A systems approach to coupled river-coastal ecosystem science and management* (Vol. 2). IOS Press.

Moss, R.H., Edmonds, J.A., Hibbard, K.A., Manning, M.R., Rose, S.K., Van Vuuren, D.P., Carter, T.R., Emori, S., Kainuma, M., Kram, T. and Meehl, G.A., 2010. The next generation of scenarios for climate change research and assessment. *Nature*, *463*(7282), pp.747-756.

Moradkhani, H. and Sorooshian, S., 2009. General review of rainfall-runoff modeling: model calibration, data assimilation, and uncertainty analysis. In *Hydrological modelling and the water cycle* (pp. 1-24). Springer, Berlin, Heidelberg.

Moriasi, D.N., Arnold, J.G., Van Liew, M.W., Bingner, R.L., Harmel, R.D. and Veith, T.L., 2007. Model evaluation guidelines for systematic quantification of accuracy in watershed simulations. *Transactions of the ASABE*, *50*(3), pp.885-900.

Morita, T., Nakićenović, N. and Robinson, J., 2000. Overview of mitigation scenarios for global climate stabilization based on new IPCC emission scenarios (SRES). *Environmental Economics and Policy Studies*, *3*(2), pp.65-88.

Mpelasoka, F.S. and Chiew, F.H., 2009. Influence of rainfall scenario construction methods on runoff projections. *Journal of Hydrometeorology*, *10*(5), pp.1168-1183.

Mujere, N. and Mazvimavi, D., 2012. Impact of climate change on reservoir reliability. *African Crop Science Journal*, *20*, pp.545-551.

Muleta, M.K., 2012. Improving model performance using season-based evaluation. *Journal of Hydrologic Engineering*, *17*(1), pp.191-200.

Müller-Wohlfeil, D.I., Bürger, G. and Lahmer, W., 2000. Response of a river catchment to climatic change: application of expanded downscaling to Northern Germany. *Climatic Change*, *47*(1), pp.61-89.

Mussa, F.E.F., 2013. Groundwater as an emergency source for drought mitigation in the Incomati River basin-case study of the Crocodile river catchment.

Musselman, K.N., Lehner, F., Ikeda, K., Clark, M.P., Prein, A.F., Liu, C., Barlage, M. and Rasmussen, R., 2018. Projected increases and shifts in rain-on-snow flood risk over western North America. *Nature Climate Change*, *8*(9), pp.808-812.

Nakicenovic, N., Alcamo, J., Grubler, A., Riahi, K., Roehrl, R.A., Rogner, H.H. and Victor, N., 2000. *Special report on emissions scenarios (SRES), a special report of Working Group III of the intergovernmental panel on climate change*. Cambridge University Press.

Nash, J.E., 1959. A note on the Muskingum flood-routing method. *Journal of geophysical research*, *64*(8), pp.1053-1056.

Nash, J.E. and Sutcliffe, J.V., 1970. River flow forecasting through conceptual models part I—A discussion of principles. *Journal of hydrology*, *10*(3), pp.282-290.

New, M., Hewitson, B., Stephenson, D.B., Tsiga, A., Kruger, A., Manhique, A., Gomez, B., Coelho, C.A., Masisi, D.N., Kululanga, E. and Mbambalala, E., 2006. Evidence of trends in daily climate extremes over southern and west Africa. *Journal of Geophysical Research: Atmospheres*, *111*(D14).

Nikulin, G., Jones, C., Giorgi, F., Asrar, G., Büchner, M., Cerezo-Mota, R., Christensen, O.B., Déqué, M., Fernandez, J., Hänsler, A. and Van Meijgaard, E., 2012. Precipitation climatology in an ensemble of CORDEX-Africa regional climate simulations. *Journal of Climate*, *25*(18), pp.6057-6078.

Nikulin, G., Lennard, C., Dosio, A., Kjellström, E., Chen, Y., Hänsler, A., Kupiainen, M., Laprise, R., Mariotti, L., Maule, C.F. and Van Meijgaard, E., 2018. The effects of 1.5 and 2 degrees of global warming on Africa in the CORDEX ensemble. *Environmental Research Letters*, *13*(6), p.065003.

Niraula, R., Norman, L.M., Meixner, T. and Callegary, J.B., 2012. Multi-gauge calibration for modeling the semi-arid Santa Cruz Watershed in Arizona-Mexico border area using SWAT. *Air, Soil and Water Research*, *5*, pp.ASWR-S9410.

Nyeko-Ogiramoi, P., Ngirane-Katashaya, G., Willems, P. and Ntegeka, V., 2010. Evaluation and inter-comparison of Global Climate Models' performance over Katonga and Ruizi catchments in Lake Victoria basin. *Physics and Chemistry of the Earth, Parts A/B/C*, *35*(13-14), pp.618-633.

O'Neill, B.C., Kriegler, E., Riahi, K., Ebi, K.L., Hallegatte, S., Carter, T.R., Mathur, R. and Van Vuuren, D.P., 2014. A new scenario framework for climate change research: the concept of shared socioeconomic pathways. *Climatic change*, *122*(3), pp.387-400.

Okello, A.S., Masih, I., Uhlenbrook, S., Jewitt, G.W.P., Van der Zaag, P. and Riddell, E., 2015. Drivers of spatial and temporal variability of streamflow in the Incomati River basin. *Hydrology & Earth System Sciences*, *19*(2).

Okello, S., 2019. *Improved Hydrological Understanding of a Semi-Arid Subtropical Transboundary Basin Using Multiple Techniques-The Incomati River Basin*. CRC Press.

Pall, P., Aina, T., Stone, D.A., Stott, P.A., Nozawa, T., Hilberts, A.G., Lohmann, D. and Allen, M.R., 2011. Anthropogenic greenhouse gas contribution to flood risk in England and Wales in autumn 2000. *Nature*, *470*(7334), pp.382-385.

Park, C., Min, S.K., Lee, D., Cha, D.H., Suh, M.S., Kang, H.S., Hong, S.Y., Lee, D.K., Baek, H.J., Boo, K.O. and Kwon, W.T., 2016. Evaluation of multiple regional climate models for summer climate extremes over East Asia. *Climate Dynamics*, *46*(7-8), pp.2469-2486.

Parry, M., Parry, M.L., Canziani, O., Palutikof, J., Van der Linden, P. and Hanson, C. eds., 2007. *Climate change 2007-impacts, adaptation and vulnerability: Working group II contribution to the fourth assessment report of the IPCC* (Vol. 4). Cambridge University Press.

Pedersen, J.S.T., Santos, F.D., Van Vuuren, D., Gupta, J., Coelho, R.E., Aparício, B.A. and Swart, R., 2021. An assessment of the performance of scenarios against historical global emissions for IPCC reports. *Global Environmental Change*, *66*, p.102199.

Pielke Sr, R.A. and Wilby, R.L., 2012. Regional climate downscaling: What's the point?. *Eos, Transactions American Geophysical Union*, *93*(5), pp.52-53.

Pinto, I., Lennard, C., Tadross, M., Hewitson, B., Dosio, A., Nikulin, G., Panitz, H.J. and Shongwe, M.E., 2016. Evaluation and projections of extreme precipitation over southern Africa from two CORDEX models. *Climatic Change*, *135*(3-4), pp.655-668.

Pitman, W.V., 1973. *A mathematical model for generating monthly river flows from meteorological data in South Africa*. University of the Witwatersrand, Department of Civil Engineering.

Pomeroy, J.W., Stewart, R.E. and Whitfield, P.H., 2016. The 2013 flood event in the South Saskatchewan and Elk River basins: Causes, assessment and damages. *Canadian Water Resources Journal/Revue canadienne des ressources hydriques*, *41*(1-2), pp.105-117.

Prudhomme, C., Reynard, N. and Crooks, S., 2002. Downscaling of global climate models for flood frequency analysis: where are we now?. *Hydrological processes*, *16*(6), pp.1137-1150.

Reason, C.J.C., Landman, W. and Tennant, W., 2006. Seasonal to decadal prediction of southern African climate and its links with variability of the Atlantic Ocean. *Bulletin of the American Meteorological Society*, *87*(7), pp.941-956.

Reynard, N.S., Prudhomme, C. and Crooks, S.M., 2001. The flood characteristics of large UK rivers: potential effects of changing climate and land use. *Climatic change*, *48*(2), pp.343-359.Reynard, N.S., Prudhomme, C. and Crooks, S.M., 2001. The flood characteristics of large UK rivers: potential effects of changing climate and land use. *Climatic change*, *48*(2), pp.343-359.

Refsgaard, J.C. and Knudsen, J., 1996. Operational validation and intercomparison of different types of hydrological models. *Water Resources Research*, *32*(7), pp.2189-2202.

Refsgaard, J.C., Højberg, A.L., Møller, I., Hansen, M. and Søndergaard, V., 2010. Groundwater modeling in integrated water resources management—visions for 2020. *Groundwater*, *48*(5), pp.633-648.

Riddell, E., Jewitt, G., Chetty, K., Saraiva Okello, A., Jackson, B., Lamba, A., Gokoo, S., Naidoo, P., Vather, T. and Thornton-Dibb, S., 2014. A management tool for the Inkomati Basin with focus on improved hydrological understanding for risk-based operational water management. *WRC*.

Roe, G.H., Montgomery, D.R. and Hallet, B., 2003. Orographic precipitation and the relief of mountain ranges. *Journal of Geophysical Research: Solid Earth*, *108*(B6).

Rogelj, J., Den Elzen, M., Höhne, N., Fransen, T., Fekete, H., Winkler, H., Schaeffer, R., Sha, F., Riahi, K. and Meinshausen, M., 2016. Paris Agreement climate proposals need a boost to keep warming well below 2 C. *Nature*, *534*(7609), pp.631-639.

Ryu, D., Crow, W.T., Zhan, X. and Jackson, T.J., 2009. Correcting unintended perturbation biases in hydrologic data assimilation. *Journal of Hydrometeorology*, *10*(3), pp.734-750.

Sauka, S., 2016. *Flood risk assessment of the Crocodile River, Mpumalanga* (Doctoral dissertation).

Schaefli, B., Hingray, B., Niggli, M. and Musy, A., 2005. A conceptual glacio-hydrological model for high mountainous catchments. *Hydrology and earth system sciences*, *9*(1/2), pp.95-109.

Schulz, A., 2006. Creating a legal framework for good transboundary water governance in the Zambezi and Incomati River basins. *Geo. Int'l Envtl. L. Rev.*, *19*, p.117.

Schulze, R.E., 1995. *Hydrology and agrohydrology: A text to accompany the ACRU 3.00 agrohydrological modelling system*. Water Research Commission.

Schulze, R.E., 2011. Approaches towards practical adaptive management options for selected water-related sectors in South Africa in a context of climate change. *Water SA*, *37*(5), pp.621-646.

Sengo, D.J., Kachapila, A., Van der Zaag, P., Mul, M. and Nkomo, S., 2005. Valuing environmental water pulses into the Incomati estuary: key to achieving equitable and sustainable utilisation of transboundary waters. *Physics and Chemistry of the Earth, Parts A/B/C*, *30*(11-16), pp.648-657.

Servat, E. and Dezetter, A., 1991. Selection of calibration objective fonctions in the context of rainfall-ronoff modelling in a Sudanese savannah area. *Hydrological Sciences Journal*, *36*(4), pp.307-330.

Sheffield, J., Goteti, G. and Wood, E.F., 2006. Development of a 50-year high-resolution global dataset of meteorological forcings for land surface modeling. *Journal of climate*, *19*(13), pp.3088-3111.

Sherman, L.K., 1932. Streamflow from rainfall by the unit-graph method. *Eng. News Record*, *108*, pp.501-505.

Shongwe, M.E., van Oldenborgh, G.J., van den Hurk, B. and van Aalst, M., 2011. Projected changes in mean and extreme precipitation in Africa under global warming. Part II: East Africa. *Journal of climate*, *24*(14), pp.3718-3733.

Sifundza, L., Masih, I. and Van der Zaag, P., 2018. Comparing the 2015-2016 drought in Southern Africa with historic droughts-the case of the Incomati River Basin. *EGUGA*, p.6979.

Sifundza, L.S., Van der Zaag, P. and Masih, I., 2019. Evaluation of the responses of institutions and actors to the 2015/2016 El Niño drought in the Komati catchment in Southern Africa: lessons to support future drought management. *Water SA*, *45*(4), pp.547-559.

Silver, M., Karnieli, A., Ginat, H., Meiri, E. and Fredj, E., 2017. An innovative method for determining hydrological calibration parameters for the WRF-Hydro model in arid regions. *Environmental Modelling & Software*, *91*, pp.47-69.

Singh, K.P., Malik, A., Mohan, D. and Sinha, S., 2004. Multivariate statistical techniques for the evaluation of spatial and temporal variations in water quality of Gomti River (India)—a case study. *Water research*, *38*(18), pp.3980-3992.

Sivakumar, B., Jayawardena, A.W. and Fernando, T.M.K.G., 2002. River flow forecasting: use of phase-space reconstruction and artificial neural networks approaches. *Journal of hydrology*, *265*(1-4), pp.225-245.

Singh, V.P. and Woolhiser, D.A., 2002. Mathematical modeling of watershed hydrology. *Journal of hydrologic engineering*, *7*(4), pp.270-292.

Slinger, J.H., Hilders, M. and Juizo, D., 2010. The practice of transboundary decision making on the Incomati River: elucidating underlying factors and their implications for institutional design. *Ecology and Society*, *15*(1).

Solomon, S., Manning, M., Marquis, M. and Qin, D., 2007. *Climate change 2007-the physical science basis: Working group I contribution to the fourth assessment report of the IPCC* (Vol. 4). Cambridge university press.

Sood, A., Muthuwatta, L. and McCartney, M., 2013. A SWAT evaluation of the effect of climate change on the hydrology of the Volta River basin. *Water international*, *38*(3), pp.297-311.

Sorooshian, S., Hsu, K.L., Coppola, E., Tomassetti, B., Verdecchia, M. and Visconti, G. eds., 2008. *Hydrological modelling and the water cycle: coupling the atmospheric and hydrological models* (Vol. 63). Springer Science & Business Media.

Stocker, T. ed., 2014. *Climate change 2013: the physical science basis: Working Group I contribution to the Fifth assessment report of the Intergovernmental Panel on Climate Change*. Cambridge university press.

Su, B., Zeng, X., Zhai, J., Wang, Y. and Li, X., 2015. Projected precipitation and streamflow under sres and rcp emission scenarios in the songhuajiang river basin, China. *Quaternary International*, *380*, pp.95-105.

Sunday, R.K.M., 2013. Rainfall and streamflow forecasting for operational water management in the Incomati Basin, Southern Africa.

Sunday, R.K.M., Masih, I., Werner, M. and Van der Zaag, P., 2014. Streamflow forecasting for operational water management in the Incomati River Basin, Southern Africa. *Physics and Chemistry of the Earth, Parts A/B/C*, *72*, pp.1-12.

Tadross, M., Jack, C. and Hewitson, B., 2005. On RCM-based projections of change in southern African summer climate. *Geophysical Research Letters*, *32*(23).

Tadross, M. and Johnston, P., 2012. Climate systems regional report: Southern Africa. *Local governments for sustainability—Africa climate systems regional report: Southern Africa, ISBN*, pp.978-0.

Tang, J., Niu, X., Wang, S., Gao, H., Wang, X. and Wu, J., 2016. Statistical downscaling and dynamical downscaling of regional climate in China: Present climate evaluations and future climate projections. *Journal of Geophysical Research: Atmospheres*, *121*(5), pp.2110-2129.

Tarek, M., Brissette, F.P. and Arsenault, R., 2020. Evaluation of the ERA5 reanalysis as a potential reference dataset for hydrological modelling over North America. *Hydrology and Earth System Sciences*, *24*(5), pp.2527-2544.

Tauacale, F.P.I, Amida Mussa, Tomazina Sithole and Marcio Mathe, 2007: Perfil Ambiental da bacia do Inkomati em Moçambique, Departamento de Geografia, Universidade Eduardo Mondlane.

Teutschbein, C. and Seibert, J., 2012. Bias correction of regional climate model simulations for hydrological climate-change impact studies: Review and evaluation of different methods. *Journal of hydrology*, *456*, pp.12-29.

Teutschbein, C. and Seibert, J., 2013. Is bias correction of regional climate model (RCM) simulations possible for non-stationary conditions?. *Hydrology and Earth System Sciences*, *17*(12), pp.5061-5077.

Thavhana, M.P., Savage, M.J. and Moeletsi, M.E., 2018. SWAT model uncertainty analysis, calibration and validation for runoff simulation in the Luvuvhu River catchment, South Africa. Physics and Chemistry of the Earth, Parts A/B/C, 105, pp.115-124.

Thrasher, B. and Nemani, R., 2015. Nasa earth exchange global daily downscaled projections (nex-gddp). *Van Vuuren DP, Edmonds J, Kainuma M, Riahi K, Thomson A, Hibbard K, Hurtt GC, Kram T, Krey V, Lamarque JF, et al.(2011): The representative concentration pathways: an overview. Climatic Change*, *109*(5).

Tong, Y., Gao, X., Han, Z., Xu, Y., Xu, Y. and Giorgi, F., 2020. Bias correction of temperature and precipitation over China for RCM simulations using the QM and QDM methods. *Climate Dynamics*, pp.1-19.

UNEP/Nairobi Convention Secretariat (2010): Environmental Profile of the Inkomati River Basin, UNEP, Nairobi Kenya, 82p

Van der Zaag, P. and Carmo Vaz, Á., 2003. Sharing the Incomati waters: cooperation and competition in the balance. Water Policy, 5(4), pp.349-368.

Van Griensven, A., Bieger, K., Hoang, L. and Arnold, J., 2018. Improved simulation of riparian wetland processes using SWAT+.

Van Liew, M.W., Arnold, J.G. and Garbrecht, J.D., 2003. Hydrologic simulation on agricultural watersheds: Choosing between two models. *Transactions of the ASAE*, *46*(6), p.1539.

Van Ogtrop, F.F., Hoekstra, A.Y. and van der Meulen, F., 2005. FLOOD MANAGEMENT IN THE LOWER INCOMATI RIVER BASIN, MOZAMBIQUE: TWO ALTERNATIVES 1. *JAWRA Journal of the American Water Resources Association*, *41*(3), pp.607-619.

Van Vuuren, D.P., Edmonds, J., Kainuma, M., Riahi, K., Thomson, A., Hibbard, K., Hurtt, G.C., Kram, T., Krey, V., Lamarque, J.F. and Masui, T., 2011. The representative concentration pathways: an overview. *Climatic change*, *109*(1), pp.5-31.

Van Vuuren, D.P., Kok, M.T., Girod, B., Lucas, P.L. and de Vries, B., 2012. Scenarios in global environmental assessments: key characteristics and lessons for future use. *Global Environmental Change*, *22*(4), pp.884-895.

Van Vuuren, D.P., Kriegler, E., O'Neill, B.C., Ebi, K.L., Riahi, K., Carter, T.R., Edmonds, J., Hallegatte, S., Kram, T., Mathur, R. and Winkler, H., 2014. A new scenario framework for climate change research: scenario matrix architecture. *Climatic Change*, *122*(3), pp.373-386.

Vaz, A.C., 2000, November. Coping with floods—the experience of Mozambique. In *1st WARFSA/WaterNet Symposium: sustainable use of water resources* (pp. 1-2).

Vaz, A.C. and Pereira, A.L., 2000. The Incomati and Limpopo international river basins: a view from downstream. *Water Policy*, *1*(2), pp.99-112.

Watson, R.T. and Team, C.W., 2001. IPCC Third Assessment Report climate change 2001: synthesis report.

Whetton, P.H., Fowler, A.M., Haylock, M.R. and Pittock, A.B., 1993. Implications of climate change due to the enhanced greenhouse effect on floods and droughts in Australia. *Climatic Change*, *25*(3), pp.289-317.

Wilkinson, M.J., Magagula, T.K. and Hassan, R.M., 2015. Piloting a method to evaluate the implementation of integrated water resource management in the Inkomati River Basin. *Water SA*, *41*(5), pp.633-642.

Winsemius, H.C., Aerts, J.C., Van Beek, L.P., Bierkens, M.F., Bouwman, A., Jongman, B., Kwadijk, J.C., Ligtvoet, W., Lucas, P.L., Van Vuuren, D.P. and Ward, P.J., 2016. Global drivers of future river flood risk. *Nature Climate Change*, *6*(4), pp.381-385.

Wu, J., Yen, H., Arnold, J.G., Yang, Y.E., Cai, X., White, M.J., Santhi, C., Miao, C. and Srinivasan, R., 2020. Development of reservoir operation functions in SWAT+ for national environmental assessments. *Journal of Hydrology*, *583*, p.124556.

Yang, C., Yu, Z., Hao, Z., Zhang, J. and Zhu, J., 2012. Impact of climate change on flood and drought events in Huaihe River Basin, China. *Hydrology Research*, *43*(1-2), pp.14-22.

Yen, H., Sharifi, A., Kalin, L., Mirhosseini, G. and Arnold, J.G., 2015. Assessment of model predictions and parameter transferability by alternative land use data on watershed modeling. *Journal of hydrology*, *527*, pp.458-470.

Yen, H., Jeong, J. and Smith, D.R., 2016. Evaluation of dynamically dimensioned search algorithm for optimizing SWAT by altering sampling distributions and searching range. *JAWRA Journal of the American Water Resources Association*, *52*(2), pp.443-455.

Yen, H., Park, S., Arnold, J.G., Srinivasan, R., Chawanda, C.J., Wang, R., Feng, Q., Wu, J., Miao, C., Bieger, K. and Daggupati, P., 2019. IPEAT+: a Built-in optimization and automatic calibration tool of SWAT+. *Water*, *11*(8), p.1681.

Zhang, H. and Huang, G.H., 2013. Development of climate change projections for small watersheds using multi-model ensemble simulation and stochastic weather generation. *Climate dynamics*, *40*(3-4), pp.805-821.

Zhang, L., Jin, X., He, C., Zhang, B., Zhang, X., Li, J., Zhao, C., Tian, J. and DeMarchi, C., 2016. Comparison of SWAT and DLBRM for hydrological modeling of a mountainous watershed in arid northwest China. *Journal of Hydrologic Engineering*, *21*(5), p.04016007.

Zhang, Y., You, Q., Chen, C. and Ge, J., 2016. Impacts of climate change on streamflows under RCP scenarios: A case study in Xin River Basin, China. *Atmospheric Research*, *178*, pp.521-534.

Zhu, T. and Ringler, C., 2012. Climate change impacts on water availability and use in the Limpopo River Basin. *Water*, *4*(1), pp.63-84.